8-2016

DEVELOPMENT OF RATIONAL COMBINATION THERAPY WITH PARP INHIBITORS AND KINASE INHIBITORS IN TNBC

Wen-Hsuan Yu

DEVELOPMENT OF RATIONAL COMBINATION THERAPY WITH PARP INHIBITORS AND KINASE INHIBITORS IN TNBC

By

Wen-Hsuan Yu, B.S.

APPROVED:

Mien-Chie Hung, PhD
Advisory Professor

Dihua Yu, M.D., Ph.D.

Jennifer Litton, M.D.

Paul Chiao, Ph.D.

Zhimin Lu, M.D., Ph.D.

APPROVED:

Dean, The University of Texas
Graduate School of Biomedical Science at Houston

DEVELOPMENT OF RATIONAL COMBINATION THERAPY WITH PARP INHIBITORS AND KINASE INHIBITORS IN TNBC

A

DISSERTATION

Presented to the Faculty of

The University of Texas

Health Science Center at Houston

and

The University of Texas

M.D. Anderson Cancer Center

Graduate School of Biomedical Sciences

In Partial Fulfillment

Of the Requirements

for the Degree of

DOCTOR OF PHILOSOPHY

by

Wen-Hsuan Yu, B.S.

Houston, Texas

August, 2016

DEDICATION

To my parents and sister:

for your unconditional love and support

for your patience and encouragement

I owe you more than I can express in words.

I couldn't have done this without you!

ACKNOWLEDGMENTS

It has been a long journey from where I began to get to know more about science. Over the past 7 years, there are so many people helped me throughout this journey. Without their guidance and help, I couldn't have done any of it.

First and for most, thank my parents, especially my dad, Jing-Lung Yu. He is the person who always respects my decision and supports everything I want to do. Although life is unexpected, I'm grateful for having a second chance to take care of him. I thank my parents for their unconditional love and support. I could not achieve my goal without them. A special thank to my sister, Wen-Yao, who helped to take care of my family and shared all my ups and downs.

I would like to offer my special thanks to my PhD advisor, Dr. Mien-Chie Hung, especially for his fully support during the time I took leave of absence for one and half year due to family issue. Without his encouragement and guidance, I couldn't overcome all challenges to pursue this dream. He is always generous to share his philosophy, scientific thinking and creative ideas with us. He also shows marked enthusiasm for research. I have learned a lot from him! I would also like to thank our collaborator in Taiwan, Dr. Min-Liang Kuo, for giving me an opportunity to continue working on bench in his lab during the time I was leave of absence. Working with his team in Taiwan further improves my independent thinking. Due to this long-term collaboration, I have chance to get one co-author paper and one co-first paper. Thank Dr. Darrel Stafford in UNC-CH, who gave me the first job in my life after graduating from NTU as research assistant and also supported me to begin my adventure in U.S.

I would like to thank all the faculty members that have served on my committees,

especially Dr. Dihua Yu, Dr. Zhimin Lu, Dr. Jennifer Litton and Dr. Paul Chiao for their constructive suggestions and guidance on my thesis project.

I want to thank all the past and present's members of Dr. Hung's laboratory. It is my pleasure to work with you in this big lab. I really enjoy the time brainstorming and chatting together, especially Shih-Shin, Aarthi, Jung-Mo, Yi-Hsin, Jennifer, Chien-Chia, Hsin-Wei, Lim, Jerry, Chao-Kai and James. Special thank to the members of PARP subgroup in Dr. Hung's lab including Dr. Yamaguchi Hirohito, Dr. Yi Du, Dr. Dong, Kathy, Jiao and Wan-Chi for daily project discussion and technical support. Thank Dr. Yi Du., who initiated this PARP project, so that creating many interesting topics as my dissertation. I want to especially thank Dr. Yamaguchi Hirohito who taught me a lot about scientific thinking and writing. It has been a privilege to work with him through my time in lab. I also want to take this opportunity to thank members of Dr. Kuo's lab. They are very generous and easy to collaborate with, especially Dr. Kuo-Tai Hua, Chi-Kuan, Rafi, Tsang-Chih and Kai Hang.

Thank all my friends around the world for the invaluable memories and endless support over the past several years! Tina, Judy, Ming-Hui, Kuo-Chan, Chih-Chao, Steve, Lin Lin and Tzu-Tang, it has been a lovely journey because of you!

In "The Road Not Taken" Frost writes, "Two roads diverged in a wood, and I- / I took the one less traveled by / And that has made all the difference." Yes, doing the PhD is a lonely road, but this journey becomes more fruitful with all of your support.

DEVELOPMENT OF RATIONAL COMBINATION THERAPY WITH PARP INHIBITORS AND KINASE INHIBITORS IN TNBC

Wen-Hsuan Yu, B.S.

Advisory Professor: Mien-Chie Hung, Ph.D.

Poly (ADP-ribose) polymerase inhibitors (PARPi) emerge as potential targeting drugs for BRCA-deficient cancers including triple negative breast cancer (TNBC). However, it has been reported that a subgroup of patients even with BRCA mutation fails to respond to PARPi in multiple clinical trials. In this study, we identified c-Met, a tyrosine kinase, phosphorylates PARP1 at Y907 and that the phosphorylation increases PARP1 activity, thereby rendering cancer cells resistant to PARPi. The combination of c-Met inhibitors (METi) and PARPi has a synergistic effect for c-Met overexpressed TNBC *in vitro* and *in vivo*. In addition to c-Met, through functional analysis, we found casein kinase 2 (CK2) is another potential PARP1 regulator. The combination of a CK2 inhibitor (CK2i) and PARPi synergistically attenuates DNA damage repair, cell cycle, cell proliferation and xenograft tumor growth. Similar to the c-Met-PARP1 axis, CK2 interacts with PARP1 in the nucleus. Moreover, CK2 can phosphorylate PARP1 *in vitro*, implicating that similar to c-Met, CK2 regulates PARP1 activity through direct phosphorylation. Together, phosphorylation of PARP1 may be used as biomarkers to guide the combinational treatment of PARPi and corresponding kinase inhibitors. Our study not only has revealed a new mechanism of PARPi resistance but also provided a marker-guided combination therapeutic strategy to stratify TNBC patients who do not respond to PARPi.

TABLE OF CONTENTS

LIST OF FIGURES

LIST OF TABLES

CHAPTER 1

INTRODUCTION

1.1 Overview of Breast Cancer

Breast cancer is the most common cancer diagnosed among US women, accounting for approximately one in three cancer populations (1). In the U.S., the rates of breast cancer death are higher than those for any other cancer except for lung cancer. According to the statistics from National Cancer Institute (NCI), there were 230,000 female breast cancer cases and caused about 40,000 deaths in 2015.

Breast cancer can be divided into different types by the tissue histopathology, including ductal carcinoma, lobular carcinoma and inflammatory breast cancer (2). Among them, ductal carcinoma is the most common type of breast cancer, making up nearly 70-80% of all breast cancer population. Staging of breast cancer by TNM system has important implications for cancer prognosis and therapy (3). The current therapies for breast cancer included surgery, radiotherapy, chemotherapy, hormone therapy and target therapy (4). Surgery is the most recommended therapy for patients with early stages (I or II) breast cancer (5). In patients with unresectable tumors (stage III or IV), chemotherapy or combination with radiotherapy, hormonal therapy, or target therapy is considered to be the standard treatment (6, 7). Until now, many effective chemotherapy drugs have been discovered to against breast cancer (8). The most common chemotherapy drugs include paclitaxel (Taxol®), docetaxel (Taxotere®), doxorubicin (Adriamycin®), epirubicin (Ellence®), methotrexate (Trexall®), 5-fluorouracil (5-FU; Adrucil®), cyclophosphamide (Cytoxan®) and carboplatin (Paraplatin®). Combination chemotherapy treatment is usually used to treat breast cancer. For example, CMF (cyclophosphamide, methotrexate and 5-FU) is a common used regimen for breast cancer (9).

Breast cancer can be divided into three subtypes by the protein expressions of estrogen receptor (ER), progesterone receptor (PR) and ERBB2 (HER2/neu), including luminal types, HER2-positive types and basal-like types (10). Luminal types breast cancer are ER-positive tumors, and the gene expression patterns of these tumors are similar to normal tissues that line the breast ducts and glands. Luminal types breast cancer can be further classified into two subtypes: luminal A and luminal B. Luminal A breast cancer tends to grow slowly, which have better prognosis. Luminal B breast cancer typically grows faster than luminal A. HER2-positive breast cancer is a breast cancer that highly expresses human epidermal growth factor receptor 2 (HER2), which can promote tumor growth, accounting for approximately 1 of 5 breast cancer cases. HER2-positive breast cancers tend to be more aggressive than luminal types breast cancer. Basal-*like* breast cancer (BLBC) makes up about 15-20% of breast cancers. Tumors that are negative for ER, PR, and HER2 expression are referred to as triple-negative breast cancers (TNBCs) (11).

1.2 Background of Triple-Negative Breast Cancer (TNBC)

As mentioned earlier, TNBC is a subtype of breast cancer that phenotypically lack of ER, PR and HER2 expressions (11). This subtype accounts for approximately 15-20% among all breast cancer patients. Majority of TNBC are high grade and invasive, resulting in distant metastases and poor survival rates. Women with TNBC do not respond to hormonal therapies or HER2-targeted agents because of the lack of ER, PR, and HER2 amplification (12). Recent studies using clinical samples indicate that TNBC and BLBC are 80% similar (13). More recently, TNBCs have been further classified into

six subtypes according to gene expression profiles (14), indicating that TNBCs are highly heterogeneous. Therefore, the development of the effective treatment strategies for TNBC is urgently needed.

BRCA1 and BRCA2 are the enzymes involved in homologous recombination (HR) DNA repair pathway. BRCA1 was first found to be involved in breast and ovarian cancer in 1990's (15). Later, BRCA2 was identified to have similar functions with BRCA1 (16). Further studies showed that BRCA1 mutations are correlated with early-onset of breast and ovarian cancers (17, 18). More detail investigation further revealed that both BRCA1 and BRCA2 are involved in the progression of breast cancer through functional loss of mutations, which is deficient in HR repair of damaged DNA (19-21). Currently, BRCA mutations are considered as key bio-markers to predict the hereditary breast or ovarian cancer. A recent study showed that more than 30% TNBC patients have BRCA mutations and BRCA1-mutation patients have same histological characteristics and clinical outcome with TNBC patients (22).

1.3 Overview of DNA Damage and Repair

DNA damage is an alteration in the chemical structure of DNA, which includes base and sugar modifications, single-strand breaks (SSBs), double-strand breaks (DSBs) and DNA-protein cross-links (23). DSBs can lead to genome rearrangements that are particularly hazardous to the cell. DNA damage could occur from various endogenous and exogenous resources. For example, oxidative DNA damage is frequently occurred by reactive oxygen species (ROS) in many human tissues, especially in tumors (24, 25). ROS could be produced from endogenous metabolic process such as oxidation, alkylation

and hydrolysis of bases (26-28). Endogenous DNA damage occurs more often than exogenous damage that is caused by external agents such as ultraviolet (UV) light, radiation, several plant toxins, mutagenic chemicals and virus infection (29, 30). DNA damages occur naturally thousands of times every day during each cell cycle in humans, and that damages must be repaired by different DNA repair mechanisms to remove different types of DNA damages and restore the DNA duplex (31). To counteract DNA damage, cells have developed specialized DNA repair systems, which can be subdivided into several distinct mechanisms based on the types of DNA damage. These processes include base excision repair (BER), mismatch repair (MMR), nucleotide excision repair, and DSBs repair, which comprise both non-homologous end-joining (NHEJ) and homologous recombination (HR) (32) .

DNA repair systems are consist of multiple repair enzymes, and allow both RNA and DNA polymerases to read accurately and duplicate the information in the genome (33). These repair mechanisms are regulated by various DNA damage response kinases, which are activated at DNA lesions. These kinases can phosphorylate repair proteins to modify their activities, or initiate a complex series of changes in the local chromatin structure near the damage sites to improve the efficiency of DNA repair (32).

1.4 Poly-ADP-Ribose Polymer (PARP) in DNA Repair

Poly (ADP-ribose) polymerase (PARP) is an enzyme that transfers poly (ADP-ribose) (PAR) chain to various acceptor proteins such as histone, DNA repair proteins and PARP itself. This process plays a critical role in DNA repair (34, 35). PARP1 is responsible for approximately 90% of the ADP-ribosyl transferase activity [poly (ADP-

ribose)ylation (PARylation)] in cells (36). When cells are exposed to alkylating agents, ionizing radiation or free radicals, PARP detects and rapidly binds to DNA strand breaks and catalyzes PARylation mainly of itself using NAD^+ as substrate (34). Upon the formation of long, branched polymers, PARP is released from DNA, and then the polymers are degraded by the PARG enzyme, allowing the access of the DNA repair machinery to the lesion sites (34).

PARP1 has a key role in BER, SSBs, and DSBs repair. In addition, PARP1 has been implicated in HR at stalled or collapsed replication forks, as well as regulating nonhomologous end-joining (NHEJ) repair (35). In response to DNA damage, PARP1 enzymatic function is activate and correlated with the extent of the damage (37). When DNA breaks are repairable, PARP1 activates the repair and cell cycle machineries; while in response to catastrophic damage, PARP1 induces cell death. For example, PARP1 binds to a DNA SSBs and catalyses the formation of PAR polymers on itself and other acceptor proteins. PAR formation is suggested to be important to protect DNA breaks, alter chromatin structure and to attract DNA repair proteins to the site of damage (38). Therefore, inhibition of PARP1 results in inactivation of the DNA repair machinery and causes more SSBs, which may subsequently induce the formation of DSBs.

1.5 Mechanism of Action of PARP Inhibitors (PARPi)

The structure of PARPi includes a nicotinamide moiety that competes with NAD^+. They are highly efficacious PARP catalytic inhibitors with IC_{50} values reaching the low nanomolar range (39). PARPi that compete with NAD^+ at the enzyme's activity site can be used in BRCA-deficient cells as single treatment acting through the principle of synthetic lethality exploiting these deficient DNA DSBs repair in these cells (40, 41).

In addition to catalytic inhibition, recent studies suggested that selective PARPi induce cytotoxicity by trapping PARP-DNA complexes (42, 43). PARP can't dissociate from the DNA and prevent DNA replication and transcription, leading to cell death.

1.6 Current Development of PARPi in Clinical Trial

Several PARPi including olaparib (AZD-2281), veliparib (ABT-888), rucaparib (AG-014699; CO-338), niraparib (MK4827), and talazoparib (BMN673) are currently using in clinical trials as single agent or combined with chemo-drugs. Among them, olaparib is the most-investigated one in cancer treatment. Olaparib (Lynparza®) is the first PARP inhibitor, which was approved as monotherapy to treat ovarian, fallopian tube, and primary peritoneal cancer in women carrying BRCA1 or BRCA2 mutations by U.S. FDA on December 19, 2014. Recently, olaparib has been evaluated as adjuvant therapy in patients with TNBC. A phase I trial that recruited total 60 TNBC patients, of whom 22 were carriers with a germline mutation of BRCA1 or BRCA2. Eight patients received 400 mg of olaparib twice daily and only one of them had reversible dose-limiting toxicity This result suggested the safety dose of olaparib (44).

More than 127 US National Cancer Institute (NCI)-registered clinical trials have been launched to evaluate a range of compounds in combination with PARPi (45). In addition to BRCA1/2 mutations, DNA repair gene deficiency, mutation of transcription regulation gene and cell cycle control dysregulation are proposed as biomarkers of cancer sensitivity to PARPi alone or in combination with cytotoxic drugs in clinical trials (46, 47). For example, in a phase I study in patients with refractory multiple myeloma (MM), the combination of PARPi, veliparib, and proteasome inhibitor, bortezomib, seemed to be

well tolerated, with strong evidence of considerable antitumor activity (ClinicalTrials.gov Identifier: NCT01495351). In another phase I study, olaparib has been combined with alkylating agent dacarbazine for treating patients with advanced solid tumors, and the results showed to be well tolerated (48). In a phase III study, the combination of gemcitabine and carboplatin with PARPi iniparib was associated with potential benefits in overall response rate (ORR) in TNBC patients treated with this regimen (49). It is worthy to note that not all patients with BRCA mutation response to PARPi in clinical trials, suggesting other mechanisms that can compensate for BRCA deficiency.

1.7 Resistance to PARP Inhibitors in Cancer Therapy

Growing numbers of studies are being conducted to explain the molecular mechanisms underlying intrinsic and acquired resistance to PARPi. Such mechanisms, for example, include secondary BRCA mutations that regain BRCA function, and enhance P-glycoprotein-mediated drug efflux (50). Inhibition of NHEJ core proteins, such as loss of 53BP1 protein, has been shown to contribute to the development of PARPi resistance by restoring HR activity (51), and deficiency in other crucial NHEJ players, Ku70/80 and DNA-PK, contributes to PARPi resistance in BRCA1-deficient cells (52). Recently, HOXA9 has been shown to contribute to PARPi resistance of MML though upregulation of HR genes (53). These important studies provide certain mechanisms to explain resistance to PARPi. However, to make PARPi effective, it is still a critical challenge to identify mechanisms that could provide biomarkers to stratify patients who will respond to PARPi treatment as well as effective rational combinational therapy for those who will not respond to PARPi.

1.8 Post-Translational Modifications (PTMs) and Regulation of PARP1

Post-translational modifications (PTMs) are enzymatic modification of proteins to indicate the protein functions and to regulate the signaling networks (54). The PTMs occur on the amino acid side chains or at the C- or N-terminal of proteins including glycosylation, phosphorylation, acetylation, methylation, ubiquitination, nitrosylation, lipidation and proteolysis. These modifications affect almost every aspect of cell function (54).

The PTMs of PARP1 have been discovered in the past few years. Most of the studies focused on how PARP1 is covalently modified and how PTMs could regulate the activity and function of PARP1. Those modifications include ADP-ribosylation, phosphorylation, acetylation, methylation, ubiquitylation and SUMOylation (55). Take phosphorylation as an example, a broad proteomic screen has identified a variety of phosphorylation sites on PARP1 (56). These phosphorylation sites have been investigated in more details in functional studies. PARP1 is phosphorylated at Ser 372 and Thr 373 by ERK1/2, and these modifications are required for PARP1 activation after DNA damage (57). PARP1 can also be phosphorylated by JNK1 at undetermined sites, which sustained PARP1 activation during H_2O_2-induced non-apoptotic cell death (58). However, phosphorylation of PARP1 does not always promote an increase in PARP1 activity (59, 60). It has been shown that protein kinase C (PKC)-mediated PARP1 phosphorylation results in decreased PARP1 DNA-binding and catalytic activity. Therefore, more studies are needed to fully understand the role of other kinases on PARP1 (59).

1.9 Overview of c-Met Kinase

Receptor tyrosine kinases (RTKs) regulate many cellular processes in mammalian development, cell function and tissue homeostasis. c-Met (MET or hepatocyte growth factor receptor (HGFR)) is one of RTKs that has been implicated to play important biological roles in mammalian cells (61). c-Met is formed by proteolytic processing of a common precursor in the post-Golgi compartment into a single-pass, disulphide-linked α/β heterodimer (62). The functional structures and domains of c-Met includes the sema domain, PSI (found in plexins, semaphorins and integrins) domain, four IPT (immunoglobulin, plexin, transcription) repeats, transmembrane (TM) domain, juxtamembrane (JM) domain and tyrosine kinase (TK) domain (62).

The ligand for c-Met is hepatocyte growth Factor (HGF), which also known as scatter factor (63). HGF can serve as a pleiotropic factor and cytokine that promotes cell proliferation, survival, motility, scattering, differentiation and morphogenesis (64). HGF is highly related to members of the plasminogen serine protease family and secreted by fibroblasts and smooth muscle cells (65). The high-affinity c-Met binding domain of HGF is in the N-terminal portion of α chain, while the β chain is important for interaction with c-Met (66). Binding of HGF leads to c-Met receptor dimerization and autophosphorylation of multiple tyrosine residues. For example, HGF induces phosphorylation of Y1230, Y1234 and Y1235 located within the catalytic loop of the tyrosine kinase domain, thus activate the intrinsic kinase activity of c-Met (67). On the other hand, binding of HGF may also phosphorylate Y1003 in the JM domain and recruit c-Cbl E3 ubiquitin ligase to monoubiquitinate c-Met, leading to the internalization and degradation by proteasome (68). Therefore, the tyrosine phosphorylation sites play

important roles in the regulation and activation of c-Met signaling.

However, dysregulation of c-Met has been found in various of human cancers, such as lung cancer, mesothelioma, colorectal cancer, head and neck cancer, esophageal cancer, gastric cancer, pancreatic cancer, sarcomas, thyroid cancer, ovarian cancer, breast cancer, cervical cancer, brain tumors, and especially hereditary papillary renal cell carcinomas (61, 66, 69). Studies have shown that c-Met can be overexpressed, mutated or amplified in cancer cells and leads to tumor progression, epithelial mesenchymal transition (EMT) and tumor metastasis (70). Therefore, targeting c-Met is an attractive strategy for cancer therapy.

1.10 Current Development of c-Met Inhibitors

Many c-Met kinase inhibitors are currently used in clinical trials such as tivantinib, savolitinib, crizotinib, foretinib, cabozantinib and etc. Among them, crizotinib and cabozantinib were the first two small molecule inhibitors to be approved by U.S. FDA (71). Crizotinib is known to target multiple kinases including anaplastic lymphoma kinase (ALK), c-Met, ROS1 and RON receptors and it is approved to use in ALK-rearranged advance non-small cell lung cancer (NSCLC) (72, 73). There are 100 US NCI-registered clinical trials have been launched to evaluate the therapeutic efficacy of crizotinib as a single drug or in combination with other compounds in various types of cancer. Currently, one phase I study of the combination of crizotinib and sunitinib is designed to test the safety and tolerability with metastatic breast cancer (ClinicalTrials.gov Identifier: NCT02074878). In addition, increasing evidence showed that c-Met is involved in resistance to many targeted therapies including EGFR inhibitors,

VEGFR inhibitors, anti-HER2 and BRAF inhibitors (74-78). For example, it has been reported that c-Met signaling can compensate for EGFR inhibition by tyrosine kinase inhibitor, erlotinib, in lung cancer (74). The combined inhibition of c-Met and EGFR can overcome the resistance. Several combination treatments of c-Met inhibitors and EGFR inhibitors have been tested in clinical trials. Moreover, the combination of VEGF inhibitor (axtinib) and c-Met inhibitor (crizotinib) increased the antitumor efficacy in RCC mice model (79). These data suggest that c-Met might be a potential target to inhibit both molecular driver and resistance regulator.

1.11 Overview of Casein Kinase 2 (CK2)

Casein Kinase 2 (CK2) is a constitutively active serine/threonine kinase and is highly conserved in eukaryotic cells (80, 81). CK2 is a tetramer of two alpha (α and α') subunits and two beta (β) subunits. Depending on different cell types, the catalytic subunits are linked via the regulatory subunits to form either the heterotetramer or homotetramer such as α2β2, αα'β2, or α'2β2 (82). However, the subunits can also exist and function individually in cells. The alpha subunits contain the catalytic kinase domain of CK2. The β subunits mediate the autophosphorylation of CK2 protein, and that is important to assemble and stable the holoenzyme. Furthermore, β subunits regulate the recruitment of distinct substrates, thus regulating the selectivity of substrate by enzyme (83). CK2 has many substrates, therefore it can regulates multiple cell functions including cell proliferation, cell differentiation, cell cycle, DNA repair, and regulation of circadian rhythm (81, 84, 85)

CK2 has been found to be overexpressed in many cancers such as ovarian and

breast cancer (86). Studies have shown that increased expression and activity of CK2 are associated with human cancers, while overexpression of CK2 in transgenic mouse models result in tumor growth (87, 88). It has been reported that CK2 phosphorylated and regulated the activity and stability of various tumor suppressor proteins such as PML, p53, and PTEN, as well as oncogenes and transcriptional activators such as c-Myc, c-Myb, c-Jun, NFkB, and β-catenin (86). Recent studies have demonstrated that CK2 could act as suppressor of apoptosis through phosphorylation of pro-apoptotic proteins, which protected them from caspase-mediated cleavage (89). Studies also showed that inhibition of CK2 sensitized tumor cells to TNF-related apoptosis-inducing ligand (TRAIL) receptor-mediated apoptosis, ionizing radiation and chemotherapeutic agents (90). In addition, several recent studies reported that CK2 could also regulate epithelial-to-mesenchymal transition (EMT), which is an early step in cancer invasion and metastasis (91).

1.12 CK2 in Cancer

It has been reported that the activity of CK2 and protein expression levels can influence the acquisition and maintenance of the emerging cancer hallmarks in several different ways that originally described by Hanahan and Weinberg (92). CK2 can regulate the expression of various proteins essential for proliferation, evading growth suppressors, avoiding immune destruction, enabling replicative immortality, tumor-promoting inflammation, invasion, metastasis, angiogenesis, regulating genome instability, resisting cell death and deregulating cellular energetics (93). These are all highly relevant to cancer progression.

Take breast cancer as an example, it has been found that overexpression of CK2α in the mammary gland of transgenic mice could promote hyperplasia and neoplasia, suggesting CK2 contributed to the development of breast cancer (94). In addition, the upregulation of CK2 activity was observed during the development of 7, 12-Dimethylbenz[a]anthracene (*DMBA*)-induced mammary tumors *in vivo* (88). In mouse models, CK2 cooperatively promotes tumor formation and progression with overexpression of oncogenes such as c-myc or with loss of tumor suppressor genes such as p53 (95, 96). Moreover, CK2 activity is higher in human breast cancer tissues compared to normal ones, indicating the pathologic relationship between CK2 and breast cancer tumorigenesis (88). Clinical breast tumor samples displayed positive correlation between CK2 and several EMT markers such as snail (91). Furthermore, at the mRNA level, both CK2α and CK2β are elevated and associated with a poor survival prognosis and metastasis in patients with all breast cancer subtypes (97). These results indicate that CK2 may play an important role in cellular transformation and tumorigenesis. Thus, targeting CK2 may serve as an effective strategy for cancer therapy. Therefore, CK2 inhibitors have been suggested as promising drugs for cancer treatment. CX-4945 is a CK2 inhibitor, which is currently under some clinical trials in patients with various advanced tumors (45).

1.13 The Role of CK2 in DNA Damage and Repair

CK2 has recently gained interest in the field of cancer research as both a regulator of survival pathways and a modulator of the DNA-repair machinery. CK2 was shown to

regulate the function of several enzymes of the DNA-repair and DNA-damage sensing machinery, such as XRCC1 and XRCC4, Rad9 and DNA-PK.

The X-ray repair cross-complementing group 1 (XRCC1) is a member of a family of XRCC proteins (98). XRCC1 can directly bind to DNA SSBs, which play important roles in DNA repair. XRCC1 interacts with PARP and DNA ligase to participate in BER and HR (99). CK2 has been shown to phosphorylate XRCC1 and thereby enable the assembly and activity of DNA SSBs repair at sites of chromosome breakage (100). CK2 can also phosphorylate XRCC4, which is known to be one of the proteins involved in non-homologous end joining (NHEJ) pathway to repair DNA DSBs (101). Furthermore, phosphorylation of XRCC4 is necessary for its interaction with PNK. This interaction is important for DNA DSBs repair. Together, these results demonstrate that CK2 regulates not only SSBs repair but also DSBs repair.

1.14 Current Development of CK2 Inhibitors

CX-4945 is a selective CK2 ATP-competitive inhibitor, initially discovered by Cylene Pharmaceuticals Incorporation (102). CX-4945 can cause cell cytotoxicity and apoptosis and some clinical trials are currently performed in different cancer types to evaluate the effectiveness of the drug. For example, in hematological tumors, CX-4945 shows anti-proliferation effects by suppressing CK2 expression and inhibiting activation of PI3K/Akt/mTOR signaling pathway, which is mediated by CK2 (103). Moreover, combined CX-4945 with other inhibitors such as PI3K inhibitors had synergistic effects (104). Therefore, CX-4945 is a potential therapeutic target for combinational treatment in human cancers.

Currently, CX-4945 is investigated in Phase I and II clinical trials in multiple human cancers. For example, the phase I study of oral CX-4945 is evaluated the safety, tolerability and highest safe dose levels of this CK2 inhibitor in patients with advanced solid tumor cancers, Castleman's Disease or multiple myeloma (ClinicalTrials.gov Identifier: NCT00891280). Another phase 1 study is designed to test the dose, safety, pharmacokinetics, and Pharmacodynamics of CX-4945 in patients with relapsed or refractory multiple myeloma (ClinicalTrials.gov Identifier: NCT01199718). The subsequent Phase I/II trial is a randomized study of antitumor activity in cholangiocarcinoma patients, comparing the standard-of-care protocol of gemcitabine plus cisplatin against treatment with CX-4945 in combination with gemcitabine plus cisplatin at the combination maximum tolerated dose (MTD) (ClinicalTrials.gov Identifier: NCT02128282).

1.15 Rationale and Hypothesis

TNBC is an aggressive subtype of breast cancer that initially responds to chemotherapy, but a majority of patients eventually develop resistance. Currently, PARPi are widely evaluated in clinical trials because TNBC has similar properties with BRCA-mutated cancers. However, some BRCA-mutated tumors are reported to be resistant to PARPi, suggesting mechanisms that can compensate for BRCA deficiency. Thus, it is critical to develop strategies to increase the effectiveness of PARPi treatment and to identify biomarkers with which to stratify TNBC patients for better therapy. PTM is important to the function of PARP1 and phosphorylation signaling is relatively easy to be targeted. Therefore, we hypothesized that PARP1 protein is regulated by its

phosphorylation. Thus, the phosphorylation status of PARP1 and the expression of the kinases that phosphorylate PARP1 may serve as appropriate biomarkers for combinational treatments. In this study, we utilized antibody array, database analysis and *in vitro* functional characterization to identify potential regulators for PARPi resistance. The long-term goal of this study is to develop the marker-guided combinational treatment of PARPi for TNBC.

CHAPTER 2

MATERIALS AND METHODS

Part of this chapter is taken verbatim by permission from the Nature publishing group: Yi Du, Hirohito Yamaguchi, Yongkun Wei, Jennifer L Hsu, Hung-Ling Wang, Yi-Hsin Hsu, Wan-Chi Lin, Wen-Hsuan Yu, Leonard, Gilbert R Lee IV, Mei-Kuang Chen, Katsuya Nakai, Ming-Chuan Hsu, Chun-Te Chen, Ye Sun, Yun Wu, Wei-Chao Chang, Wen-Chien Huang, Chien-Liang Liu, Yuan-Ching Chang, Chung-Hsuan Chen, Morag Park**,** Philip Jones, Gabriel N Hortobagyi & Mien-Chie Hung. Blocking c-Met mediated PARP1 phosphorylation enhances anti-tumor effects of PARP inhibitors. Nature Medicine, 2016, 22(2), 194-201(105)

2.1 Cell Culture

All cells were obtained from American Type Culture Collection (ATCC). Cells were cultured in Dulbecco's Modified Eagle's Medium cells (DMEM) or in RPMI 1640 and maintained at 37 °C in 5% CO_2. All mediums were supplemented with 10% FBS.

2.2 Transfection, Plasmids and RNAi

Plasmid DNA transfection was conducted by Lipofectamin 2000 (Thermo Fisher Scientific) according to the manufacture's instruction. The plasmid of Myc-CK2β (Addgene plasmid, #27091) was obtained from Addgene. The plasmids that express HA-PARP1, V5-PARP1 and Flag-c-Met were constructed on pCDH-CMV-MCS-EF1-Puromycin vector (#CD510B-1; System Biosciences). For stable knockdown of c-Met or PARP1 and c-Met or PARP1 overexpression studies, breast cancer cells were transfected with pGIPZ shRNA (control) vector (Thermo Fisher Scientific, Rockford, IL) or pLKOshRNA vector Sigma-Aldrich (St. Louis, MO) and pCDH-neo vector (System Biosciences, Mountain View, CA). siRNA transfection was conducted with use of Amexa Nucleofactor II (Lonza Group Ltd., Basel, Switzerland) according to the manufacture's instruction. Sequences of shRNA and siRNA are listed in Table 2.1.

Table 2.1 Information about shRNA and RNAi

Name	Purpose	Sequence or other information
Met	shRNA	CCATCCAGAATGTCATTCT; GCATTAAAGCAGCGTATC; GCATTAAAGCAGCGTATC*; TGTGTTGTATGGTCAATAA; CCTTCAGAAGGTTGCTGAGTA;
PARP1	shRNA	TGGAAAGATGTTAAGCATTTA*
CK2α	siRNA	SASI_Hs01_00110178; Clone ID (From Sigma-Aldrich)
CK2α'	siRNA	SASI_Hs01_00087712; Clone ID (From Sigma-Aldrich)

*Targeting the 3′-UTR.

2.3 Chemicals and Inhibitors

Hydrogen peroxide (#216763), and sodium arsenite solution (#35000) were obtained from Sigma-Aldrich (St. Louis, MO). PARP inhibitors ABT-888 (Veliparib, #CT-A888) and AG-014699 (Rucaparib, #CT-AG01) were from ChemieTek (Indianapolis, IN); AZD-2281 (Olaparib, #S1060) and BMN-673 (Talazoparib, #S7048) were from Selleck Chemicals (Houston, TX). c-Met kinase inhibitors crizotinib (#C-7900) and foretinib (#F-4185) were from LC Laboratories (Woburn, MA). CK2 kinase inhibitor CX-4945 (Silmitasertib, #200843) was from MedKoo (Chaple Hill, NC). CDK2 inhibitor SNS-032 (BMS-387032, #S1145) and PKC inhibitor sotrastaurin (#S2791) were from Selleck Chemicals (Houston, TX).

2.4 Immunoprecipitation, Immunoblotting and Antibodies

For immunoprecipitation assay, cell lysates were obtained with modified RIPA buffer (25mM Tris-HCl pH7.6, 150mM NaCl, 1% NP40, 1mM DTT). Protein complexes were pulled down from antibody/lysate (1 mg, overnight incubation at 4 °C) by protein A/G beads. Protein complexes were then washed 5 times and subsequently released by SDS-loading buffer. The immunoblot assay was conducted following standard procedures. All primary antibodies were used according to the manufactory datasheet. The mouse phospho-Y907-PARP1 antibody was generated against a phosphorylated synthetic peptide (ADMVSKSAN-Yp-CHTSQGD) at China Medical University, Center of Molecular Medicine. Detailed information about all of the antibodies is listed in the Table 2.2.

Table 2.2 Antibodies List Used in this Study

Protein	Company	Purpose	Catalog number
Tubulin	Sigma-Aldrich	WB	T5168
Flag	Sigma-Aldrich	WB, IP	F3165
Actin	Sigma-Aldrich	WB	A2066
γ-H2AX	EMD Millipore	WB, IF	05-636
GST	Santa Cruz	WB	sc-53909
HA	Santa Cruz	WB, IP	sc-805
V5	ThermoFisher	WB, IP	MA5-15253
Myc	Roche	WB, IP	11667203001
c-Met	Cell Signaling	WB, IP, IF	8198
Phosphor-Met (Tyr1234/1235)	Cell Signaling	WB	3077
CK2α	Cell Signaling	WB, IP	2656
PARP1	Cell Signaling	WB, IP, IF	9532
PARP1	BD Pharmingen	IF	556362
PARP1	Santa Cruz	WB	sc-7150
CK2α prime	Abcam	WB	Ab10474
CK2β	Abcam	WB	Ab133576
CK2β	Bethyl Lab	IP, IF	A301-984A
PAR	Trevigen	WB	4335

2.5 ROS Detection

The assay was performed as previously described (105). Cells were seeded in the 12- or 96- well plates. After overnight growth, cells were incubated with 10 μM 2′,7′-dichlorofluorescindiacetate (DCFDA) in PBS for 30mins. Cells were washed and the media replaced with PBS. 2′,7′-dichlorofluorescein (DCF) was measured under a Zeiss microscope with spectra of 495 nm excitation/529 nm emission. Fluorescence intensity was measured by AxioVision software. The mean ± s.d. of DCF intensity from five images in each cell line was calculated.

2.6 Hierarchical Clustering and Display

The assay was performed as previously described (105). Clustering of any set of PARP1-associated kinase genes expression with TNBC signature genes (*ERBB2*, *ESR1*, and *PGR*) from The Cancer Genome Atlas database was analyzed with the Cluster and TreeView program (106). Briefly, for any set of PARP1-associated kinases, an upper-diagonal similarity matrix was computed by using average-linkage clustering. This algorithm was determined by computing a dendrogram. The heat map was represented graphically by coloring each cell on the basis of the measured fluorescence ratio. Log ratios of 0 (a ratio of 1.0 indicates that the genes are unchanged) were colored in black, positive log ratios were colored in red, and negative log ratios were colored in green.

2.7 Confocal Microscopy Analysis of γ-H2AX Foci

The assay was performed as previously described (105). Cells grown on chamber slides (Labtek, Scotts Valley, CA) were treated as described in the text. After washing

with ice-cold PBS, cells were fixed, permeabilized, and incubated with γ-H2AX antibodies and fluorescence-labeled secondary antibodies. Immunostained cells were examined by Zeiss LSM 710 laser-scanning microscope (Carl Zeiss, Thornwood, NY) with a 63X/1.4 objective. The ZEN and AxioVison (Carl Zeiss) software programs (NIH, Bethesda, MD) were used for data analysis.

2.8 Comet Assay

Comet assay was performed following procedure described previously with some modifications (107). Briefly, cells were sandwiched in agarose and subjected to electrophoresis in either alkaline electrophoresis buffer (0.3 N NaOH, 1 mM EDTA) or neutral electrophoresis buffer (0.3M Sodium acetate and 0.1M Tris-Cl, adjusted to pH 8.3). To prepare gel sandwich, basal layer was made by applying 1.2% agarose in PBS to frosted microscope slide. Second layer is made of mixing equal amount of cell suspensions (10^6 cells/ml in PBS) with 1.2% low gelling temperature agarose. Third layer is made of 1.2 % low gelling temperature agarose. After gel sandwich solidified, the slides were immersed in ice-cold lysis buffer (2.5 M NaCl, 100 mM EDTA, 10 mM Tris-Cl (pH 10), 1 % N-laurylsarcosine, 0.5 % Triton and 10 % DMSO) and stored at 4˚C for at least 2 hours. For alkaline comet assay, slides were immersed in alkaline electrophoresis buffer for 20 mins at 4˚C before electrophoresis at 20 V, 0.3 A for 25 mins. While for neutral comet assay, slides were immersed in neutral electrophoresis buffer for 1 hour at 4˚C before electrophoresis at 14 V, 0.01 A for 1 hour. After electrophoresis, slides were stored in 0.4 M Tris-Cl (pH 7.5) before staining DNA with propidium iodide. The slides were subjected to examination with fluorescence microscope and image of at least 50 cells per treatment was recorded and the migration of

DNA was quantified by CometScore (TriTek Corp.) by the parameter of percentage of DNA in tail (%T).

2.9 Duolink Assay

Cells were prepared for fluorescence microscopy analysis. Primary antibodies were incubated with cells and a pair of oligonucleotide-labeled antibodies (PLA probes). Ligation and amplification were done according to the manufacturer's instructions (Duolink Assay Kit, Sigma-Aldrich) before mounting the slide for measurement under confocal microscope. The mean ± s.d. of PLA signal intensity from 50 cells in each treatment group was calculated.

2.10 MTT Assay

Cells were seeded at 1,500 cells/well in a 96-well plate overnight, then treated with indicated inhibitors at various concentrations for 72 hours. Then cells were incubated in 100 μL of sterile MTT (0.5 mg/mL; Sigma) for 2 hours at 37°C, followed by removal of the culture medium and addition of 100 μL of dimethyl sulfoxide. Absorbance was measured by fluorescent plate readers at spectra of 560 nm excitation/590 nm emission. Survival curves were expressed as mean ± s.d. relative to DMSO-treated control from three independent experiments.

2.11 Clonogenic Cell Survival Assay

Cells were plated into 6- or 12-well plates for overnight incubation, and then cells were treated with indicated inhibitors followed by 8 days of incubation. The colonies

were fixed and stained with 0.5% crystal violet, washed, dried and imaged. The number of colonies were quantified by ImageJ.

2.12 Dual-Drug Combination Assay

Cell growth of different treatment as indicated in text was measured by MTT assay or clonogenic cell survival assay. Synergistic effects of multiple drugs were determined by Chou and Talalay method to calculate the combination index (CI) using the software Calcusyn (108). CI values of <1, 1, and >1 indicate synergistic, additive, and antagonistic effects, respectively.

2.13 *In Vitro* Kinase Assay

For c-Met and PARP1 study, recombinant glutathione *S*-transferase (GST)-WT PARP1 (Ala374-Trp1014 of human PARP1) and mutants (GST-Y907F and GST-Y986E) were expressed by induction of isopropyl β-D-1-thiogalactopyranoside (IPTG) and purified with glutathione agarose beads. After cold-PBS washing three times, beads were suspended with 500 µl 1X kinase buffer, with 50 µl saved for western blotting with GST. The beads were spun down and 100 µM ATP, 0.5 µg human recombinant active c-Met protein and 50 µCi [γ-^{32P}]-ATP were added in 50 µl kinase buffer at 30 °C for 15–30 min. For CK2 and PARP1 study, recombinant His-PARP1 (Sino Biological, #11040-H08B-20) and His-CK2α (Life Technologies, #PV3248) were incubated in 1X kinase buffer with 100 µM ATP and 50 µCi [γ-^{32P}]-ATP at 30 °C for 30 min. The kinase reaction was stopped by heating at 100 °C for 10 min in SDS loading dye. All samples were subjected to two identical SDS-PAGE assays. One was used for coomassie blue staining of total

proteins. The second gel was dried and used to detect phosphorylation of substrate by autoradiography.

2.14 Cell Cycle Analysis

Determination of cell cycle distribution was performed by BD FACS Canto II (BD Biosciences) and analyzed by FlowJo. Cells were treated with DMSO or indicated doses of inhibitos for 72 hours, cells were collected, washed with PBS, and fixed with 75% ethanol for at least overnight at -20 °C. Fixed cells were collected by centrifugation and washed with PBS to discard ethanol. Cells were resuspended in 500 µl PBS containing 400 µg/ml propidium iodide (PI) and 0.2 mg/ml RNAase and incubated in 37°C for 15 min. The stained cells were stored in 4 °C and detected on flow cytometer within 48 hours.

2.15 Mouse Xenograft Model

All animal procedures were conducted under the approval of the Institutional Animal Care and Use Committee (IACUC) at The University of Texas MD Anderson Cancer Center (protocol number 10-14-07231). MDA-MB 231 (5×10^5), HCC1937 (2×10^6) cells and BT549 (5×10^6) cells were injected into the mammary fat pads of female nude mice (Swiss Nu/Nu) of 6–8 weeks of age (Department of Experimental Radiation Oncology Breeding Core, The University of Texas MD Anderson Cancer Center). When the tumor volume reached ~50 mm^3, mice were treated with vehicle, crizotinib (5 mg/kg, p.o) and foretinib (5 mg/kg, p.o), AG-014699 (5 mg/kg, p.o) and ABT-888 (25 mg/kg, p.o) were administered to mice five times per week as single agents or in combination for

the number of days specified in the figure legends; while AZD-2281 (25 mg/kg, p.o) and CX-4945 (6.25 mg/kg, i.p) were administered to mice daily as single agents or in combination for two weeks. Tumor was measured at the indicated time points, and tumor volume was calculated by the formula length × width^2 × ½. Tumors were not allowed to grow larger than allowed by the animal welfare protocol.

2.16 Statistical Analysis

Each sample was assayed in triplicate in this study. For *in vitro* analysis, each experiment was repeated at least three times. All error bars represent standard deviation (s.d.). Student's *t* test was used to compare two groups of independent samples. Repeated-measures ANOVA analysis was used to evaluate the statistical significance of dose curve response. Correlations were analyzed using the Pearson chi-square test. A *P* value of < 0.05 was considered statistically significant. No statistical methods were used to determine sample size.

CHAPTER 3

RESULTS

Figures 3.1 to 3.5 are obtained and modified by permission from the Nature publishing group: Yi Du, Hirohito Yamaguchi, Yongkun Wei, Jennifer L Hsu, Hung-Ling Wang, Yi-Hsin Hsu, Wan-Chi Lin, Wen-Hsuan Yu, Leonard, Gilbert R Lee IV, Mei-Kuang Chen, Katsuya Nakai, Ming-Chuan Hsu, Chun-Te Chen, Ye Sun, Yun Wu, Wei-Chao Chang, Wen-Chien Huang, Chien-Liang Liu, Yuan-Ching Chang, Chung-Hsuan Chen, Morag Park**,** Philip Jones, Gabriel N Hortobagyi & Mien-Chie Hung. Blocking c-Met–mediated PARP1 phosphorylation enhances anti-tumor effects of PARP inhibitors. Nature Medicine, 2016, 22(2), 194-201(105)

Results

3.1 ROS Levels is Associated with PARP1 Activity in TNBC

3.1.1 TNBCs Showed Higher Oxidative DNA Damage and ROS Levels in TNBCs than Non-TNBCs

Reactive oxygen species (ROS) levels are higher in multiple types of cancer cells compared with normal cells (109), and a high level of ROS scavenger enzymes has been correlated with good prognosis in TNBC (110). ROS is a major resource for inducing oxidative DNA damage. Therefore, first we asked whether oxidative DNA damage and ROS levels were higher in TNBCs compared to non-TNBCs. We examined cellular 8-hydroxydeoxyguanosine (8-OHdG), an oxidative DNA damage marker to determine the DNA damage levels in multiple TNBC cells by immunofluorescence staining (Figure 3.1.1.1). For ROS levels, we detected the ROS marker 2′,7′-dichlorofluorescein (DCF) by fluorescence microscope (Figure 3.1.1.2). After data analysis, we found that 8-OHdG and DCF signals were higher in TNBC cell lines than in non-TNBC cell lines. Together, these results indicate that oxidative DNA damage and ROS levels in TNBC were higher than the ones in non-TNBC.

Figure 3.1.1.1 TNBC Cell Lines Showed Higher Oxidative Damage DNA than Non-TNBC Cell Lines

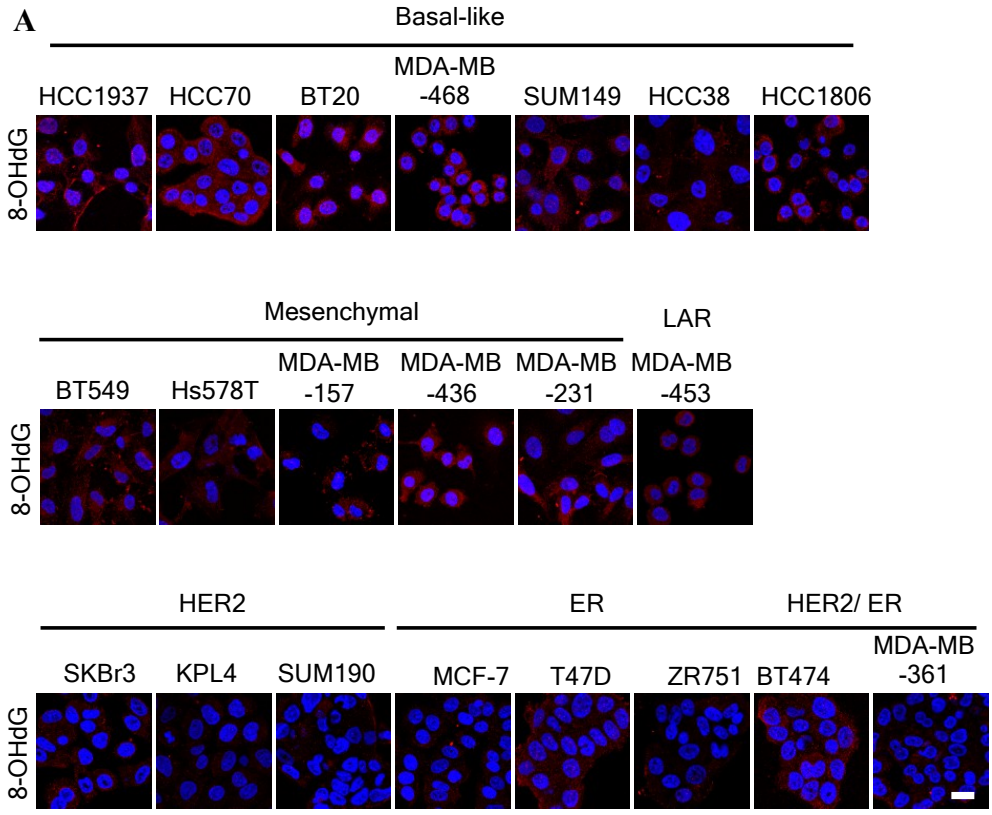

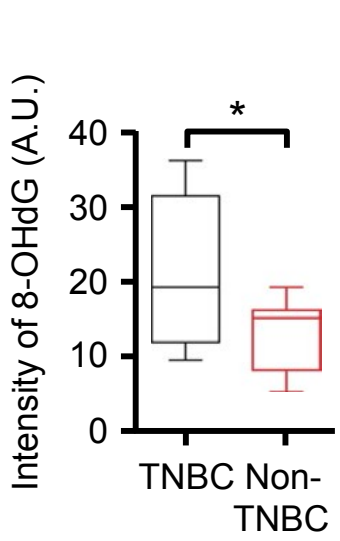

Figure 3.1.1.1 TNBC Cell Lines Showed Higher Oxidative Damage DNA than Non-TNBC Cell Lines

(A) A panel of breast cancer cell lines was stained with 8-OHdG antibody and immunofluorescence signals were detected by fluorescence microscope. Red, 8-OHdG; Blue, DAPI. Bar, 20 μm.

(B) Quantification of the fluorescence intensity signals by AxioVision software was shown.

Experiments in figure 3.1.1.1 were conducted by Yi Du.

Figure 3.1.1.2 TNBC Cell Lines Showed Higher ROS Levels than Non-TNBC Cell Lines

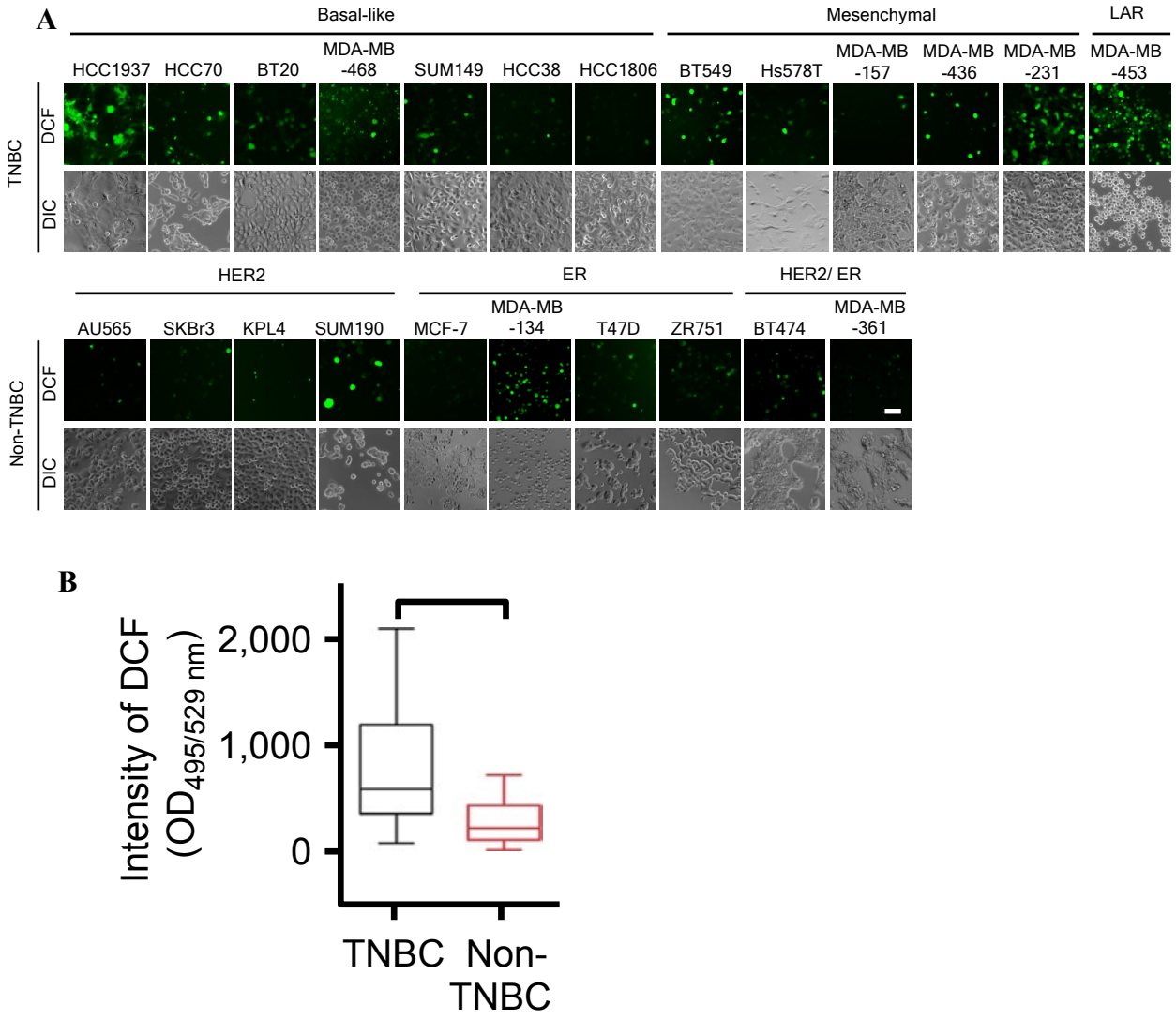

(A) The DCF signals and differential interference contrast (DIC) images of various breast cancer cells. DCF signals (green) were detected by fluorescence microscope. Bar, 100 μm.

(B) Quantification of fluorescence intensity by AxioVision software was shown.

Experiments in figure 3.1.1.2 were conducted by Yi Du.

3.1.2 PARP1 Activity is Higher in TNBCs than Non-TNBCs

PARP1 is the key molecular for ROS-induced DNA damage repair. Our previous data showed that ROS level is higher in TNBC than non-TNBC. Next, we asked whether PARP1 activity was higher in TNBC than non-TNBC cell lines. We determined poly(ADP)-ribose (PAR) levels, which represent cellular PARP activity, by western blot in a panel of TNBC and non-TNBC cell lines. Indeed, PAR expression was higher in TNBC cell lines compared to non-TNBC cell lines (Figure 3.1.2). These data suggest that PARP activity in TNBC is higher than that in non-TNBC. Together with the results from Figure 3.1.1, these data suggest that there may be positive association between ROS and activity of PARP in TNBC.

Figure 3.1.2 PARP1 Activity is Higher in TNBC cell lines than Non-TNBC cell lines

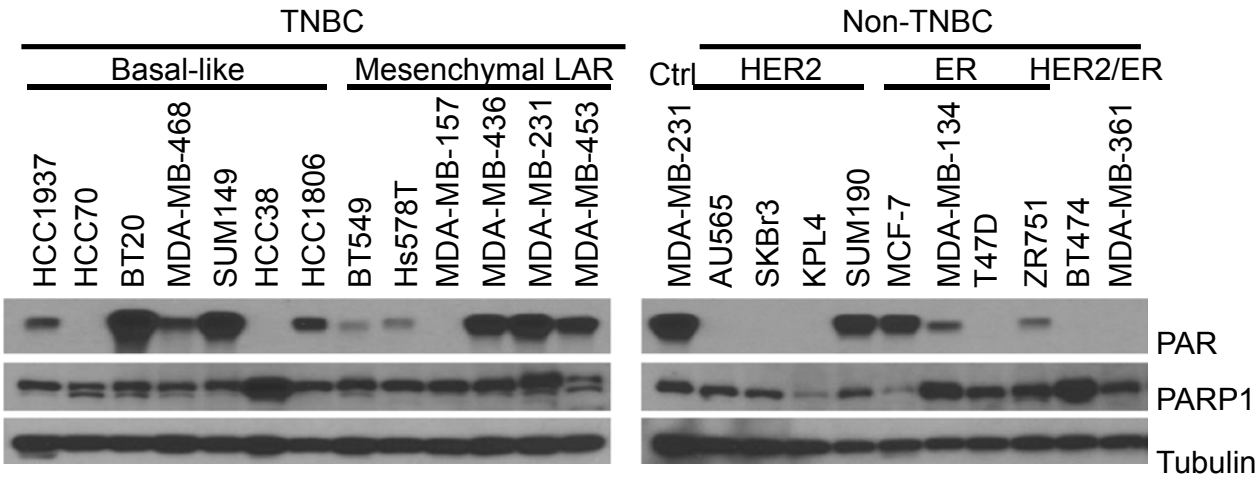

Immunoblot showing the expression of PAR and PARP1 in a panel of breast cancer cells. LAR, luminal androgen receptor. ER, estrogen receptor; HER2, human epidermal growth factor receptor 2.

Experiments in figure 3.1.2 were conducted by Yi Du and Wen-Hsuan Yu.

3.2 ROS Induce the Association of c-Met and PARP1

3.2.1 c-Met Interacts with PARP1 upon ROS Stimulation

Next, we investigated the molecular mechanism regulating PARP activity under ROS-induced DNA damage. We searched for PARP1 interacting proteins, especially tyrosine kinases (TKs) since many of them are druggable targets, which will make the future clinical application easier. Furthermore, it is known that ROS activate receptor tyrosine kinases (RTKs) (111). Therefore, we used phospho-RTK antibody array to screen PARP1 associated TKs in the cells treated with sodium arsenite (As), a ROS inducer (data not shown). Also, we are interested in the target, which overexpressed in TNBC. According to the criteria, we first focused on c-Met, which gave the highest score of PARP1 interaction upon ROS stimulation.

We further verified the association between c-Met and PARP1 by co-immunoprecipitation (Co-IP). MDA-MB 231 and HCC1937 cells, and 293T cells overexpressing c-Met and PARP1 were stimulated with H_2O_2 and subjected to Co-IP (Figure 3.2.1). The data demonstrate that c-Met indeed interacts with PARP1 upon ROS stimulation.

Figure 3.2.1 c-Met Interacts with PARP1 upon ROS Stimulation

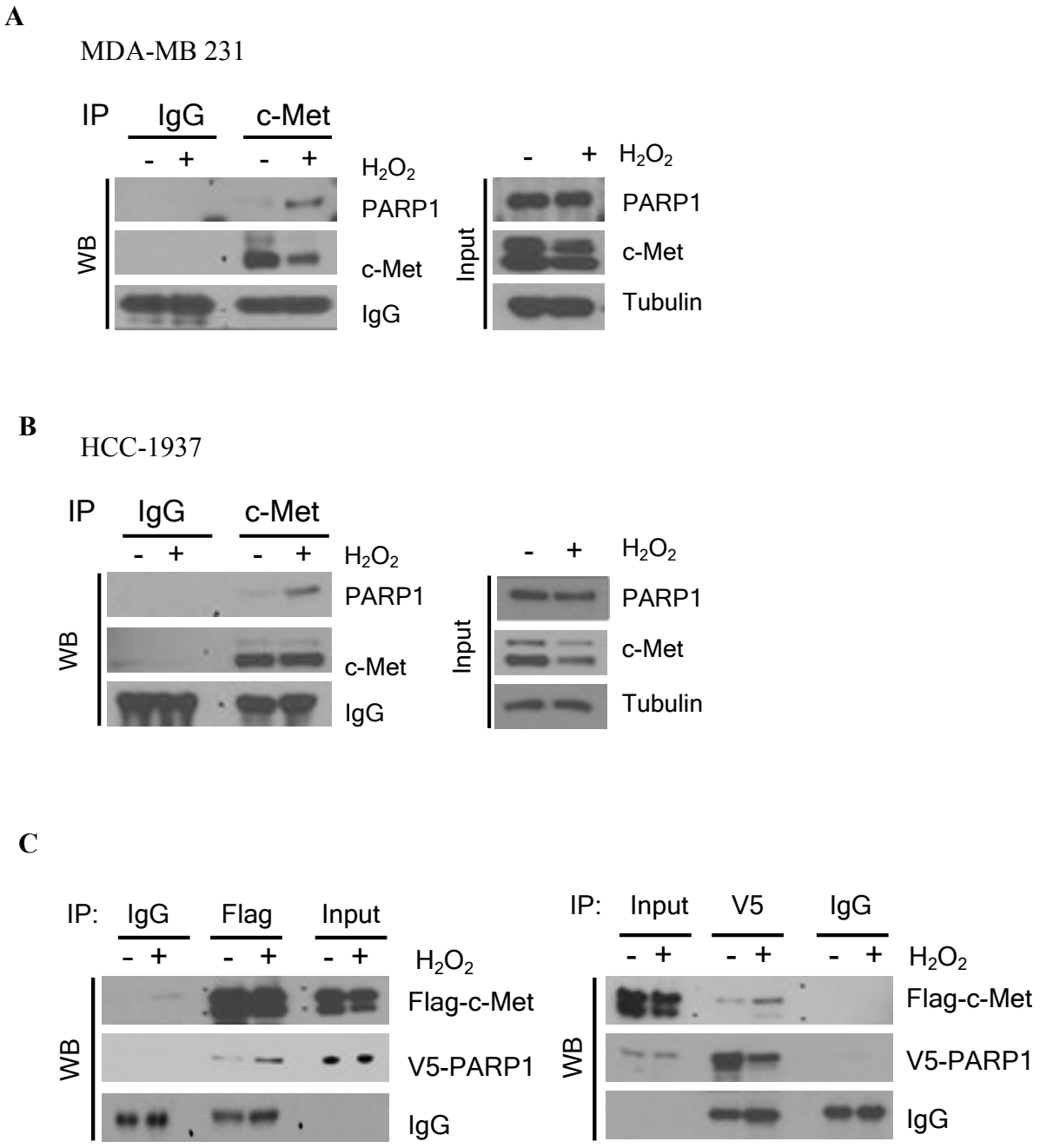

Figure 3.2.1 c-Met Interacts with PARP1 upon ROS Stimulation

(A)(B) MDA-MB 231 cells (A) and HCC 1937 cells (B) were treated with 20 mM H_2O_2 treatment for 30 min and subjected to Co-IP with anti-c-Met antibody, followed by western blot to detect the interaction of PARP1 and c-Met.

(C) HEK 293T cells transfected with V5-PARP1 and Flag-c-Met were treated with 10 mM H_2O_2 for 15 min and subjected to Co-IP with anti-Flag tag or anti-V5 tag antibodies, followed by western blot with the indicated antibodies.

Experiments in figure 3.2.1 were conducted by Yi Du.

3.2.2 The Interaction between c-Met and PARP1 is Mainly in the Nucleus upon ROS Stimulation

c-Met and PARP1 are known to be mainly located in cell surface membrane and the nucleus, respectively. However, it has been reported that c-Met can translocate into the nucleus (112). Therefore, we asked where the interaction between c-Met and PARP1 occurs. To address this question, we performed cell fractionation with Co-IP analysis and Duolink assay. Co-IP using nuclear/cytoplasmic fractions showed that the interaction between c-Met and PARP1 occurred in both the cytoplasmic and nuclear fractions, and that the interaction was enhanced by H_2O_2 treatment in MDA-MB 231 with ectopic expression of HA-tagged PARP1 (Figure 3.2.2 A). Duolink assay further verified the results that c-Met and PARP1 interactions primarily in nucleus (Figure 3.2.2 B). Together, these data suggest that c-Met translocates into the nucleus and interacts with PARP1 upon ROS stimulation.

Figure 3.2.2 The Interaction between c-Met and PARP1 is Mainly in the Nucleus upon ROS Stimulation

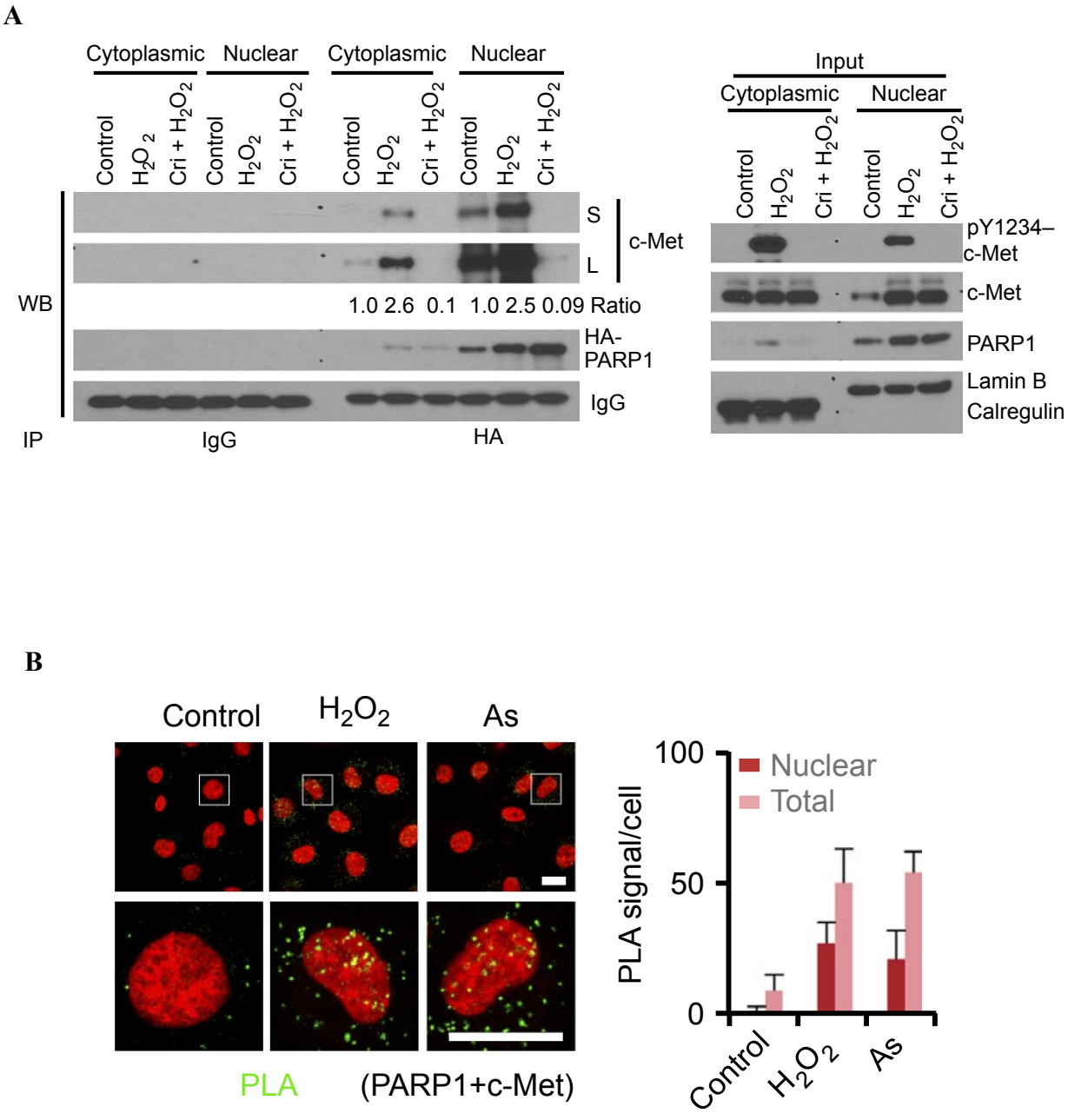

Figure 3.2.2 The Interaction between c-Met and PARP1 is Mainly in the Nucleus upon ROS Stimulation

(A) MDA-MB-231 cells with ectopic expression of HA-tagged PARP1 were treated with 20 mM H_2O_2 for 30 min and with or without a 1-hour pre-treatment with 2 μM crizotinib (Cri). The interaction of PARP1 and c-Met in cytosolic and nuclear fractions by Co-IP/Western blot. S, short exposure. L, long exposure.

(B) Proximity ligation assay to detect co-localization of PARP1 and c-Met in MDA-MB 231 cells treated with 20 mM H_2O_2 or 20 μM sodium arsenite (AS). Quantification of PLA signals from 50 cells was shown in the right panel. Bar, 20 μm.

Experiments in figure 3.2.1 were conducted by Yi Du.

3.3 Inhibition of c-Met Sensitizes TNBC Cells to PARP Inhibitor

3.3.1 Knockdown of c-Met Enhances the Sensitivity to PARP Inhibitor in TNBC Cells

We showed that c-Met could interact with PARP1. Therefore, we hypothesized that c-Met may regulate PARP1 activity and affect tumor the response to PARPi. To test this hypothesis, we knocked down c-Met in MDA-MB 231 by shRNA and treated the cells with different PARPi including olaparib (AZD-2281), rucaparib (AG-014699) and veliparib (ABT-888). We then evaluated the role of c-Met under PARP inhibition by MTT assay (Figure 3.3.1 A) and soft agar assay (Figure 3.3.1 B). The results with different assays showed that knockdown of c-Met sensitized MDA-MB 231 to PARPi in MTT assay and soft agar assays. We also knocked down c-Met in HCC-1937 cells, which have BRCA1 mutation but are resistant to PARPi. These cells also became more sensitive to PARPi after knockdown of c-Met (Data not shown). These data suggest that c-Met contributes to the PARPi resistance in TNBC.

Figure 3.3.1 Knockdown of c-Met Enhances the Sensitivity to PARP Inhibitor in TNBC Cells

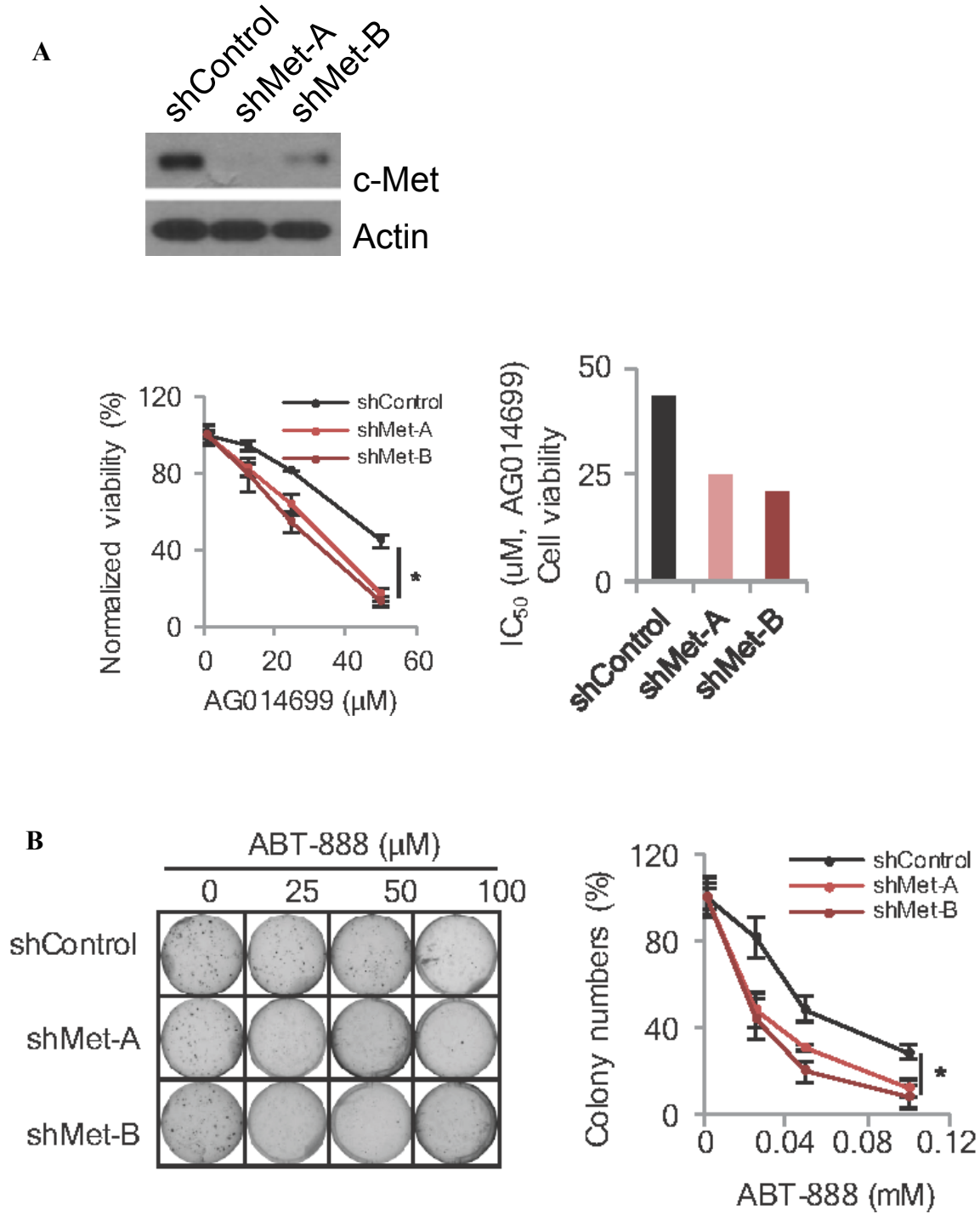

Figure 3.3.1 Knockdown of c-Met Enhances the Sensitivity to PARP Inhibitor in TNBC Cells

(A) Western blot of c-Met showing shRNA efficiency in MDA-MB 231 cells (upper panel). c-Met-knockdown MDA-MB 231 cells were treated with the different concentration of AG-014699, and subjected to MTT assay. IC50 of AG-014699 was shown in the right panel.

(B) c-Met-knockdown MDA-MB 231 cells were treated with ABT-888, and subjected to soft agar colony formation assay. Quantification of colony number was shown in right panel.

Experiments in figure 3.3.1 were conducted by Yi Du, Hirohito Yamaguchi and Wen-Hsuan Yu.

3.4 c-Met Phosphorylates PARP1 at Tyrosine 907 (Y907) and Increases Its Function.

3.4.1 c-Met Phosphorylates PARP1 at Y907

Our previous data demonstrated that c-Met physically associated with PARP1 and also inhibition of c-Met sensitized TNBC to PARPi. Therefore, we hypothesized that c-Met could phosphorylate PARP1 under oxidative stress. We first used software (NetworKIN 2.0) to predict the potential tyrosine residues in PARP1 that is phosphorylated by c-Met. Tyrosine 907 (Y907), which located on the H-Y-E motif in the catalytic domain of PARP1, was predicted as a potential phosphorylation site.

Using recombinant PARP1 proteins with/without the mutation in Y907 (tyrosine to phenylalanine, Y907), we verified Y907 phosphorylation by c-Met by *in vitro* kinase assay (Figure 3.4.1.1). We also raised the specific antibody against p-Y907 of c-Met, and demonstrated that in response to ROS stimulation, PARP1 is phosphorylated (Figure 3.4.1.2 A). Moreover, the phosphorylation of PARP1 at Y907 is abolished in c-Met-knockdown MDA-MB 231 cells (Figure 3.4.1.2 B). Together, these data suggest that c-Met mediates phosphorylation of PARP1 at Y907 *in vivo.*

Figure 3.4.1.1 c-Met Phosphorylates PARP1 at Y907 by *in vitro* Kinase Assay

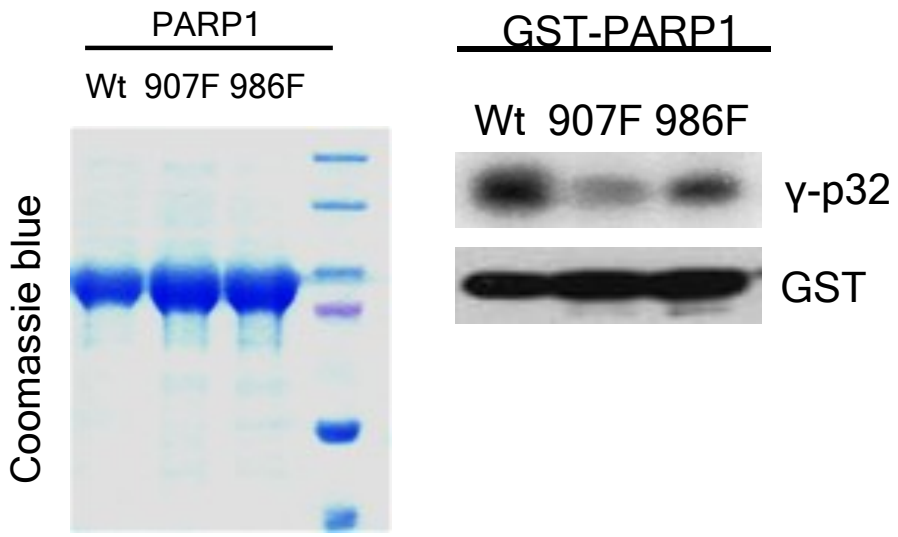

Left panel, coomassie blue staining of GST fusion wild-type PARP1 and PARP1 Y907F and Y986F mutants. Right panel, *In vitro* kinase assay, GST fusion wild-type PARP1 and PARP1 Y907F and Y986F mutants were incubated with purified c-Met in kinase buffer in the presence of [γ-32P]-ATP. Phosphorylated PARP1 was measure by autoradiography.

Experiments in figure 3.4.1 were conducted by Yi Du, Hung-Ling Wang and Wei-Chao Chang.

Figure 3.4.1.2 c-Met Phosphorylates PARP1 at Y907 upon ROS Stimulation

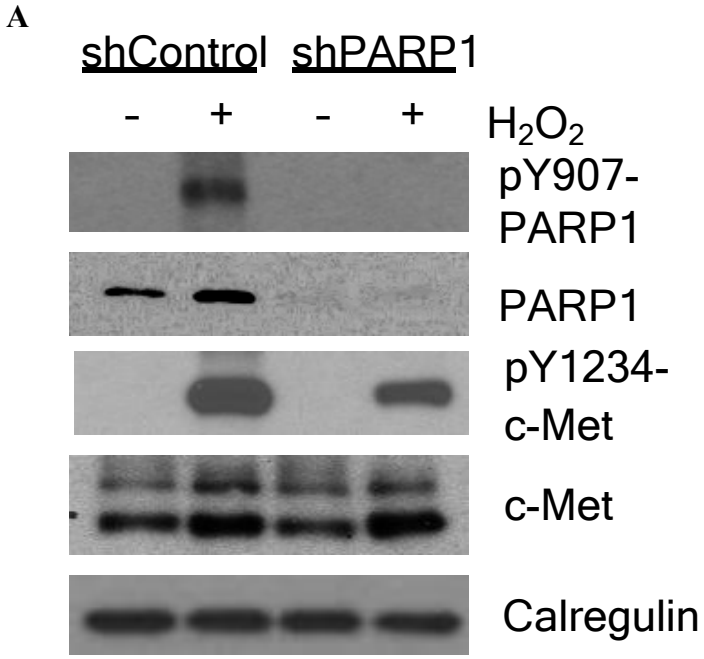

(A) Immunoblot showing the expression of pY907-PARP1. MDA-MB 231 wild type and PARP1-knockdown cells were treated with 20 mM H_2O_2 for 30 min, and subjected to western blot with the indicated antibodies.

B

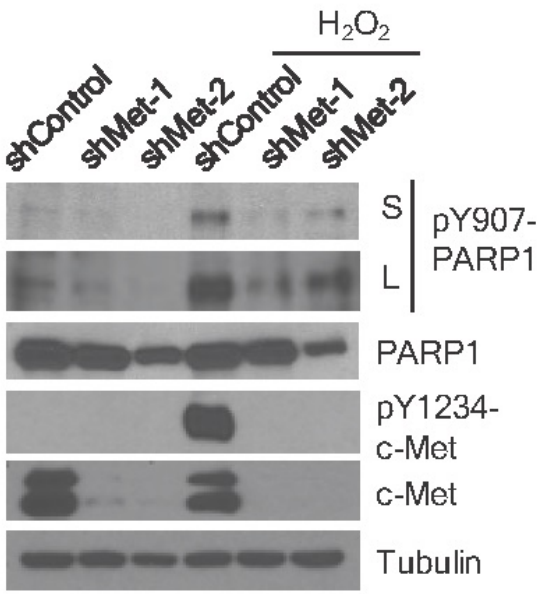

(B) Immunoblot showing the expression of pY907-PARP1. MDA-MB 231 wild type and c-Met-knockdown cells were treated with 20 mM H_2O_2 for 30 min, and subjected to western blot with the indicated antibodies.

Experiments in figure 3.4.1.2 were conducted by Yi Du, Hung-Ling Wang, Wan-Chi Lin and Wen-Hsuan Yu.

3.4.2 Phosphorylation of PARP1 at Y907 Enhances PARP1 Activity

Next, we further investigated whether PARP1 Y907 phosphorylation contributes to PARP function and PARPi resistance. To address this question, we stably re-expressed WT, Y907F (non-phosphorylatable) or Y907E (phosphomimetic)-mutant PARP1 in PARP1-knockdown MDA-MB 231 cells, and used these stable cells for various assay. First, we determined DNA damage repair ability in these stable cell lines by comet assay. The data showed that the cells expressing Y907F PARP1 exhibited more DNA strand breaks than the one expressing wild type PARP1, while the cells with Y907E did lower than the one with wild type (Figure 3.4.2 A). Second, we evaluated PARP activity by measuring the expression of PAR and Y907F PARP1 showed less PARP activity than wild type PARP1, while Y907 did higher than wild type one (Figure 3.4.2 B). Moreover, the cells expressing Y907F PARP1 were more sensitive to PARPi than the cells expressing wild type, while the cells with Y907E PARP1 were more resistant to PARPi than the one with wild type PARP1 by colony formation assay (Figure 3.4.2 C). Together, these findings supported our hypothesis that phosphorylation of PARP1 at Y907 contributes to PARP activity and attenuates the response to PARPi in TNBC.

Figure 3.4.2 Phosphorylation of PARP1 at Y907 Contributes to PARP Function and PARP Inhibitor Resistance

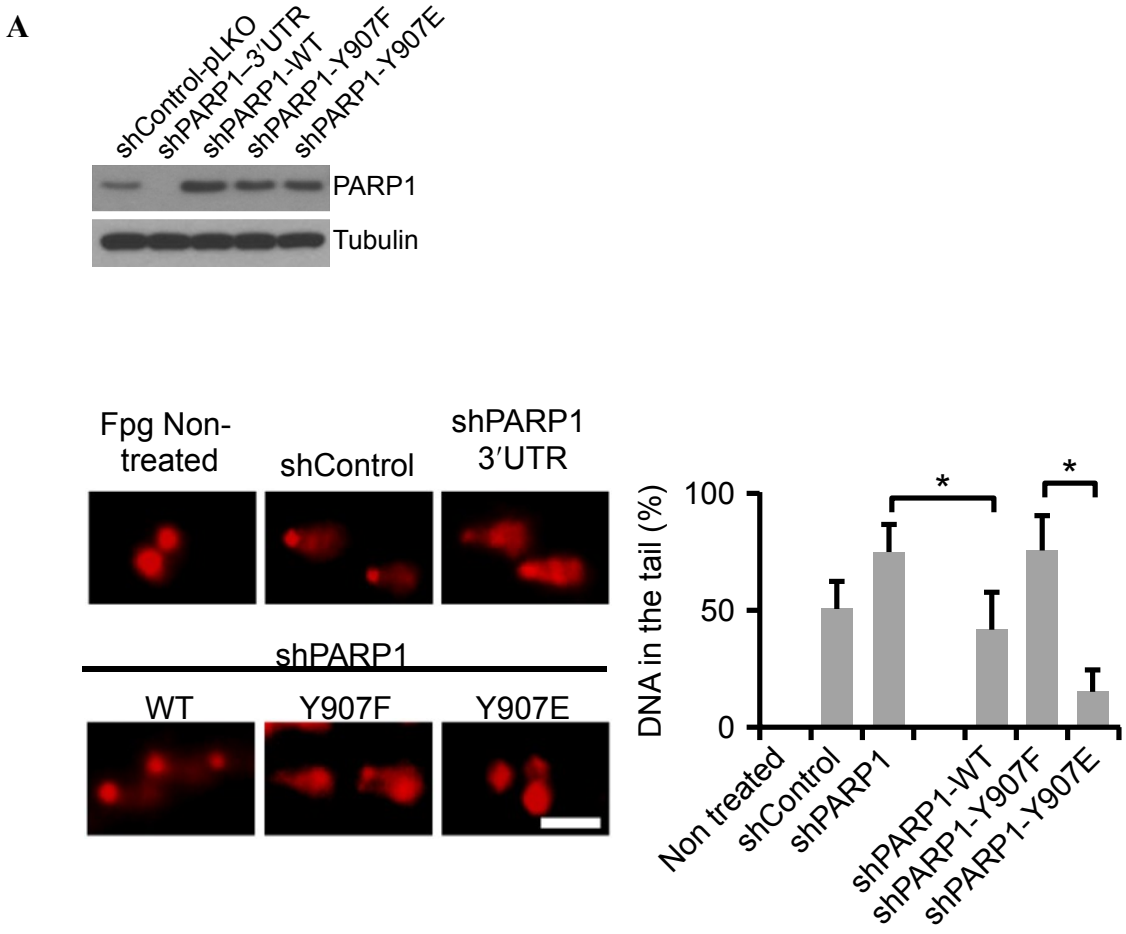

(A) DNA strand breaks were measured by comet assay with pre-incubation with formanidopyrimidine DNA glycosylase (Fpg) in PARP1-WT-, PARP1-Y907E-, or PARP1-Y907F-expressing MDA-MB 231 stable cells treated with 20 mM H_2O_2 for 30 min. Immunoblot showing expression of PARP1 in PARP1-knockdown MDA-MB 231 cells and WT PARP1 or the Y907 mutant re-expressing MDA-MB 231 cells. The quantified intensity of damaged DNA was shown in right panel. Bar, 100 μm.

B

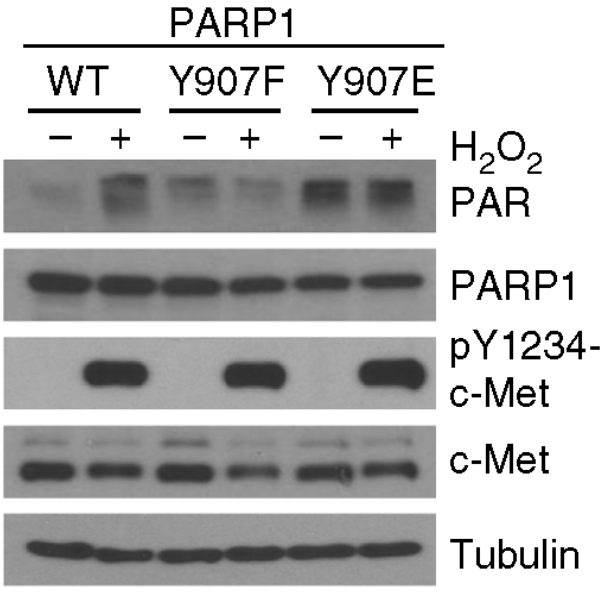
PARP1
WT
Y907F
Y907E
− + − + − +
H_2O_2
PAR
PARP1
pY1234-
c-Met
c-Met
Tubulin

C

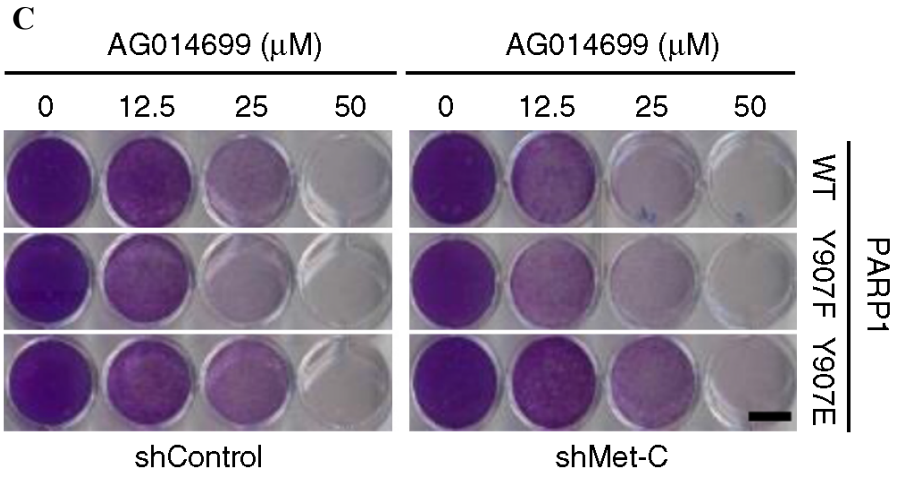
AG014699 (μM)
AG014699 (μM)
0 12.5 25 50 0 12.5 25 50
WT
Y907F
Y907E
PARP1
shControl
shMet-C

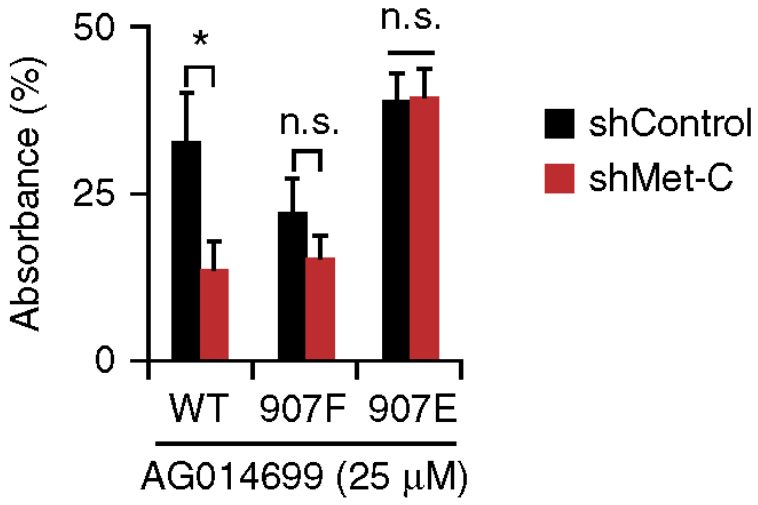
50
25
0
Absorbance (%)
*
n.s.
n.s.
WT 907F 907E
AG014699 (25 μM)
shControl
shMet-C

Figure 3.4.2 Phosphorylation of PARP1 at Y907 Contributes to PARP Function and PARP Inhibitor Resistance

(B) Immunoblot showing PAR expression in the MDA-MB 231 stable cells as described in (A) with or without 20 mM H_2O_2 for 30 min.

(C) MDA-MB 231 stable cells as described in (A) were treated with indicated concentration of AG-014699 and subjected to clonogenic formation assay for 8 days. Bar, 10 mm. *$P < 0.05$, Student's t-test. n.s., not significant.

Experiments in figure 3.4.2 were conducted by Yi Du, Hirohito Yamaguchi, Wan-Chi Lin, Wen-Hsuan Yu, Mei-Kuang Chen and Katsuya Nakai.

3.5 The Clinical Relevance of c-Met and Phosphorylation of PARP1 at Y907

3.5.1 c-Met and p-Y907 PARP1 Expression is Positively Correlated in TNBC

To investigate the clinical significance of our findings, we performed IHC staining with p-Y907 and c-Met antibodies in TNBC tissue microarray. The results demonstrated a positive correlation between c-Met and p-Y907 PARP1 (Figure 3.5.1).

Figure 3.5.1 The Correlation between c-Met and p-Y907 PARP1 is Positive in TNBC

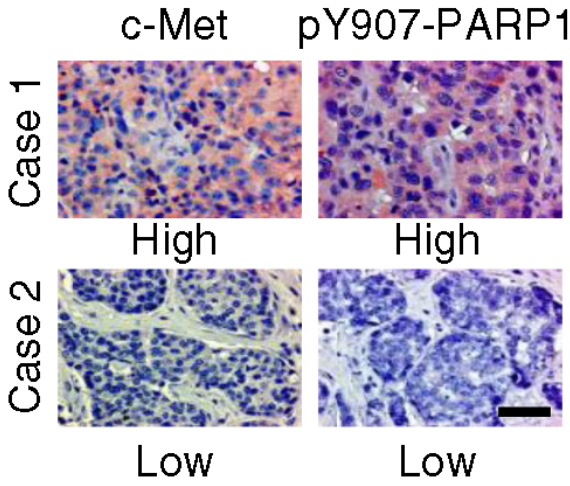

Representative images of immunohistochemical staining for pY907-PARP1 and c-Met from tissue microassay of TNBC (77 cases). Bar, 100 μm.

Experiments in figure 3.5.1 were conducted by Yi Du and Yongkun Wei.

3.5.2 The Combination of c-Met and PARP Inhibitor Has Synergistic Effect in TNBC Cells *in vitro* and *in vivo*

Finally, we examined the therapeutic efficacy of the combination of METi (foretinib and crizotinib) and PARPi (ABT-888 and AG-014699). We performed the dual-drug combination analysis in MDA-MB 231 and HCC 1937 by MTT assay and clonogenic cell survival assay. Using combination index (CI), we evaluated synergistic effects. The results showed that the combination exhibited synergistic inhibition of cell growth in TNBC cell lines (Figure 3.5.2.1).

We then evaluated the combination effect in MDA-MB 231 xenograft mice model. The combination treatment (AG-014699-crizotinib and ABT-888-foretinib) substantially reduced tumor growth compared to either inhibitor alone or vehicle (Figure 3.5.2.2). Thus, this combination is effective against TNBC both *in vitro* and *in vivo*, suggesting METi and PARPi serve as an effective therapeutic strategy to treat TNBC with c-Met overexpression.

Figure 3.5.2.1 The Combination of c-Met and PARP Inhibitor Has Synergistic Effect in TNBC Cells *in vitro*

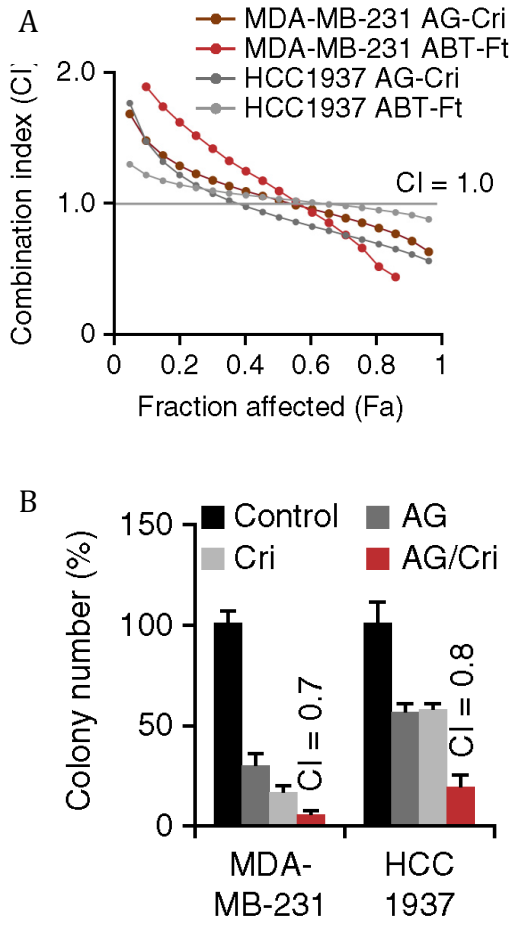

(A) CI plots of the combination of AG-014699 (AG) and crizotinib (Cri) or ABT-888 (ABT) and foretinib (Ft) in both MDA-MB 231 and HCC 1937.

(B) The synergistic effect of crizotinib and AG-014699 in MDA-MB 231 cells and HCC1937 cells was measured by soft agar assay after a 4-week treatment. Quantification of relative colony numbers and CI values was shown.

Experiments in figure 3.5.2.1 were conducted by Yi Du, Hirohito Yamaguchi and Wen-Hsuan Yu.

Figure 3.5.2.2 The Combination of c-Met and PARP Inhibitor Has Synergistic Effect in TNBC Cells *in vivo*

A

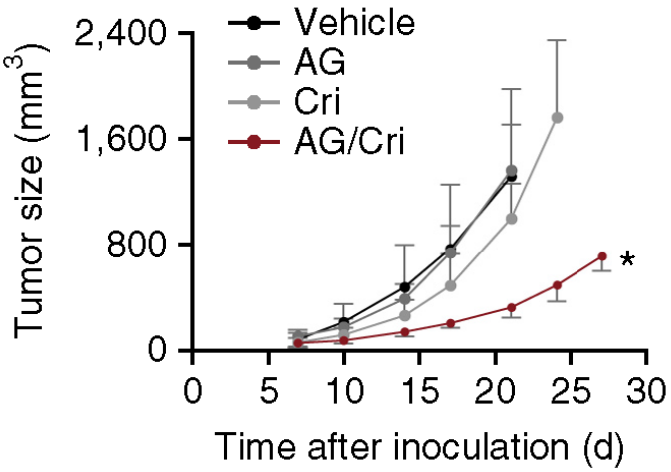

B

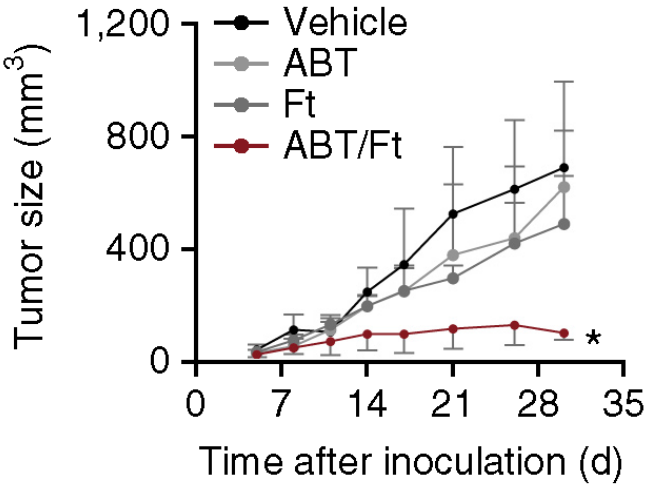

Figure 3.5.2.2 The Combination of c-Met and PARP Inhibitor Has Synergistic Effect in TNBC Cells *in vivo*

(A) MDA-MB 231 cells were inoculated into the mammary fat pads of nude mice (10 mice per group). When the tumor reached ~50 mm^3, mice were orally administered AG-014699 (10 mg/kg), crizotinib (5 mg/kg), or the combination five times per week. Tumor volume was measured at the indicated time points. *$P < 0.05$, Student's t-test.

(B) Same as (A), but the mice were orally treated with ABT-888 (25 mg/kg), foretinib (5 mg/kg), or the combination.

Experiments in figure 3.5.2.2 were conducted by Yi Du, Hirohito Yamaguchi, Wan-Chi Lin, Wen-Hsuan Yu, Mei-Kuang Chen and Chun-Te Chen.

3.6 CK2 is The Potential PARP1 Regulator

3.6.1 Identification of Druggable PARP1-Associated Serine/Threonine Kinase in TNBC by Bioinformatics Analysis of Public Database and Mass Spectrometry Data

In addition to tyrosine kinases, previous studies have shown that multiple serine/threonine (S/T) residues within important regulatory domains and motifs in PARP1 are phosphorylated by kinases (56). To identify other S/T kinases that are involved in the regulation of PAPR1, first we screened potential PARP1-associated S/T kinases from online databases and published mass spectrometry databases (56, 113) as well as our own mass spectrometry analysis data of PARP1 binding proteins. We identified thirteen S/T kinases that potentially interact with PARP1 (Table 3.1). Then, we analyzed the patient samples from TCGA database (The Cancer Genome Atlas) to select genes that are overexpressed in TNBC compared with other subtypes of breast cancer (Figure 3.6.1). From the data, we found six out of thirteen PARP1-associated S/T kinases overexpressed in TNBC. Furthermore, we especially focused on the S/T kinases whose inhibitors are currently used in the clinic or in clinical trials, and therefore could be readily tested in combination in clinical trials. Based on the above criteria, CDK2, PKCβ and CK2 are three candidates for PARP1 regulators (Table 3.2).

Table 3.1 Thirteen PARP1-Associated S/T Kinases

Kinase	Entrez gene name	
CDK8	Cyclin-dependent kinase 8	BioGRID Database
MAPK13	Mitogen-activated protein kinase 13	BioGRID Database
ERK1/2	Mitogen-activated protein kinase 1	(56, 57)
CDK5	Cyclin-dependent kinase 5	(56, 114)
CDK2	Cyclin-dependent kinase 2	(115)
JNK1	c-jun N-terminal kinase	(56, 58)
CaMK-II	Calcium/calmodulin-dependent protein kinase II	(56, 116)
PKCβ	Protein kinase C, beta	(56, 117)
AMPKα2	protein kinase, AMP-activated, alpha 1 catalytic subunit	(56)
PKA	Protein kinase, cAMP-dependent, catalytic, alpha	(113)
CK2	Casein Kinase 2	(113) Our Mass Spec data
ZAK	Mitogen-activated protein kinase kinase kinase MLT	Our Mass Spec data
WNK1	Serine/threonine-protein kinase WNK1	Our Mass Spec data

Figure 3.6.1 Expression of Six PARP1-Associated S/T Kinases mRNA Correlates with TNBC from TCGA Database

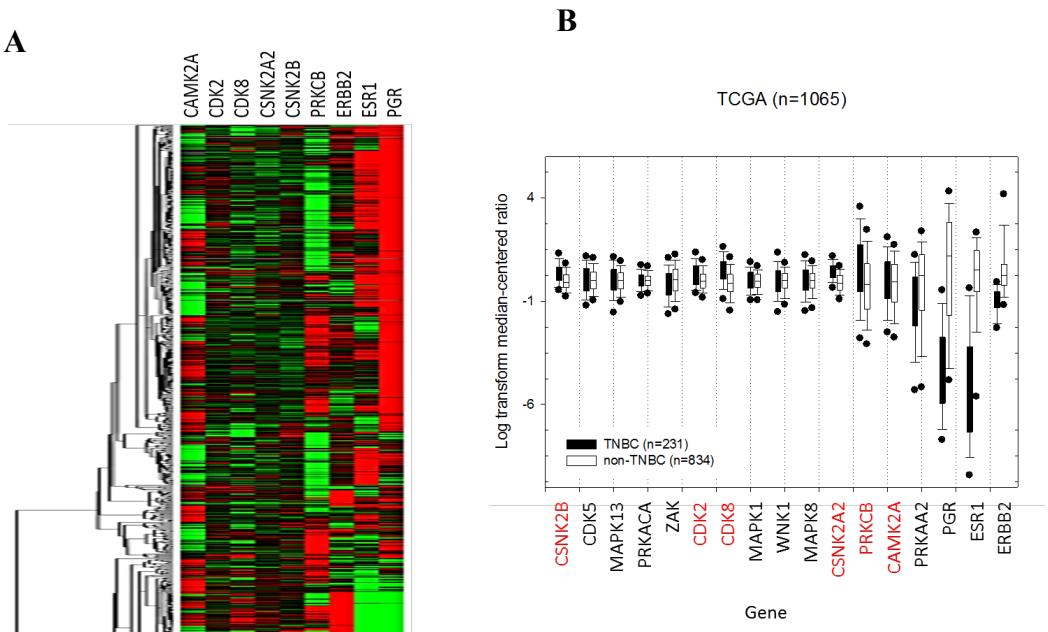

(A) Hierarchical clustering analysis of mRNA expression six PARP1-associated S/T kinases and breast cancer markers in TCGA database. Red represents high gene expression, and green represents low gene expression.

(B) Box plot generated from original and log2-tranformed mRNA expression levels of thirteen PARP1-associated S/T kinases. The genes highlighted in red correlate with TNBC.

Table 3.2 Three Druggable PARP1-Associated S/T Kinases

Kinase	Entrez gene name	Drugs	Clinical Trials
CDK2	Cyclin-dependent kinase 2	**SNS-032**, Sunesis Pharmaceuticals	Phase I trials in select advanced solid tumors
PKCβ	Protein kinase C, beta	**Sotrastaurin(AEB071)**, Norvatis	PhaseIb/II in uveal melanoma
CK2	Casein Kinase 2	**CX-4945**, Cylene, Senhwa Biosciences	Phase1/2 in cholangiocarcinoma

3.6.2 Dual-Drug Combination Effect of CDK2, PKCβ, CK2 and PARP Inhibitors in TNBC cells

Next, we performed dual-drug combination assay to further investigate the anti-TNBC efficacies of combination of a CDK2 inhibitor (SNS-032), a PKCβ inhibitor (sotrastaurin), a CK2 inhibitor (CX-4945) and four PARPi (olaparilb [AZD-2281], Veliparib [ABT-888], talazoparib [BMN-673], and rucaparib [AG-014699]). We first determined IC50 of each drug in MDA-MB 231 and BT549 cell lines by MTT assay. Then, we performed the combination index (CI) theorem of Chou-Talalay to offer a quantitative definition for the addictive effect (CI = 1), synergism (CI < 1), and antagonism (CI > 1) in dual-drug combinations to test synergistic efficacy as determined by MTT assay.

As shown in Figure 3.6.2.1, MDA-MB 231 treated with CX-4945, SNS-032, sotrasaturin, and four different PARP inhibitors alone or in combination at various concentrations. CI-Fa (fraction affected) values as a function of fractional inhibition were plotted to determine drug interactions by computer simulation (CompuSyn). For example, a fixed ratio of BMN-673 and CX-4945 combination (BMN-673/CX-4945 = 10:1) was determined by the IC50s of the individual drugs. The CI-Fa plot of this combination showed that the strongest synergism at 97% ED (effective dose) with CI value of 0.49 in MDA-MB 231 cells. However, the combination of BMN-673 and sotrasaturin or SNS-032 at 97% ED were antagonism with CI above 1. Therefore, the combination with the best therapeutic effect among three kinase inhibitors with BMN-673 was CX-4945. We performed the same analysis for all dual-drug combinations in BT549 (Figure 3.6.2.2). The CI values of dual-drug combinations in the different cell lines were summarized as

Table 3.3. According to these results, the best synergism was observed in the combination of CX-4945 with PARPi (BMN-673 and AZD-2281) in MDA-MB231 and BT549 at 97% EDs with CI value of 0.49 and 0.31, respectively. CX-4945 is a CK2 inhibitor, and therefore CK2 may be a potential kinase to regulate PARP1.

Figure 3.6.2.1 The Effect of Dual-Drug Combinations of Kinase Inhibitors and PARP Inhibitors in MDA-MB 231

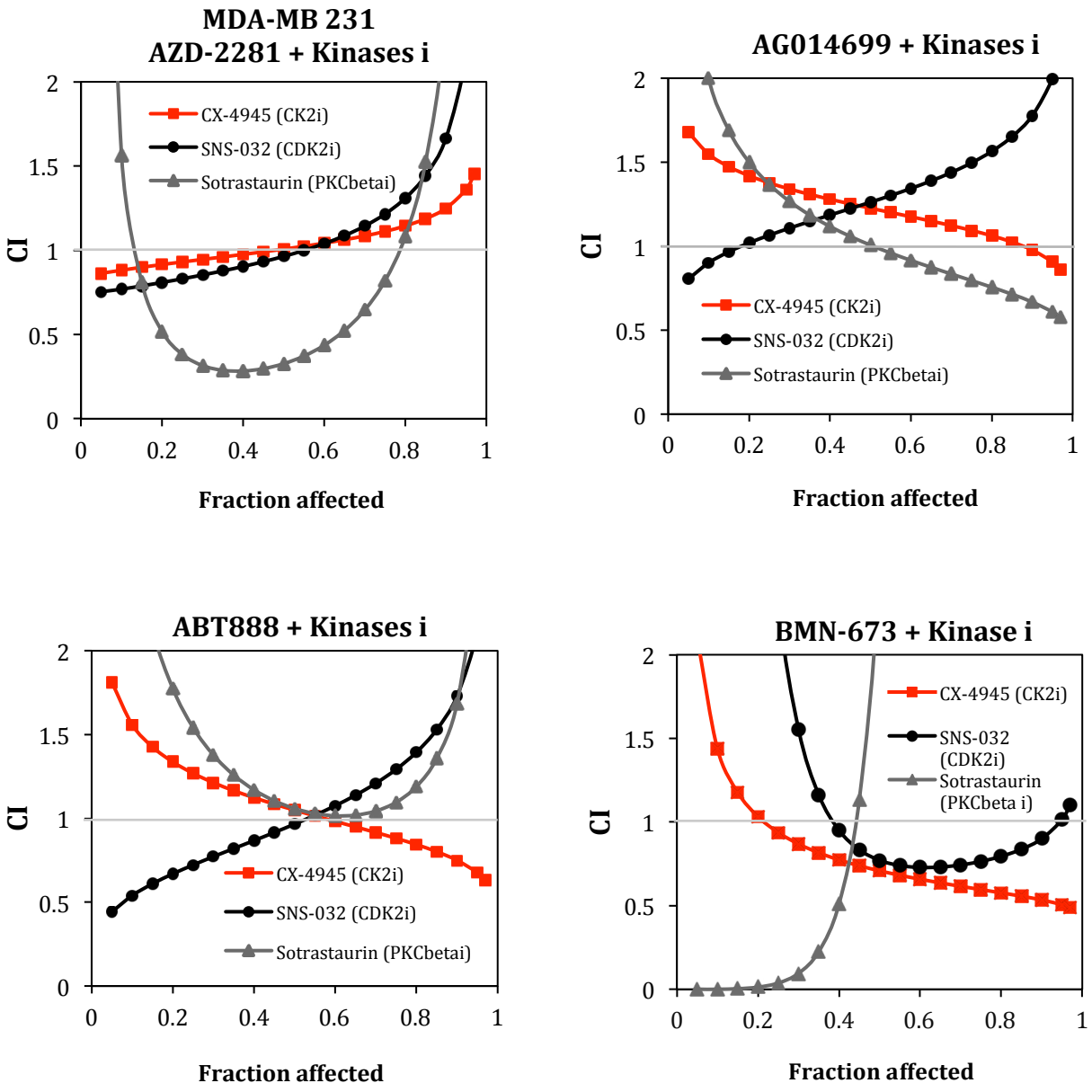

Figure 3.6.2.1 The Effect of Dual-Drug Combinations of Kinase Inhibitors and PARP Inhibitors in MDA-MB 231

CI plots for the dual drug combinations of PARPi (AZD-2281, AG-014699, ABT-888 and BMN-673) and kinase inhibitors (CX-4945, SNS-032 and sotrastaurin) in MDA-MB 231. Cells were treated with the combinations at various concentrations for 72 hours. CI values were plotted as a functional of fractional inhibition as determined by MTT assay.

Figure 3.6.2.2 The Effect of Dual-Drug Combinations of Kinase Inhibitors and PARP Inhibitors in BT549

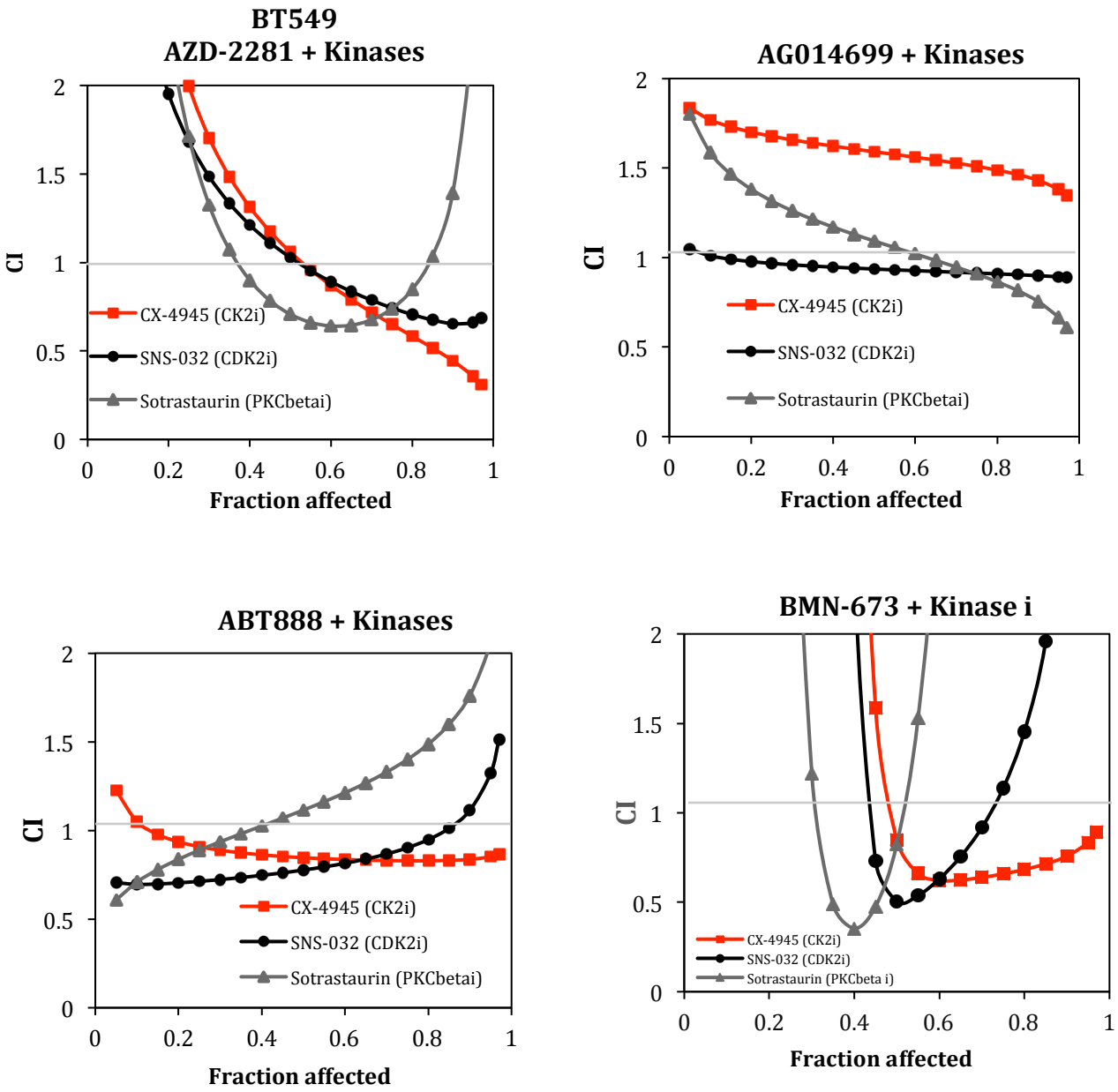

BT549 cells were used for the same assay described in Figure 3.6.2.1.

Table 3.3 Summary of CI Values of Dual-Drug Combinations in TNBC Cell Lines

	CI			
Drug combination	**ED50**	**ED75**	**ED90**	**ED97**
MDA-MB 231				
CX/AZD	1.01	1.11	1.25	1.45
CX/AG	1.23	1.09	0.98	0.86
CX/ABT	1.05	0.88	0.75	0.63
CX/BMN	0.71	0.60	0.53	0.49
SNS-AZD	0.96	1.22	1.66	2.61
SNS-AG	1.26	1.50	1.78	2.17
SNS-ABT	0.97	1.29	1.73	2.43
SNS-BMN	0.77	0.76	0.90	1.10
SO/AZ	0.33	0.82	2.41	8.58
SO/AG	1.01	0.80	0.67	0.58
SO/ABT	1.06	1.10	1.69	3.50
SO/BMN	2.52	264.25	39643.70	16130000.00
BT549				
CX/AZD	1.06	0.65	0.45	0.31
CX/AG	1.59	1.51	1.43	1.35
CX/ABT	0.85	0.83	0.84	0.86
CX/BMN	0.85	0.66	0.76	0.89
SNS-AZD	1.03	0.74	0.65	0.68
SNS-AG	0.94	0.91	0.90	0.89
SNS-ABT	0.78	0.90	1.11	1.51
SNS-BMN	0.50	1.14	2.91	8.67
SO/AZD	0.71	0.74	1.39	3.36
SO/AG	1.09	0.91	0.75	0.61
SO/ABT	1.12	1.40	1.76	2.30
SO/BMN	0.83	25.94	830.79	46999.70

3.6.3 The Protein Expression of CK2 in Breast Cancer Cell Lines

From the previous TCGA data analysis, we found that the mRNA level of CK2 is significantly correlated with TNBC. Therefore, we wondered whether the protein level of CK2 is also overexpressed in TNBC. To address this question, we selected a panel of breast cancer cell lines to examine the protein expression level of CK2. Generally, we found that all the breast cancer cell lines expressed both CK2α and CK2β. However, TNBC expressed higher amount of CK2α protein compared to non-TNBC by immunoblotting assay.

Figure 3.6.3 Expression of CK2 Protein Correlates with TNBC Cell Lines

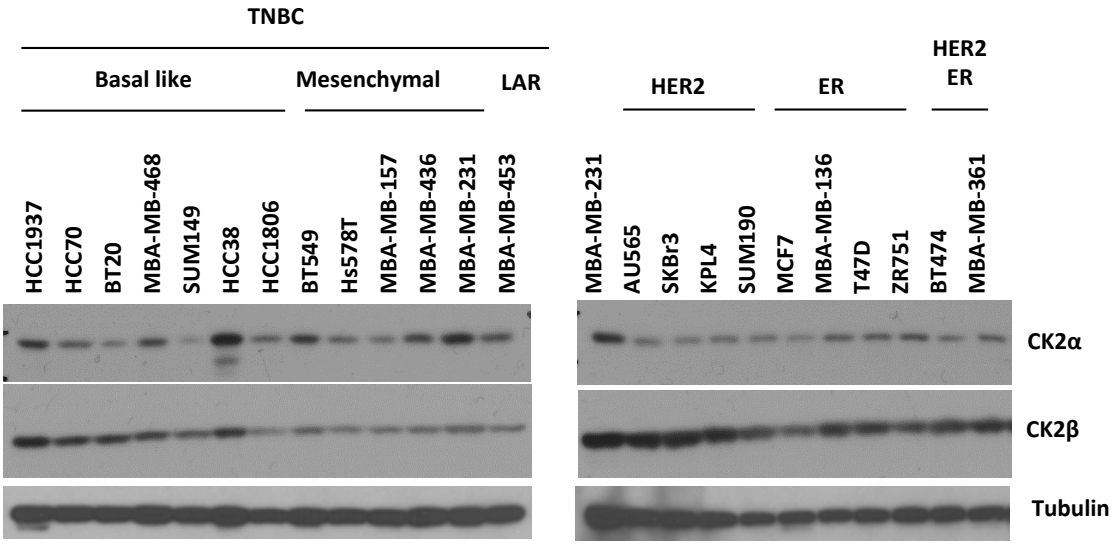

Immunoblot showing the protein expression of CK2α and CK2β in a panel of breast cancer cell lines.

LAR, luminal androgen receptor. ER, estrogen receptor; HER2, human epidermal growth factor receptor 2.

3.7 Inhibition of CK2 Sensitizes TNBC Cells to PARP Inhibitor

3.7.1 The Combination of CK2 and PARP Inhibitors Has Synergistic Effect in TNBC

Knowing that the combination with the strongest synergism is CK2 and PARPi and also CK2 is overexpressed in TNBC, we asked whether the dual-drug combinations affect on the tumorigenic potential of TNBC cells. To address this question, first we performed dual-drug combination assay in TNBC cells by colony formation assay. The result showed that inhibition of CK2 by CX-4945 rendered MDA-MB 231 cells more sensitive to all four PARPi, as indicated by inhibiting colony forming (Figure 3.7.1.1). The relative number of colonies were quantified by ImageJ. For example, AG-014699 alone at 0.8 μM resulted in ~35% colony formation inhibition; while CX-4945 alone at 0.4 μM resulted in ~10% colony formation inhibition. Addition of both AG-014699 and CX-4945 at a fixed drug ratio (0.4uM AG-014699/ 0.8uM CX-4945) resulted in ~65% colony formation reduction that was shown to be synergism by calculating CI value (CI=0.58) with the Chou and Talalay method (Figure 3.7.1.1 A). Data analysis indicated that the CI values of different combinations of CX-4945 and PARPi are all below 1 in MDA-MB 231. Synergistic inhibition of CX-4945 and PARPi was also observed in BT549 by clonogenic cell survival assay (Figure 3.7.1.2). Consistent with cell proliferation MTT assay, these data suggested CX-4945 and PARPi show synergy with PARPi.

Figure 3.7.1.1 The Combination of CK2 and PARP Inhibitors Has Synergistic Effect in MDA-MB 231

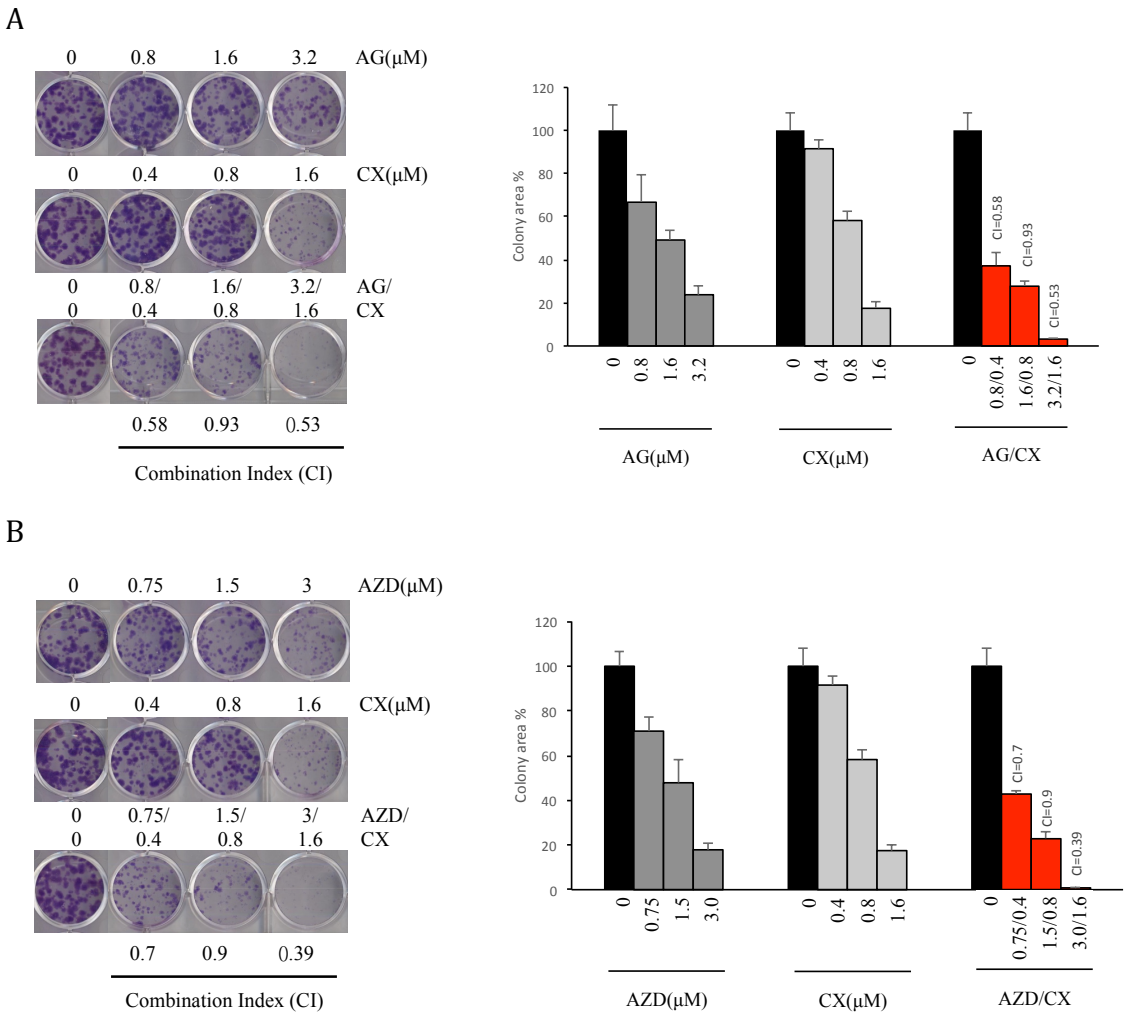

(A) The effect of the combination of CK2i and PARPi was determined by clonogenic assay in MDA-MB 231. Cells were treated with AG-014699 (AG) and CX-4945 (CX), alone or in combination at various concentrations as indicated for 8 days. CI value is quantified as previous described. The quantified result of visible colonies was shown in right panel. Error bars indicate the SD (n=3).

(B) Same as (A) but cells were treated with AZD-2281 (AZ) and CX-4945 (CX).

C

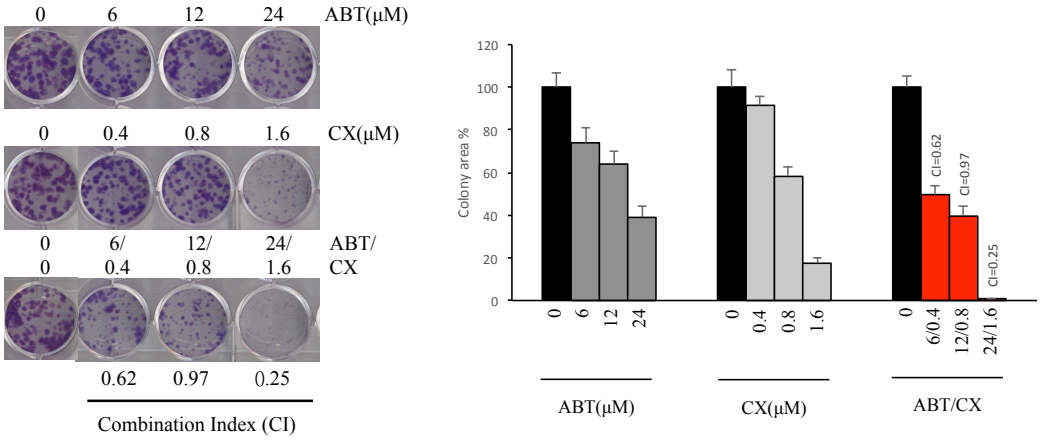

D

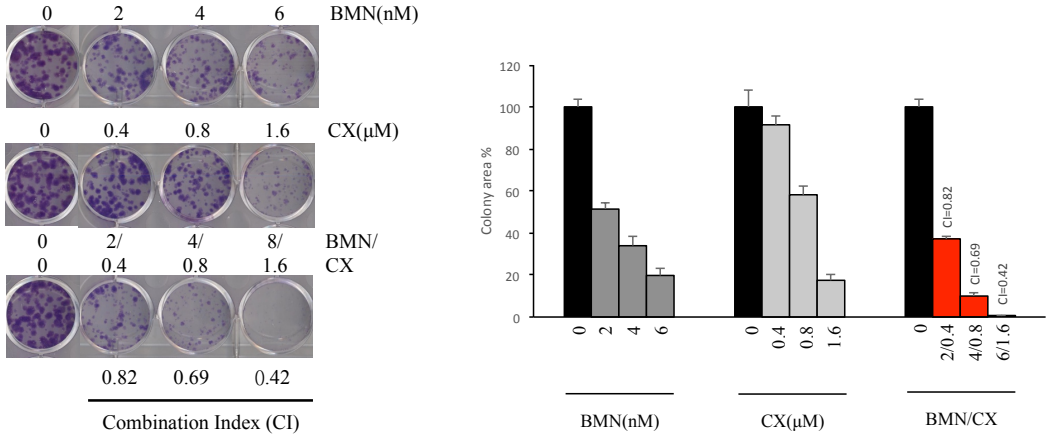

(C) Same as (A) but cells were treated with ABT-888 (ABT) and CX-4945 (CX).

(D) Same as (A) but cells were treated with BMN673 (BMN) and CX-4945 (CX).

Figure 3.7.1.2 The Combination of CK2 and PARP Inhibitors Has Synergistic Effect in BT549

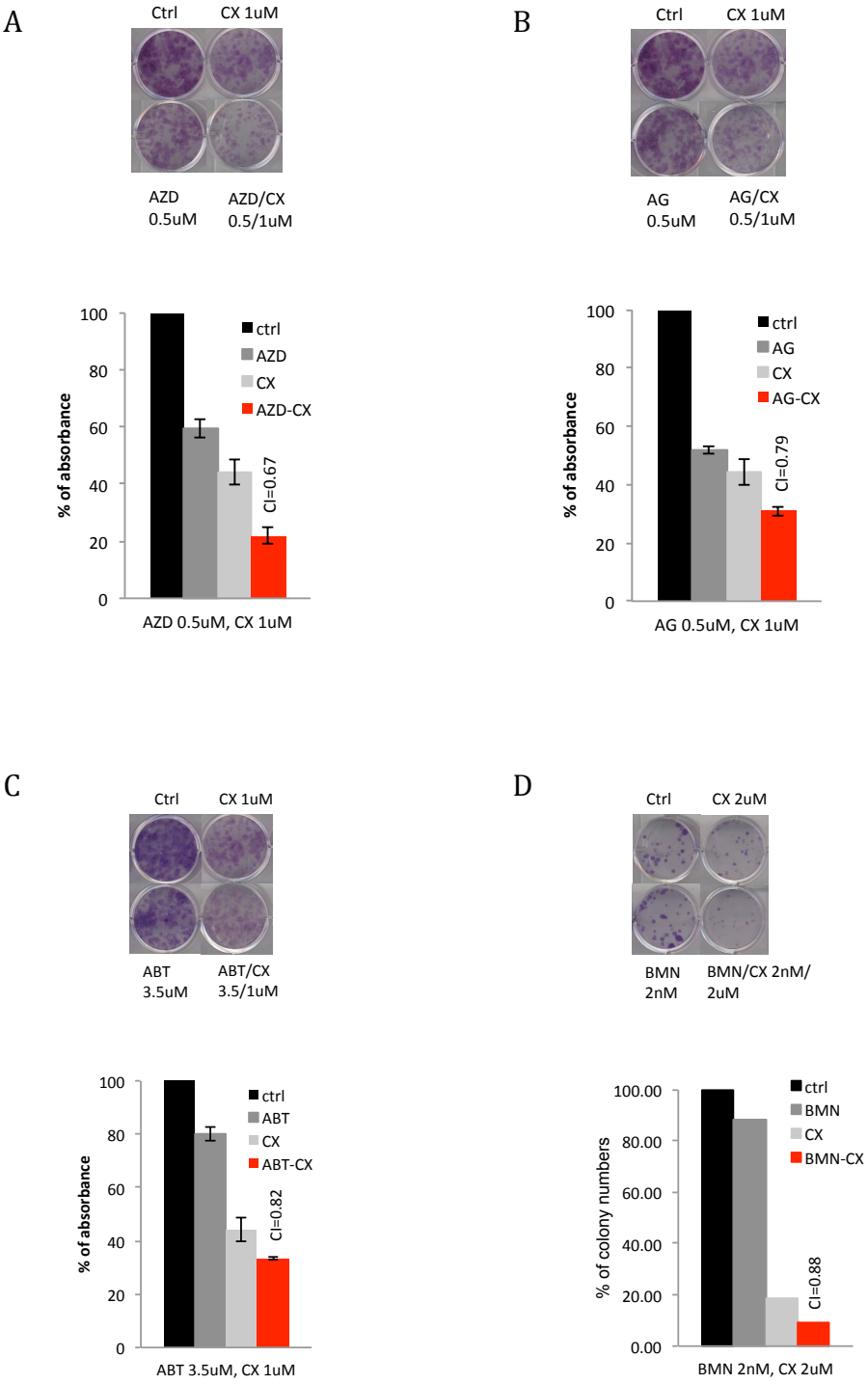

Figure 3.7.1.2 The Combination of CK2 and PARP Inhibitors Has Synergistic Effect in BT549

(A) Similar to (Figure 3.7.1.1) but BT549 cells were used in the assay. Cells were treated with AZD-2281 (AZ; 0.5 umol/L) and CX-4945 (CX; 1umol/L), alone or in combination for 10 days.

(B) Same as (A) but cells were treated with AG-014699 (AG; 0.5 umol/L) and CX-4945 (CX; 1umol/L).

(C) Same as (A) but cells were treated with ABT-888 (ABT; 3.5 umol/L) and CX-4945 (CX; 1umol/L).

(D) Same as (A) but cells were treated with BMN-673 (BMN; 2 nmol/L) and CX-4945 (CX; 2umol/L).

3.7.2 Knockdown of CK2 Enhances the Sensitivity to PARP Inhibitor in TNBC Cells

To further validate that CK2 influences the sensitivity to PARPi in TNBC, we used small interference RNA to knockdown CK2 and examined the colony forming ability after PARPi (AG-014699 and ABT-888) treatment. We knocked down CK2α and CK2α', which are catalytic subunits of CK2 protein, because CX-4945 targets the activity of both CK2α and α' (Figure 4.7.2 A). The results of colony formation assay showed that knockdown of both CK2α and CK2α' significantly increased the PARPi (AG-014699) sensitivity in MDA-MB 231. This data suggests that CK2 contributes to PARPi resistance in TNBC cells.

Figure 3.7.2 Knockdown of CK2 Enhances the Sensitivity to PARP Inhibitor in TNBC cells

A

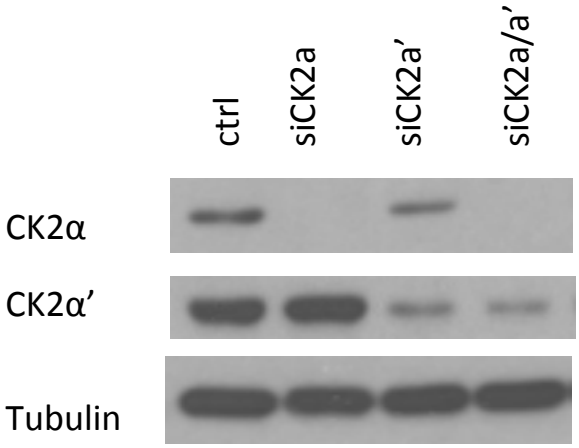

B

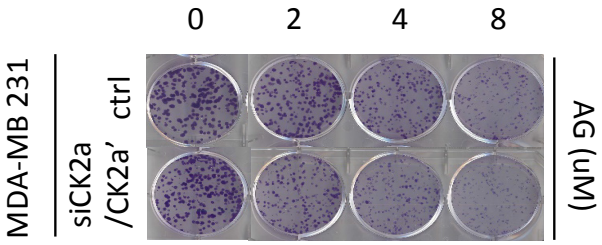

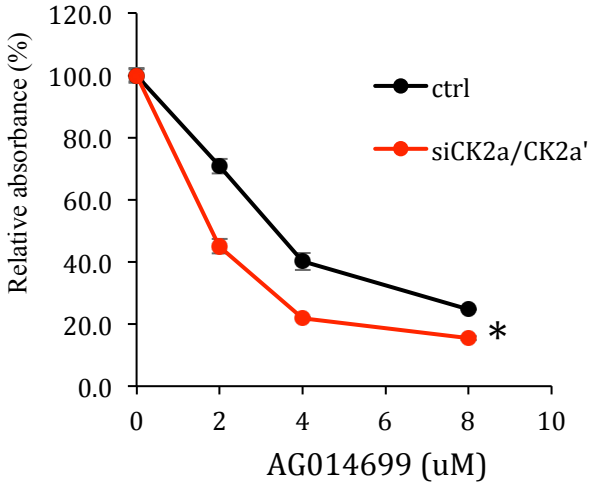

Figure 3.7.2 Knockdown of CK2 Enhances the Sensitivity to PARP Inhibitor in TNBC cells

(A) CK2α and CK2α' expression was determined by western blot to show siRNA efficiency in MDA-MB 231.

(B) CK2α/α' knockdown MDA-MB 231 cells were treated with the indicated concentrations of AG-014699 for 8 days and subjected to clonogenic cell survival assay. Quantification of clonogenic cells (n=3) was shown. $*P < 0.05$, Student's t-test.

3.7.3 The Combination of CK2 and PARP Inhibitors Has Synergistic Effect *in vivo*

Next, we evaluated the effect of the combination treatment of CK2i and PARPi in a TNBC xenograft mice model. In the BT549 xenograft tumor model, the mice were treated with AZD-2281 orally (25 mg/kg, p.o) and intraperitoneal injection of CX-4945 (6.25mg/kg, i.p) alone, or in combination daily for 14 days. The mice tumor volume was measured every two days. Consistent with our previous findings from in vitro assays, the combination treatment was more effective in reducing tumor growth than was either alone treatment or vehicle control ($p < 0.05$) (Figure 3.7.3). The mice body weight remained almost the same after treatment.

Together, the data from *in vitro* and *in vivo* studies suggested that CK2 contributes to PARPi resistance and inhibition of CK2 enhances PARPi sensitivity in TNBC.

Figure 3.7.3 The Combination of CX-4945 and AZD-2281 Inhibits Tumor Growth in BT549 Orthotopic Xenograft Mice Model

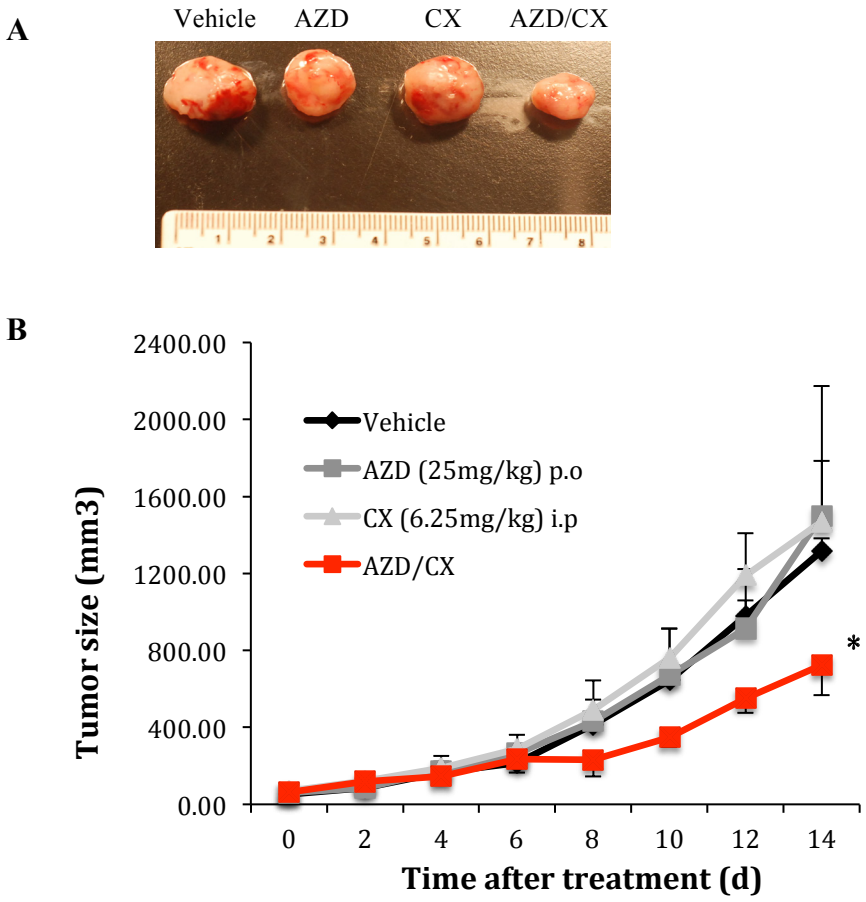

(A) Representative images of xenograft BT549 tumors from each group as indicated. AZD, AZD-2281; CX, CX-4945; AZD/CX, AZD-2281 and CX-4945 combination.

(B) BT549 cells were inoculated into the mammary fat pads of nude mice (3 mice per group). When the tumor reached ~60 mm^3, mice were administered AZD-2281 (AZD, 25mg/kg, p.o), CX-4945 (CX, 6.25mg/kg, i.p), or the combination (AZD/CX) daily for 14 days. Tumor volume was measured at the indicated time points. *$P < 0.05$, Student's t-test.

3.8 Mechanism of the Synergistic Effect of PARP Inhibitor and CK2 Inhibitor

3.8.1 Inhibition of CK2 and PARP Increases DNA Strand Breaks

We already showed that the combination of PARPi and CK2i has a synergistic effect in TNBC cells. It is known that inhibition of PARP1 accumulates DNA strand breaks and results in DNA damage. Therefore, to establish the mechanism of PARPi sensitization in response to inhibition of CK2, we first investigated whether inhibition of both CK2 and PARP1 enhanced DNA strand breaks compared to inhibition of PARP alone. We performed comet assay to investigate the extent of DNA damage after treatment of AG-014799 and CX-4945 alone or the combination in MDA-MB 231 for 18 hours. The results showed that the cells with combination treatment had higher tail intensity, which is indicative of increased DNA strand breaks compared to single treatment and control (Figure 3.8.1.1). Similarly, in BT549 cells, the combination treatment of AZD-2281 and CX-4945 had more DNA strand breaks than control and the single treatment (Figure 3.8.1.2). These results suggest that the inhibition of both CK2 and PARP1 results in more DNA damage than the inhibition of either one.

Figure 3.8.1.1 Inhibition of CK2 and PARP Increases DNA Strand Breaks in MDA-MB 231

A

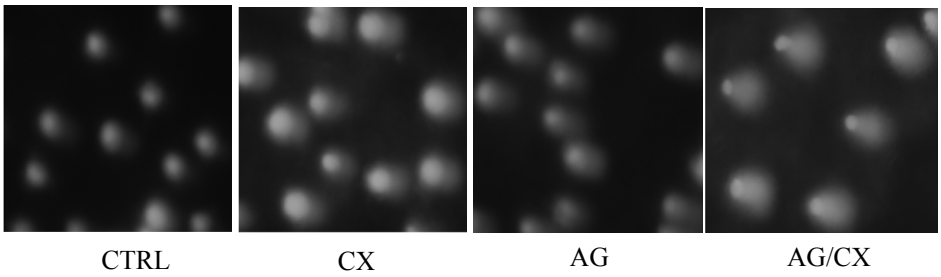

B

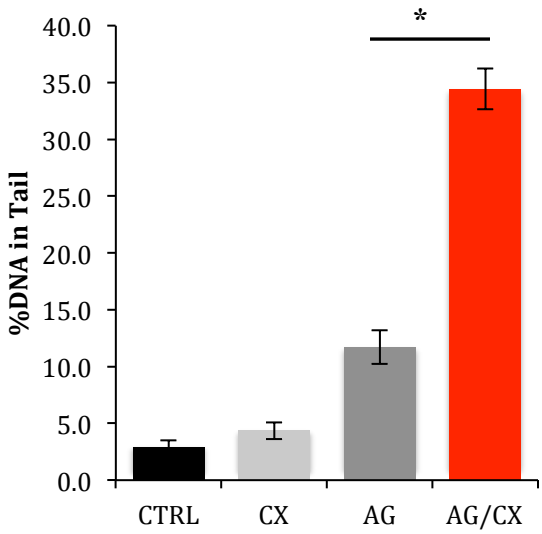

(A) DNA strand breaks were measured by comet assay in MDA-MB 231 cells. Cells were treated with AG-014699 (AG, 10 umol/L), CX-4945 (CX, 5 umol/L) or the combination (AG/CX) for 18 hours.

(B) Quantification of the intensity of damaged DNA using the parameter of percentage of DNA in tail. *$P < 0.05$, Student's t-test.

Figure 3.8.1.2 Inhibition of CK2 and PARP Increases DNA Strand Breaks in BT549

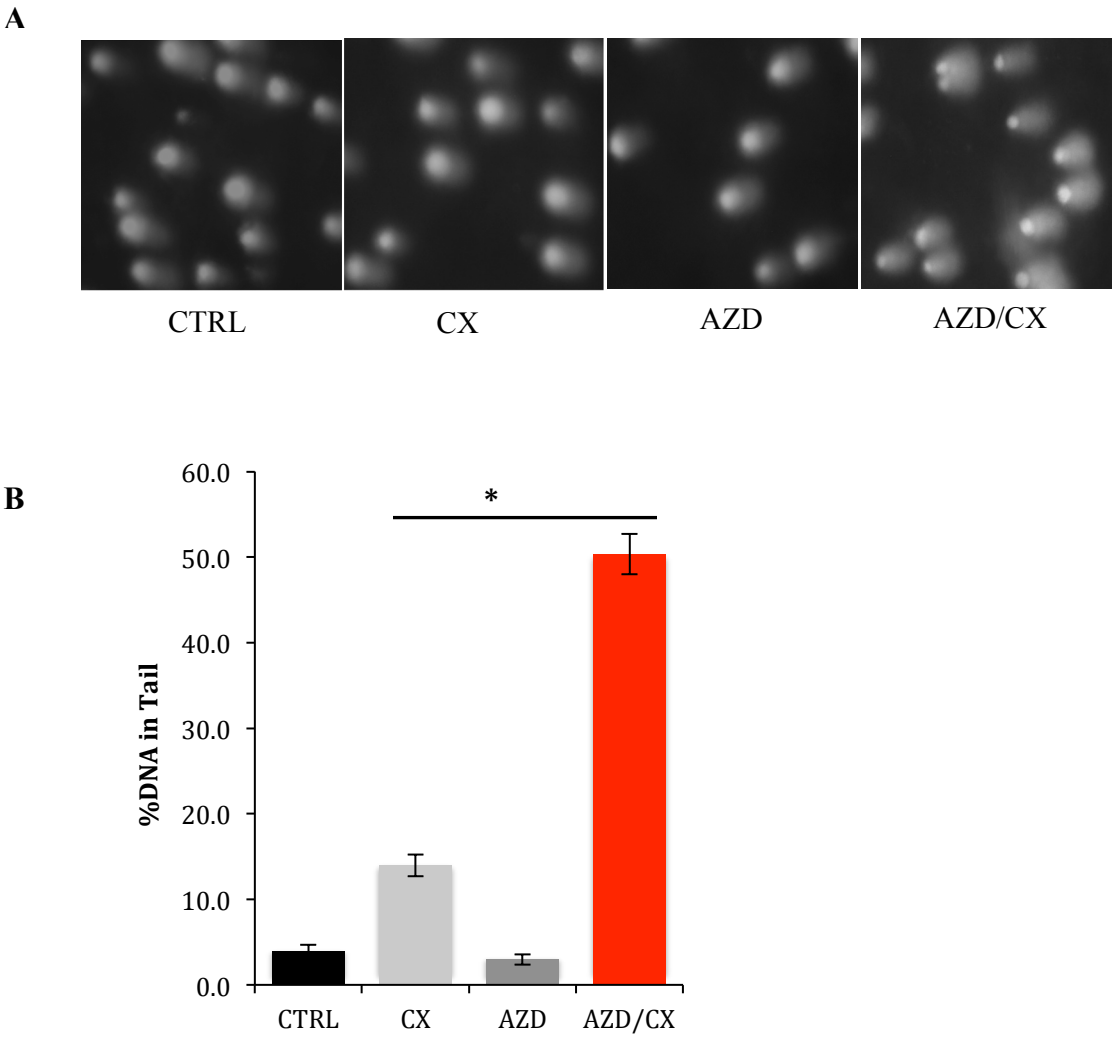

(A) BT549 cells were treated with AZD-2281 (AZD, 10 umol/L), CX-4945 (CX, 5 umol/L) or the combination (AZD/CX) for 18 hours and subjected to comet assay.

(B) Quantification of the intensity of damaged DNA using the parameter of percentage of DNA in tail. *$P < 0.05$, Student's t-test.

3.8.2 Inhibition of CK2 and PARP Enhances γ-H2AX Foci Formation

H2AX phosphorylation (γ-H2AX) is an early step in the DNA double strand break (DSB) repair pathway. Therefore, it is used as a marker for measuring DNA DSBs. We showed that inhibition of CK2 by CX-4945 increases DNA strand breaks by comet assay. Next, we asked whether the combination treatment increases γ-H2AX foci formation compared to single treatment. Using immunofluorescence, γ-H2AX foci were measured in MDA-MB 231 cells by treated with AG-014699, CX-4945, and the combination for 48 hours (Figure 3.8.2 A). Consistent with the results in comet assay, inhibition of CK2 by CX-4945 enhanced the sensitivity of cells to PARPi-induced γ-H2AX foci formation about 10 fold compared to the untreated cells (Figure 3.8.2 B). This result further validated that inhibition of CK2 increased PARPi-induced DNA DSBs.

Figure 3.8.2 Inhibition of CK2 and PARP Enhances γ-H2AX Foci Formation

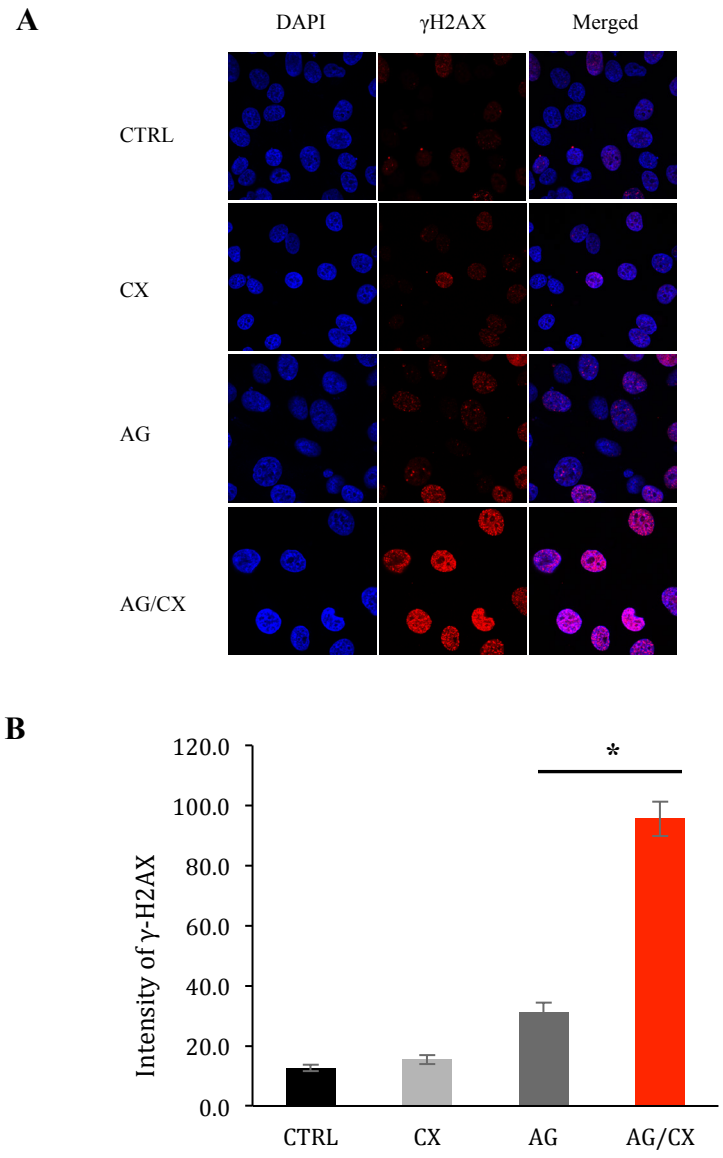

(A) MDA-MB 231 cells were treated with AG-014699 (AG, 10 umol/L), CX-4945 (CX, 5 umol/L) or the combination (AG/CX) for 48 hours. γ-H2AX (red) was detected by immunofluorescence confocal microscopy.

(B) Quantification of γ-H2AX foci formation was shown. *$P < 0.05$,'s t-test.

3.8.3 Inhibition of CK2 and PARP Results in Cell Cycle Arrest in G2/M Phase

We showed that the combination of CK2i and PARPi had higher efficacy than the single treatment. To further understand the underlying mechanism of the drug combination, we examined whether the combination treatment affect on the cell cycle. To address this question, we treated MDA-MB 231 cell lines with AG-014699, CX-4945 or the combination for 72 hours, and then the cell cycle status was detected by flow cytometry. The results showed that CX-4945 and AG-014699 treatment alone increased G2/M-phase when compared with the untreated cells by around 2% and 15%, respectively; while the combination significantly increased G2/M-phase around by 60% (Figure 3.8.3.1). The similar results were shown in BT549, in which a 40% increase in G2/M-phase by the combination of CX-4945 and AZD-2281 compared with the untreated cells was observed (Figure 3.8.3.2). This data suggest that the inhibition of both CK2 and PARP induces G2/M-arrest of cell cycle. This is consistent with our previous cell proliferation data (Figure 3.7.1.1 and 3.7.1.2), which showed that the greater growth retardation in the combination treatment. Moreover, we didn't observe the significant increase of sub-G1 population in both cell lines, suggesting the combination doesn't induce apoptosis.

Figure 3.8.3.1 Inhibition of CK2 and PARP Results in Cell Cycle Arrest in G2/M Phase in MDA-MB 231

A

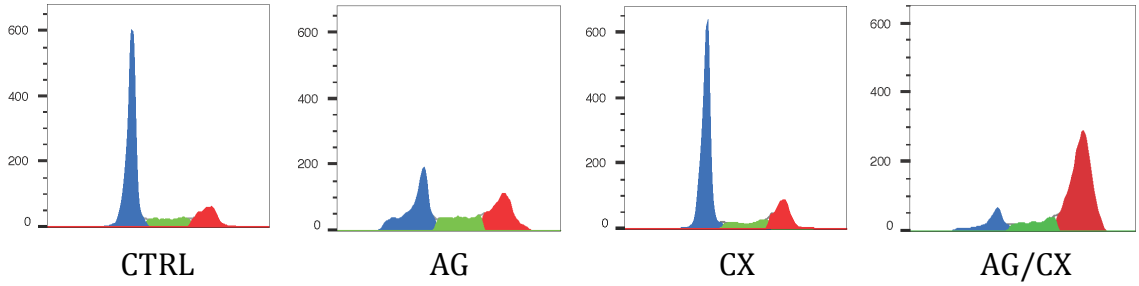

B

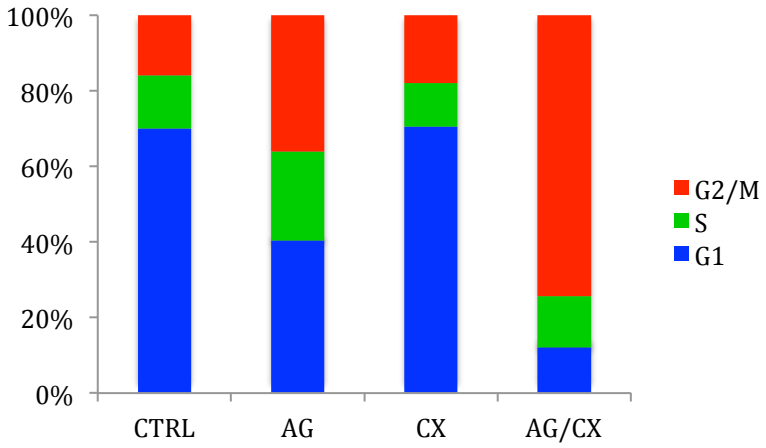

(A) MDA-MB 231 cells were treated with AG-014699 (AG, 10 umol/L), CX-4945 (CX, 5 umol/L) or the combination (AG/CX) for 72 hours. The DNA content was stained with propidium iodide (PI). The cell cycle distribution was analyzed by flow cytometry.

(B) Quantification of each cell cycle phase was shown.

Figure 3.8.3.2 Inhibition of CK2 and PARP Results in G2/M-Phase Arrest in BT549

A

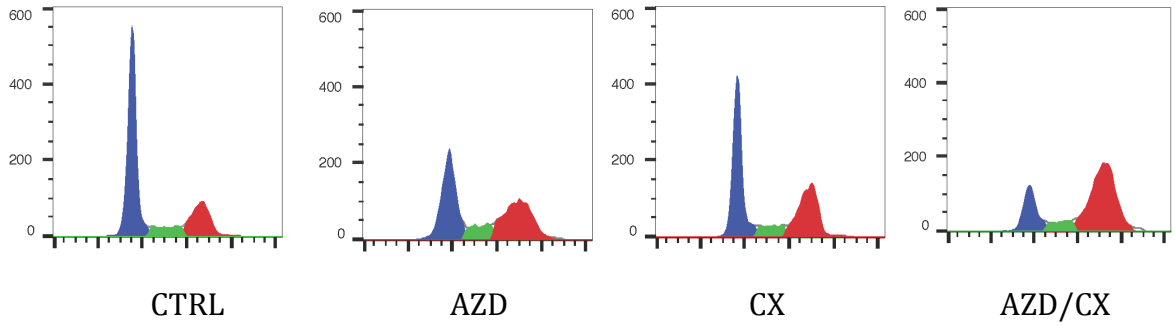

B

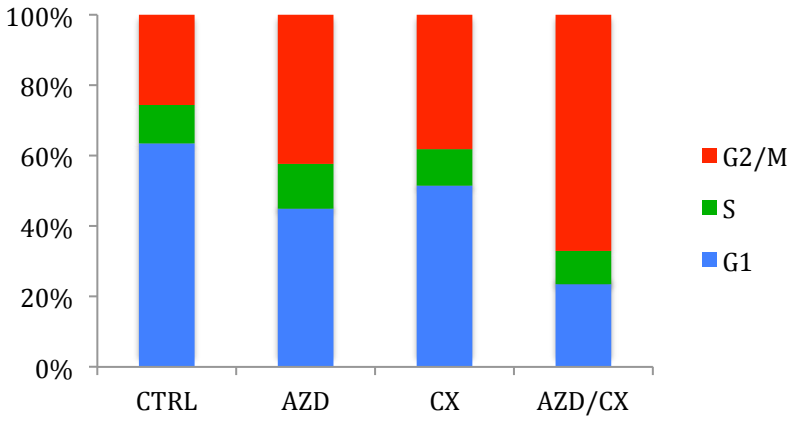

(A) BT549 cells were treated with AZD-2281 (AZD, 10 umol/L), CX-4945 (CX, 5 umol/L) or the combination (AZD/CX) for 72 hours. The cell cycle distribution was analyzed by flow cytometry.

(B) Quantification of each cell cycle phase was shown.

3.9 CK2 Associates with PARP1

3.9.1 CK2 Physically Interacts with PARP1

As mentioned in Table 3.1, our and others mass spectrometry data showed that CK2 is one of PAPR1 associated kinases, and we further validated whether CK2 indeed interacts with PARP1 protein. CK2β subunit is critical for substrate binding, therefore we first overexpressed CK2β and PARP1 exogenously in 293T cells and detected the interaction of CK2β and PARP1 by Co-IP/western blot. We pulled down myc-CK2β and immunobotted HA-PARP1. Indeed, the data showed that Myc-CK2β interacts with HA-PARP1 (Figure 3.9.1.1). Next, we performed Co-IP assay to test whether endogenous PARP1 interacts with endogenous CK2β in MDA-MB 231 and BT549. We pulled down PARP1 or CK2β and immunoblotted CK2β or PARP1, respectively. The data also showed that endogenous CK2β interacts with endogenous PARP1 (Figure 3.9.1.2). To further investigate where the interaction between CK2 and PARP1 occurs inside the cells, we performed proximity-ligation assay in BT549 cells. We found the majority of interaction happened in the cell nucleus (Figure 3.9.1.3).

Figure 3.9.1.1 Exogenous CK2 Interacts with PARP1

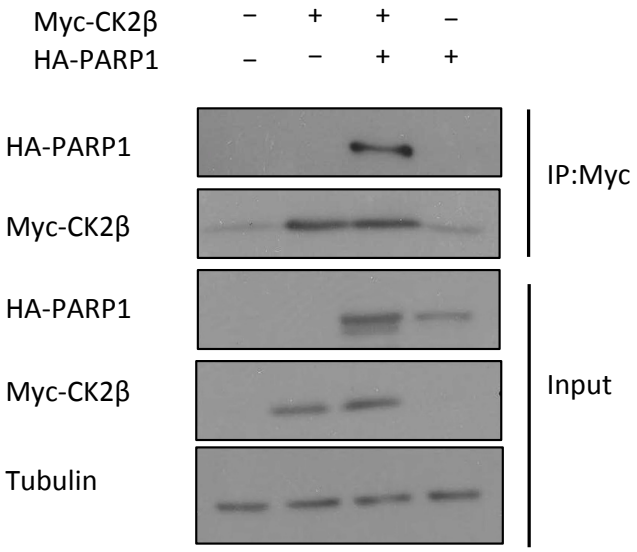

HA-PARP1 and Myc-CK2β were ectopically expressed in HEK 293FT cells, and then the association of PARP1 and CK2β was detected by Co-IP/Western blot.

Figure 3.9.1.2 Endogenous CK2 Interacts with Endogenous PARP1

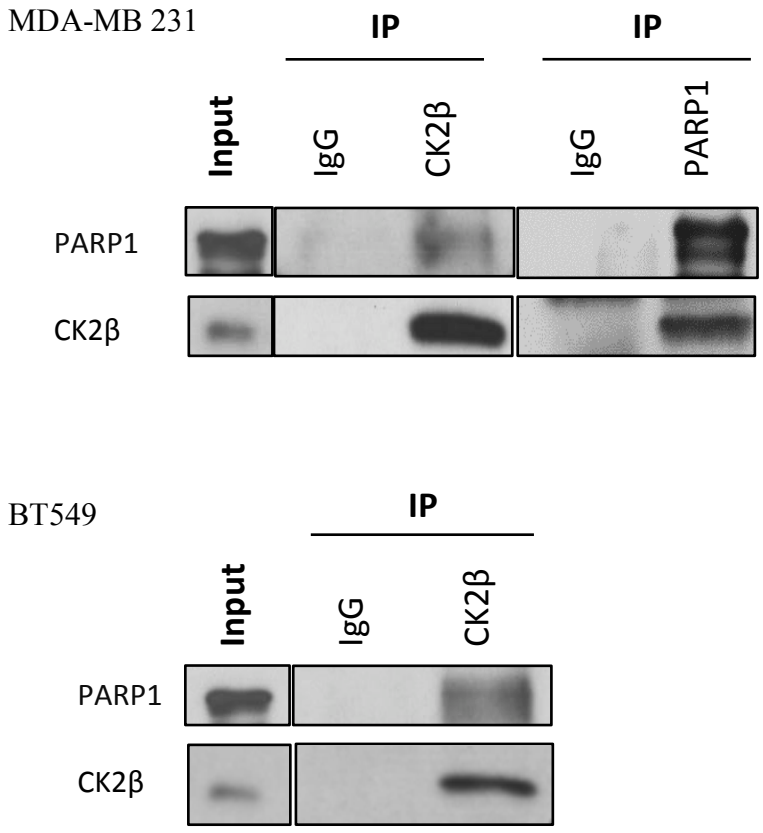

The interaction of endogenous PARP1 and CK2β were determined by Co-IP/western blot. MDA-MB 231 and BT549 were subjected to Co-IP with anti-CK2β or anti-PARP1 antibodies, followed by western blot with the indicate antibodies.

Figure 3.9.1.3 CK2 Interacts with PARP1 in the Nucleus

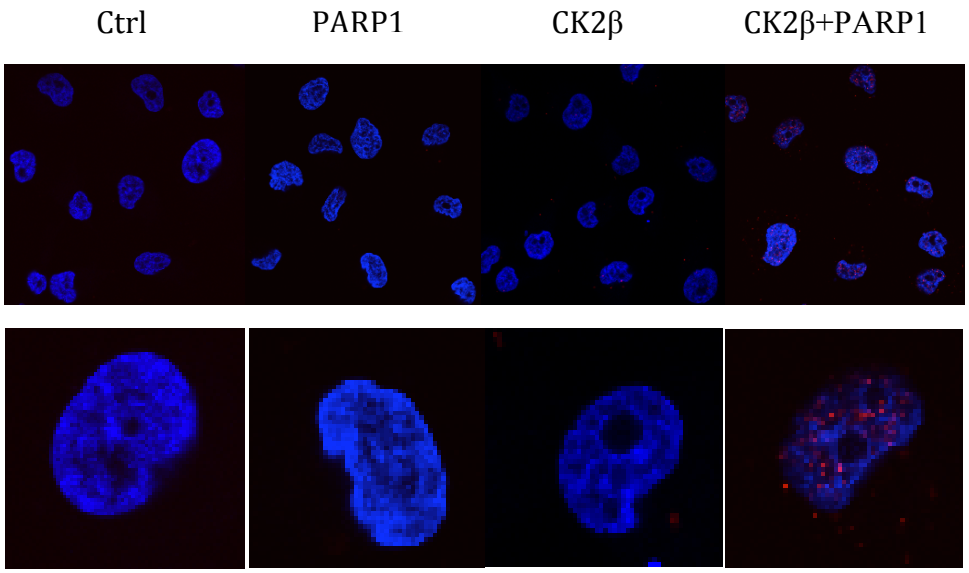

(Proximity ligation assay in BT549)

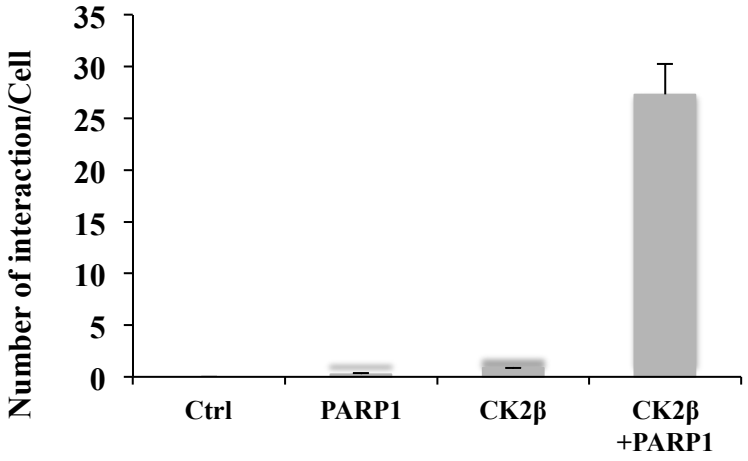

Proximity ligation assay (PLA) to analyze co-localization of PARP1 and CK2β (red) in BT549 cells. Representative images (upper panel) and quantification of PLA signals from 50 cells (lower panel) were shown.

3.9.2 CK2 Phosphorylates PARP1

Our data demonstrated that CK2 physically associated with PARP1 and also inhibition of CK2 sensitized TNBC to PARPi. Therefore, we hypothesized that CK2 could phosphorylate PARP1 and regulates its function.

Using recombinant PARP1 and CK2α proteins, we verified PAPR1 phosphorylation by CK2α by *in vitro* kinase assay detecting [γ^{32}P]-ATP (Figure 3.9.2). Next, we identified the phosphorylation site of PARP1 by CK2α by mass spectrometry. Some potential S/T phosphorylation sites on PARP1 were detected by mass spectrometry analysis. We are further validating the functional effect of the potential phosphorylation sites.

Figure 3.9.2 CK2 Phosphorylates PARP1 *in vitro*

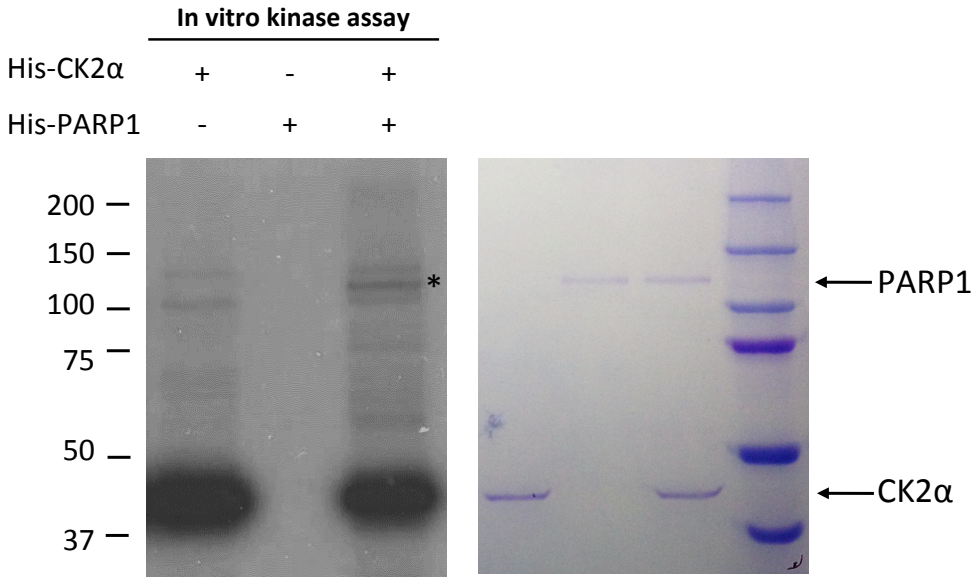

In vitro kinase assay to validate CK2-mediated phosphorylation of PARP1. Recombinant of His-CK2α and His-PARP1 proteins were incubated in kinase assay buffer in the presence of [γ^{32}P]-ATP. Phosphorylated PARP1 and CK2α were visualized by autoradiography. Total PARP1 and CK2α proteins were visualized by coomassie blue staining. *, phosphorylated PARP1.

CHAPTER 4

DISCUSSION and FUTURE WORKS

4.1 Summary of Current Findings

Our study revealed a new mechanism of PARPi resistance in TNBC and provided biomarkers to stratify patients for a rational combinational treatment with PARPi. Specifically, we identified c-Met, a tyrosine kinase, phosphorylates PARP1 at Y907 and that the phosphorylation increases PARP1 activity and resistance to PARPi. The combination of METi and PARPi has synergistic effect on c-Met overexpressed TNBC. In addition to c-Met, through database and our mass spectrometry analysis, we found CK2 is another potential PARP1 regulator. Briefly, CK2 is also overexpressed in TNBC, which is determined by TCGA analysis. The functional analysis showed that a CK2i plus PARPi exhibited synergy. The combination of a CK2i and PARPi attenuates DNA damage repair, cell cycle, and tumor growth. Similar to c-Met-PARP1 axis, CK2 interacts with PARP1 in the nucleus. This interaction may cause specific phosphorylation on PARP1 and further elevate PARP1 activity. The potential phosphorylation sites by CK2 are still under investigation. Overall, inhibition of upstream kinases could sensitize PARPi-resistant cancer cells to PARPi. A phosphorylation profile in the PARP1 may provide marker-guided combination therapies to stratify TNBC patients (Figure 4.1).

Figure 4.1 The Working Model of PARPi Resistance Induced by c-Met and CK2

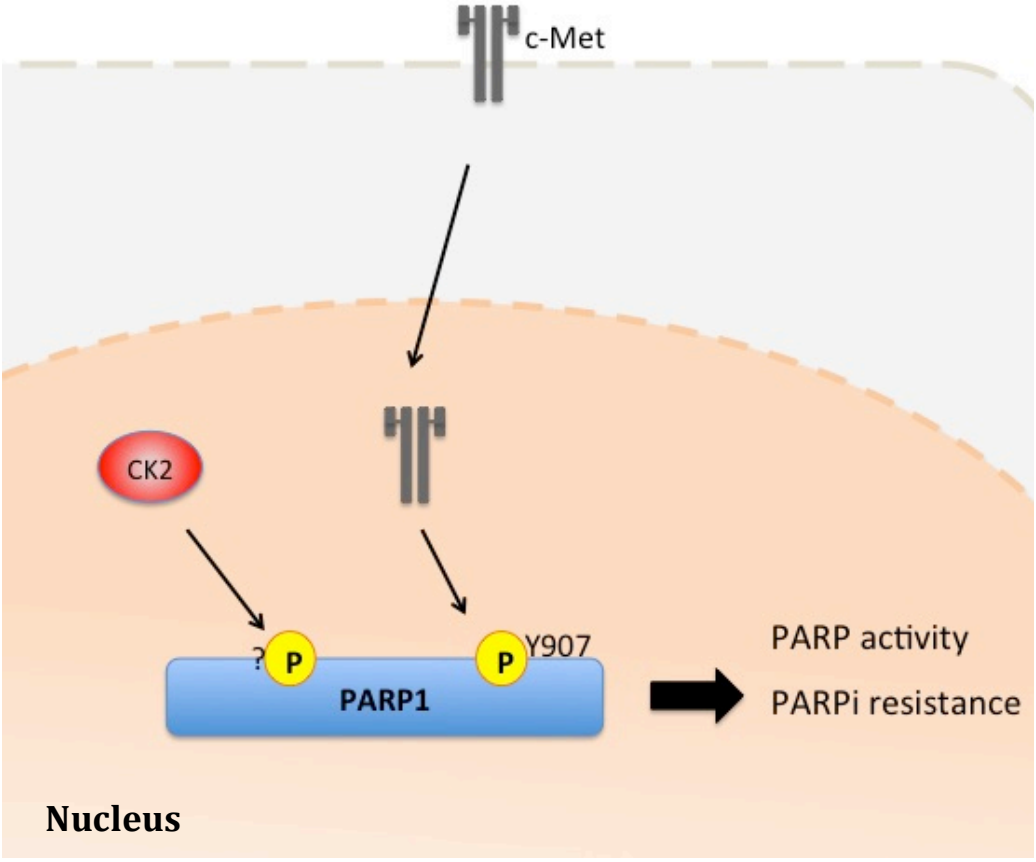

c-Met regulates the phosphorylation of PARP1 at Y907 and CK2 phosphorylates PARP1 (The sites are under investigation) and enhances the PARP activity, leading to PARPi resistance.

4.2 Translational Application from Current Study

4.2.1 PARP1 Could be Regulated by Multiple Kinases

PARP is currently the most promising drug target for BRCA-mutated TNBC, and multiple PARPi have been developed and tested in clinical trials including a single treatment or combinational treatment with other DNA-damage reagents and/or chemotherapy (39). However, not every patient with BRCA mutations responded to PARPi (46). Therefore, our studies provide other biomarkers to stratify patients who will respond to PARPi, and also develop effective combination therapies for those who will not respond to PARPi. We especially focused on the kinases that are inhibitors currently used in the clinic or in clinical trials, allowing for easier applying our biomarkers and combination therapies into clinical trials compared with the conventional drug development processes.

TNBC is known to be heterogenous. Previous studies have been shown that various kinases can phosphorylate the same substrates and resulted in signal crosstalk (118-120). Therefore, it is not surprised that PARP1 can be regulated by multiple kinases from our current study (including c-Met and CK2) in TNBC. In addition to c-Met and CK2, we found that EGFR could interact and phosphorylate with PARP1. Other group also indicated that the inhibition of both EGFR and PARP induces synthetic lethality in TNBC. Therefore, it is worthwhile to investigate the relationship between PARP1 and EGFR. Furthermore, from TCGA database analysis, we found that c-Met, EGFR and CK2 gene overexpression may cover at least 70% of TNBC. Thus, we expect that our combination treatment with PARPi and these kinase inhibitors may benefit most of TNBC patients.

4.2.2 Different Cancer Types may Show Different Response to the Same Combined Treatment

Although the first PARPi (olaparib, AZD-2281) was approved by the U.S. Food and Drug Administration (FDA) for treatment of advanced BRCA-mutant ovarian cancer in December, 2014, high percentage of patients carrying BRCA mutations do not respond to PARPi in ovarian cancer (121). We wondered whether our combination treatment could further apply to ovarian cancer. From our preliminary data, the combination of CK2i and PARPi showed strong synergistic effect in CK2 overexpressed ovarian cell lines (Figure 4.2). It has been reported that high expression of CK2 gene is correlated with poor survival in ovarian cancer patients (97). Therefore, it is worthwhile to investigate the interaction of CK2 with PARP1 in ovarian cancer. Moreover, we asked whether Y907 could also be a biomarker for the combination treatment of METi and PARPi in ovarian cancer. Surprisingly, we found that in some ovarian cell lines the phosphorylation of PARP1 at Y907 upon ROS stimulation can not be suppressed by METi, crizotinib. Thus, we suspected that other kinases might also be involved in the phosphorylation of PARP1 at Y907.

Besides TNBC and ovarian cancer, we also tested the combinational effect of c-Met and PARP inhibitors in liver cancer and lung cancer, in which PARPi is currently being tested in multiple clinical trials. We demonstrated the combinational treatment of c-Met and PARP inhibitors reduced the tumor growth in the c-Met-expressing H1993 non-small lung cancer xenograft mice model (105). Interestingly, our preliminary data showed that the combination of METi and PARPi is not synergy in some liver cancer cell

lines, suggesting other mechanisms may compromise the inhibition of c-Met and PARP in liver cancer.

Together, the present study suggested that our strategy of targeting PARP and its upstream kinase is applicable to multiple cancer types. However, as described above, PARP1 is likely to be regulated by distinct kinases in different cancer type. Thus, the detail mechanisms of how PARP1 is regulated by other kinases in different cancer types are still waiting for further investigation.

Figure 4.2 The Dual-Drug Combination of CK2 and PARP Inhibitors in Multiple Ovarian Cancer Cell Lines Shows Synergistic Effect

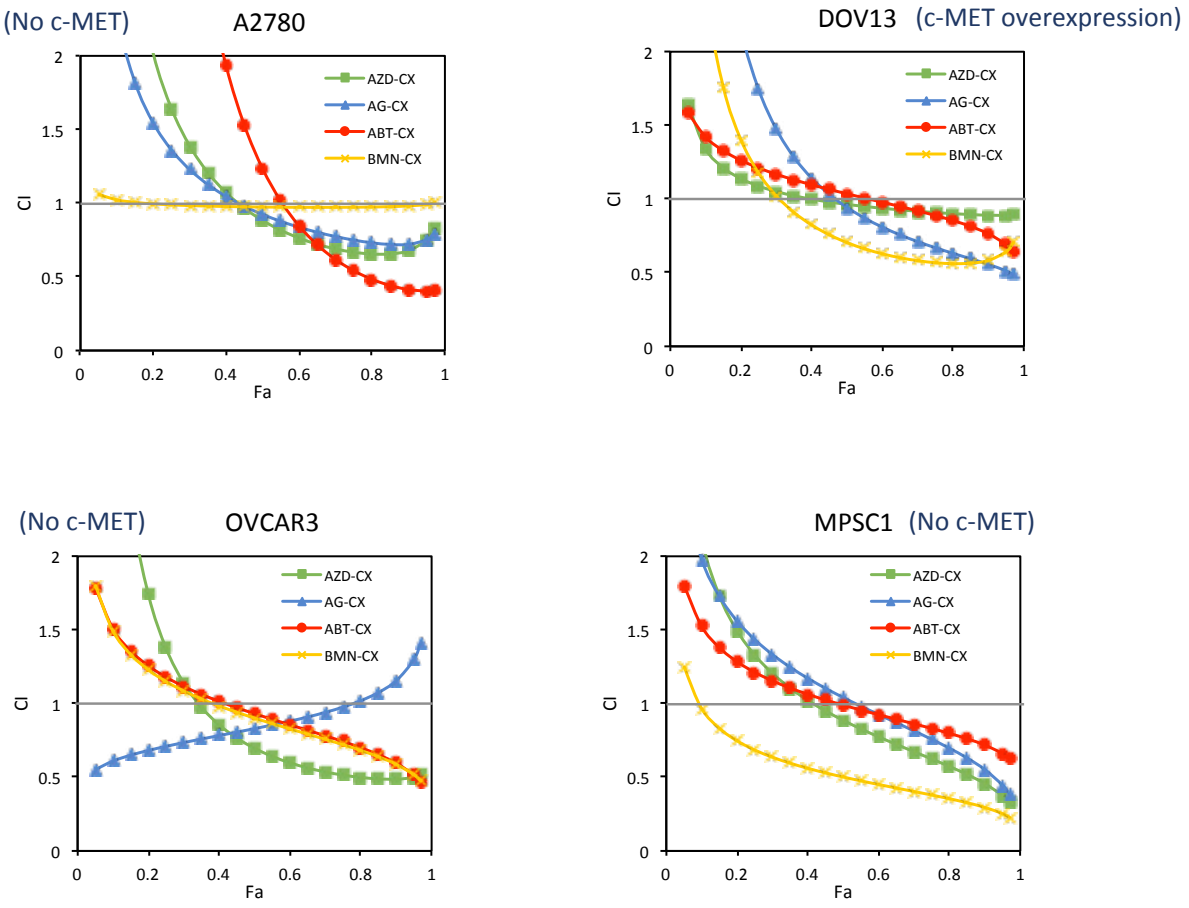

CI plots for the dual drug combinations of PARPi (AZD-2281, AG-014699, ABT-888 and BMN-673) and CX-4945 in various ovarian cancer cells.

4.3 Beyond BRCA Mutation and Deficiency

PARPi are used in BRCA mutation patients through the principle of synthetic lethality (122, 123). Although preclinical studies indicate that PARPi shows higher response rates in patients carrying BRCA mutations, a high percentage of patients with BRCA mutations do not respond to PARPi (124). In addition, some TNBC patients with wild-type BRCA still respond to PARPi, therefore BRCA mutation may not be the only biomarker to stratify patients for PARPi treatment. The concept of "BRCAness" emerged as a profile of cancers that share traits with BRCA1 or BRCA2 mutated tumors (47). A recent paper further supported this concept that in prostate cancer, patients whose tumors have a set of DNA repair gene deficiency (ATM, FANCA, CHEK2, PALB2, HDAC2 RAD51, MLH3, ERCC3, MER11, NBN, BRCA1 and BRCA2) associates with Olaparib response (125). In our study, we found that the combination of METi and PARPi is synergy in both BRCA wild-type and BRCA mutated TNBC cell lines. For example, HCC1937 cells harbor *BRCA* mutations but resistant to PARPi. From western blot analysis, we found that HCC1937 cells expressed higher levels of c-Met(105). After knocking down c-Met, HCC1937 cells became more sensitive to PARP inhibition (105). We also knocked down the *BRCA1* and *BRCA2* expression in MDA-MB-231 cell line and subjected it to PARPi. Interestingly, there is no significant change for PARPi IC50 in BRCA1/2 knockdown MDA-MB231 cell lines (105). These results suggested that independent to BRCA1/2 status, c-Met overexpression could be a marker to stratify patients. However, we didn't know whether c-Met or CK2 overexpression is associated with other DNA repair genes deficiency in these cell lines. We could further analyze other DNA repair genes status in our current model system.

Furthermore, several studies have shown that CK2 regulated DNA DSB repair pathway. It has been reported that CK2 could phosphorylate BRCA1 at S1572, but the consequences of this interaction and phosphorylation is still unclear (126). In our study, we showed that the inhibition of CK2 and PARP1 enhanced DNA DSBs, therefore it might be interesting to investigate whether the inhibition of CK2 also impairs the DNA DSBs repair through the suppression of BRCA1 activity in the future.

4.4 Different PARP Inhibitors Combined with the Same Kinase Inhibitor may Show Different Combination Efficacy

PARPi originally were designed by inhibiting the catalytic activity PARP1/PARP2 (127). However, recently some studies demonstrated that catalytic inhibition is not the only mechanism by which PARPi show cytotoxic effects (42). Some PARPi such as BMN-673, AZD-2281 and AG-014699 may trap PARP1 and PARP2 on damaged DNA (42). Trapping PARP-DNA complexes prevent DNA replication and transcription, leading to cell death more effectively than catalytic inhibition (128). It has been reported that the capacity to trap PARP varies significantly among several PARPi (43). Our study showed that c-Met and CK2 can phosphorylate PARP1 and enhance its activity. Y907 is associated with PARP1 catalytic function. However, so far whether the specific kinases involved in the regulation of PARP-DNA complex is not clear yet. Interestingly, we found that the combination efficacies of different PARPi combined with CK2i are not the same, suggesting catalytic inhibition may not be the only mechanism in our study. The different trapping ability to PARP by PARPi may be one of the possibilities leading to variable combinational effect. Taken together, whether c-Met,

CK2 or other kinase may phosphorylate PARP to affect PARP-DNA complex is an interesting topic for further study. Moreover, selection of the appropriate PARPi for each combination therapy is important for maximizing the success of clinical trials.

4.5 Increased DNA Double Strand Breaks and Replication Stress by the Combination Treatment of CK2 and PARP in TNBC

Our data showed that the combination of CK2i and PARPi enhanced more DNA strand breaks and phosphorylation of H2AX than the single treatment or untreated control, suggesting increased DNA damage by the combination. CK2 is known to be involved in the phosphorylation of multiple DNA single strand break and double strand break repair machineries such as XRCC1, XRCC4 and MRN complex (100, 129). It has been reported that inhibition CK2 delays γ-H2AX removal and reduces clonogenic survival of irradiated mammalian cells (130). Therefore, inhibition of CK2 may not only reduce PARP1 activity but also abrogate double strand break repair machinery, resulting in synthetic lethality.

Cell-cycle arrest causes the inhibition of proliferation. The G2/M checkpoint in cell cycle prevents DNA-damaged cells from entering mitosis and allows them for the repair of DNA that is damaged in late S or G2 phases before entering to mitosis (131). In our study, we observed the increase of cell-cycle arrest at G2/M phase by the combined treatment of CK2i and PARPi. As mentioned previously, AZD-2281 and AG-014699 have been shown to exhibit a stronger potency to trap PARP1 and PARP2 to DNA (43). Protein tightly bound to DNA and consequently stalling the replication fork can cause replicative stress, leading to accumulation of G2-phase cell subpopulation (132). The

increase in G2-phase that we observed in cells treated with either CX-4945 and AZD-2281 or AG-014699 may reflect their PARP-trapping ability and induction of replicative stress response. However, from cell cycle analysis, the sub-G1 population is not significantly increased in the combination treatment for 72 hours. The data from annexin V and PI staining also supported it (data not shown). It suggested that the combination may cause strong cytostaticity but mild cytotoxicity. We may consider combining chemo-drug or ionized radiation (IR) with our current combination to induce DNA damage more strongly, enhancing a cytotoxic effect in cells.

4.6 Roles of Nuclear CKα and CK2β

CK2 can form either the monomeric subunit or heterotetrameric subunit, which depends on different cell types and cellular function (97, 133). Our data showed that PARP1 co-immunoprecipitates with CK2β and is phosphorylated by CK2α. We have tried to detect the potential phosphorylation sites of PARP1 by CK2 using mass spectrometry analysis. However, so far we have not successfully identified the potential phosphorylation sites of PARP1 by CK2. There's one possibility that we performed *in vitro* kinase assay by using recombinant CK2α and PARP1 only, but CK2α itself may not have strong binding ability to PAPR1 without CK2β, the substrate-binding unit. Since CK2α and CK2β can form tetramer, we suspected that PARP1 might be a substrate targeted by the holoenzyme. Therefore, it might be better using immunoprecipitation-kinase assay to identify the phosphorylation sites of PARP1 by CK2 than *in vitro* kinase assay.

Early studies have shown that cancer cells demonstrated a higher expression of CK2 in nuclear matrix when compared to normal cells (134, 135). Traditionally, CK2

was considered as a constitutively active kinase. However, studies have shown that CK2 is activated in response to growth factor stimuli such as EGF (136, 137). In addition, it has been reported that CK2 can rapid translocate to the nuclear compartment upon heat shock and UV radiation (138). Using duolink assay, we observed the interaction of PARP1 and CK2β was mainly in the nucleus in basal-level, suggesting without any stimulation CK2 could interact with PARP1 in response to endogenous DNA damage.

4.7 Roles of Nuclear c-Met

A group of receptor tyrosine kinases (RTKs) have been found to translocate to nucleus such as EGFR, ErbB4 and c-Met (139-141). It has been proposed that RTKs translocate into nucleus from cell membrane is through a vesicle membrane-associated pathway. Take EGFR as an example, EGFR is carried by endocytic vesicles and transported from the cell surface to Golgi apparatus, the ER, the mitochondria, and the nucleus (142). The study has shown that nuclear localization signals (NLSs) and importin-β are involved in the nuclear translocation of EGFR (143). In our current study, we found that nuclear translocation of c-Met in response to ROS stimulation required a motor protein, dynein and SNARE (soluble NSF attachment protein receptor) protein syntaxin 6 (105). These two molecules are known to involve in cell trafficking. Thus, it suggested that c-Met may use the similar nuclear translocation pathway to EGFR.

A previous report showed that the translocation of the full-length c-Met into the nucleus plays an important role in activating calcium signals (112). Furthermore, the constitutive activation of nuclear c-Met is associated with aggressiveness of MDA-MB231 (144). In our study, c-Met translocated into the nucleus upon ROS stimulation.

The interaction of PARP1 and c-Met is also observed mainly in the nucleus, suggesting a distinct function of nuclear c-Met in DNA damage response from cell surface c-Met activated by a ligand.

Since multiple RTKs translocate to the nucleus, some of them may also interact and phosphorylate PARP1. Indeed, our preliminary showed that EGFR interact and phosphorylate PARP1. EGFR is known to be overexpression in many cancer types including TNBC (145). Moreover, it has previously been shown that the combination of cetuximab (EGFR mAb) plus ABT-888 (PARPi) and that of lapatinib (EGFR/HER2 inhibitor) plus ABT-888 induce synthetic lethality in head and neck cancer and TNBC, respectively (146, 147). Thus, we suspect the underlying mechanisms of EGFR signaling contributed to PARPi sensitivity may be similar to c-Met-PARP1 axis.

4.8 Future Directions

On the basis of our current study, c-Met and CK2 can positively regulate PARP1 function and activity through phosphorylation in TNBC. More importantly, the phosphorylation of PARP1 contributes to PARPi resistance. The combination of METi and PARPi or CK2i and PARPi is likely a promising approach for overcoming resistance in TNBC. Regarding to this direction, there are still many extended questions remaining for further investigation. The potential future works from basic to translational aspect are list as below:

(1) We have already shown that CK2 can phosphorylate PARP1. Therefore, what is the specific S/T site of PARP1 phosphorylated by CK2 and contribute to PARPi resistance?

(2) In addition to TNBC, does the combined inhibition of Met and PARP or CK2 and PARP also exhibit synergistic therapeutic effects in other cancer types?

(3) Our long-term goal is to use the phosphorylation profile in PARP1 protein as biomarkers to stratify patients for appropriate combination therapies. Are there any other potential phosphorylation sites of PARP1 contribute to PARPi resistance?

(4) There are some kinases whose inhibitors are not available currently on our list. Do these kinases contribute to PARPi resistance as well?

(5) What are the detail mechanisms for c-Met translocation into the nucleus and phosphorylation of PARP1 in response to ROS stimulation?

(6) Does phosphorylation of PARP1 affect a PARP-DNA complex?

(7) Currently, many chemotherapeutic drugs combined with PARPi are tested in clinical trials. Can our combinations enhance chemo-drug sensitivity and improve the therapeutic efficacy?

BIBLIOGRAPHY

1. **DeSantis CE, Fedewa SA, Goding Sauer A, Kramer JL, Smith RA, Jemal A.** 2016. Breast cancer statistics, 2015: Convergence of incidence rates between black and white women. CA Cancer J Clin **66:**31-42.
2. **Weigelt B, Reis-Filho JS.** 2009. Histological and molecular types of breast cancer: is there a unifying taxonomy? Nat Rev Clin Oncol **6:**718-730.
3. **Senkus E, Kyriakides S, Ohno S, Penault-Llorca F, Poortmans P, Rutgers E, Zackrisson S, Cardoso F.** 2015. Primary breast cancer: ESMO Clinical Practice Guidelines for diagnosis, treatment and follow-up. Ann Oncol **26 Suppl 5:**v8-30.
4. **Sledge GW, Mamounas EP, Hortobagyi GN, Burstein HJ, Goodwin PJ, Wolff AC.** 2014. Past, present, and future challenges in breast cancer treatment. J Clin Oncol **32:**1979-1986.
5. **Schnitt SJ, Moran MS, Houssami N, Morrow M.** 2015. The Society of Surgical Oncology-American Society for Radiation Oncology Consensus Guideline on Margins for Breast-Conserving Surgery With Whole-Breast Irradiation in Stages I and II Invasive Breast Cancer: Perspectives for Pathologists. Arch Pathol Lab Med **139:**575-577.
6. **Penault-Llorca F, Radosevic-Robin N.** 2016. Biomarkers of residual disease after neoadjuvant therapy for breast cancer. Nat Rev Clin Oncol doi:10.1038/nrclinonc.2016.1.

7. **Miller E, Lee HJ, Lulla A, Hernandez L, Gokare P, Lim B.** 2014. Current treatment of early breast cancer: adjuvant and neoadjuvant therapy. F1000Res **3:**198.

8. **Hassan MS, Ansari J, Spooner D, Hussain SA.** 2010. Chemotherapy for breast cancer (Review). Oncol Rep **24:**1121-1131.

9. **Kimmick GG, Cirrincione C, Duggan DB, Bhalla K, Robert N, Berry D, Norton L, Lemke S, Henderson IC, Hudis C, Winer E.** 2009. Fifteen-year median follow-up results after neoadjuvant doxorubicin, followed by mastectomy, followed by adjuvant cyclophosphamide, methotrexate, and fluorouracil (CMF) followed by radiation for stage III breast cancer: a phase II trial (CALGB 8944). Breast Cancer Res Treat **113:**479-490.

10. **Carey LA, Perou CM, Livasy CA, Dressler LG, Cowan D, Conway K, Karaca G, Troester MA, Tse CK, Edmiston S, Deming SL, Geradts J, Cheang MC, Nielsen TO, Moorman PG, Earp HS, Millikan RC.** 2006. Race, breast cancer subtypes, and survival in the Carolina Breast Cancer Study. JAMA **295:**2492-2502.

11. **Chavez KJ, Garimella SV, Lipkowitz S.** 2010. Triple negative breast cancer cell lines: one tool in the search for better treatment of triple negative breast cancer. Breast Dis **32:**35-48.

12. **Liedtke C, Mazouni C, Hess KR, Andre F, Tordai A, Mejia JA, Symmans WF, Gonzalez-Angulo AM, Hennessy B, Green M, Cristofanilli M, Hortobagyi GN, Pusztai L.** 2008. Response to neoadjuvant therapy and long-

term survival in patients with triple-negative breast cancer. J Clin Oncol **26:**1275-1281.

13. **Weigelt B, Baehner FL, Reis-Filho JS.** 2010. The contribution of gene expression profiling to breast cancer classification, prognostication and prediction: a retrospective of the last decade. J Pathol **220:**263-280.

14. **Lehmann BD, Bauer JA, Chen X, Sanders ME, Chakravarthy AB, Shyr Y, Pietenpol JA.** 2011. Identification of human triple-negative breast cancer subtypes and preclinical models for selection of targeted therapies. J Clin Invest **121:**2750-2767.

15. **Hall JM, Lee MK, Newman B, Morrow JE, Anderson LA, Huey B, King MC.** 1990. Linkage of early-onset familial breast cancer to chromosome 17q21. Science **250:**1684-1689.

16. **Wooster R, Neuhausen SL, Mangion J, Quirk Y, Ford D, Collins N, Nguyen K, Seal S, Tran T, Averill D, et al.** 1994. Localization of a breast cancer susceptibility gene, BRCA2, to chromosome 13q12-13. Science **265:**2088-2090.

17. **Castilla LH, Couch FJ, Erdos MR, Hoskins KF, Calzone K, Garber JE, Boyd J, Lubin MB, Deshano ML, Brody LC, et al.** 1994. Mutations in the BRCA1 gene in families with early-onset breast and ovarian cancer. Nat Genet **8:**387-391.

18. **Futreal PA, Liu Q, Shattuck-Eidens D, Cochran C, Harshman K, Tavtigian S, Bennett LM, Haugen-Strano A, Swensen J, Miki Y, et al.** 1994. BRCA1 mutations in primary breast and ovarian carcinomas. Science **266:**120-122.

19. **Roy R, Chun J, Powell SN.** 2012. BRCA1 and BRCA2: different roles in a common pathway of genome protection. Nat Rev Cancer **12:**68-78.

20. **Venkitaraman AR.** 2001. Functions of BRCA1 and BRCA2 in the biological response to DNA damage. J Cell Sci **114:**3591-3598.

21. **Li S, Ting NS, Zheng L, Chen PL, Ziv Y, Shiloh Y, Lee EY, Lee WH.** 2000. Functional link of BRCA1 and ataxia telangiectasia gene product in DNA damage response. Nature **406:**210-215.

22. **Greenup R, Buchanan A, Lorizio W, Rhoads K, Chan S, Leedom T, King R, McLennan J, Crawford B, Kelly Marcom P, Shelley Hwang E.** 2013. Prevalence of BRCA mutations among women with triple-negative breast cancer (TNBC) in a genetic counseling cohort. Ann Surg Oncol **20:**3254-3258.

23. **Rastogi RP, Richa, Kumar A, Tyagi MB, Sinha RP.** 2010. Molecular mechanisms of ultraviolet radiation-induced DNA damage and repair. J Nucleic Acids **2010:**592980.

24. **Iida T, Furuta A, Kawashima M, Nishida J, Nakabeppu Y, Iwaki T.** 2001. Accumulation of 8-oxo-2'-deoxyguanosine and increased expression of hMTH1 protein in brain tumors. Neuro Oncol **3:**73-81.

25. **Li D, Firozi PF, Zhang W, Shen J, DiGiovanni J, Lau S, Evans D, Friess H, Hassan M, Abbruzzese JL.** 2002. DNA adducts, genetic polymorphisms, and K-ras mutation in human pancreatic cancer. Mutat Res **513:**37-48.

26. **Chance B, Sies H, Boveris A.** 1979. Hydroperoxide metabolism in mammalian organs. Physiol Rev **59:**527-605.

27. **Loft S, Poulsen HE.** 1996. Cancer risk and oxidative DNA damage in man. J Mol Med (Berl) **74:**297-312.

28. **De Bont R, van Larebeke N.** 2004. Endogenous DNA damage in humans: a review of quantitative data. Mutagenesis **19:**169-185.

29. **Jackson SP, Bartek J.** 2009. The DNA-damage response in human biology and disease. Nature **461:**1071-1078.

30. **Jackson AL, Loeb LA.** 2001. The contribution of endogenous sources of DNA damage to the multiple mutations in cancer. Mutat Res **477:**7-21.

31. **Lieber MR.** 2010. The mechanism of double-strand DNA break repair by the nonhomologous DNA end-joining pathway. Annu Rev Biochem **79:**181-211.

32. **Altieri F, Grillo C, Maceroni M, Chichiarelli S.** 2008. DNA damage and repair: from molecular mechanisms to health implications. Antioxid Redox Signal **10:**891-937.

33. **Sirbu BM, Cortez D.** 2013. DNA damage response: three levels of DNA repair regulation. Cold Spring Harb Perspect Biol **5:**a012724.

34. **Schreiber V, Dantzer F, Ame JC, de Murcia G.** 2006. Poly(ADP-ribose): novel functions for an old molecule. Nat Rev Mol Cell Biol **7:**517-528.

35. **Herceg Z, Wang ZQ.** 2001. Functions of poly(ADP-ribose) polymerase (PARP) in DNA repair, genomic integrity and cell death. Mutat Res **477:**97-110.

36. **Puigvert JC, Sanjiv K, Helleday T.** 2016. Targeting DNA repair, DNA metabolism and replication stress as anti-cancer strategies. FEBS J **283:**232-245.

37. **Schiewer MJ, Knudsen KE.** 2014. Transcriptional roles of PARP1 in cancer. Mol Cancer Res **12:**1069-1080.

38. **Bryant HE, Helleday T.** 2006. Inhibition of poly (ADP-ribose) polymerase activates ATM which is required for subsequent homologous recombination repair. Nucleic Acids Res **34:**1685-1691.

39. **Rouleau M, Patel A, Hendzel MJ, Kaufmann SH, Poirier GG.** 2010. PARP inhibition: PARP1 and beyond. Nat Rev Cancer **10:**293-301.

40. **Farmer H, McCabe N, Lord CJ, Tutt AN, Johnson DA, Richardson TB, Santarosa M, Dillon KJ, Hickson I, Knights C, Martin NM, Jackson SP, Smith GC, Ashworth A.** 2005. Targeting the DNA repair defect in BRCA mutant cells as a therapeutic strategy. Nature **434:**917-921.

41. **Bryant HE, Schultz N, Thomas HD, Parker KM, Flower D, Lopez E, Kyle S, Meuth M, Curtin NJ, Helleday T.** 2005. Specific killing of BRCA2-deficient tumours with inhibitors of poly(ADP-ribose) polymerase. Nature **434:**913-917.

42. **Murai J, Huang SY, Das BB, Renaud A, Zhang Y, Doroshow JH, Ji J, Takeda S, Pommier Y.** 2012. Trapping of PARP1 and PARP2 by Clinical PARP Inhibitors. Cancer Res **72:**5588-5599.

43. **Murai J, Huang SY, Renaud A, Zhang Y, Ji J, Takeda S, Morris J, Teicher B, Doroshow JH, Pommier Y.** 2014. Stereospecific PARP trapping by BMN 673 and comparison with olaparib and rucaparib. Mol Cancer Ther **13:**433-443.

44. **Tutt A, Robson M, Garber JE, Domchek SM, Audeh MW, Weitzel JN, Friedlander M, Arun B, Loman N, Schmutzler RK, Wardley A, Mitchell G,**

Earl H, Wickens M, Carmichael J. 2010. Oral poly(ADP-ribose) polymerase inhibitor olaparib in patients with BRCA1 or BRCA2 mutations and advanced breast cancer: a proof-of-concept trial. Lancet **376:**235-244.

45. **Sonnenblick A, de Azambuja E, Azim HA, Jr., Piccart M.** 2015. An update on PARP inhibitors--moving to the adjuvant setting. Nat Rev Clin Oncol **12:**27-41.

46. **Ganguly B, Dolfi SC, Rodriguez-Rodriguez L, Ganesan S, Hirshfield KM.** 2016. Role of Biomarkers in the Development of PARP Inhibitors. Biomark Cancer **8:**15-25.

47. **Lord CJ, Ashworth A.** 2016. BRCAness revisited. Nat Rev Cancer **16:**110-120.

48. **Khan OA, Gore M, Lorigan P, Stone J, Greystoke A, Burke W, Carmichael J, Watson AJ, McGown G, Thorncroft M, Margison GP, Califano R, Larkin J, Wellman S, Middleton MR.** 2011. A phase I study of the safety and tolerability of olaparib (AZD2281, KU0059436) and dacarbazine in patients with advanced solid tumours. Br J Cancer **104:**750-755.

49. **O'Shaughnessy J, Schwartzberg L, Danso MA, Miller KD, Rugo HS, Neubauer M, Robert N, Hellerstedt B, Saleh M, Richards P, Specht JM, Yardley DA, Carlson RW, Finn RS, Charpentier E, Garcia-Ribas I, Winer EP.** 2014. Phase III study of iniparib plus gemcitabine and carboplatin versus gemcitabine and carboplatin in patients with metastatic triple-negative breast cancer. J Clin Oncol **32:**3840-3847.

50. **Fojo T, Bates S.** 2013. Mechanisms of resistance to PARP inhibitors--three and counting. Cancer Discov **3:**20-23.

51. **Bunting SF, Callen E, Wong N, Chen HT, Polato F, Gunn A, Bothmer A, Feldhahn N, Fernandez-Capetillo O, Cao L, Xu X, Deng CX, Finkel T, Nussenzweig M, Stark JM, Nussenzweig A.** 2010. 53BP1 inhibits homologous recombination in Brca1-deficient cells by blocking resection of DNA breaks. Cell **141:**243-254.

52. **Patel AG, Sarkaria JN, Kaufmann SH.** 2011. Nonhomologous end joining drives poly(ADP-ribose) polymerase (PARP) inhibitor lethality in homologous recombination-deficient cells. Proc Natl Acad Sci U S A **108:**3406-3411.

53. **Esposito MT, Zhao L, Fung TK, Rane JK, Wilson A, Martin N, Gil J, Leung AY, Ashworth A, So CW.** 2015. Synthetic lethal targeting of oncogenic transcription factors in acute leukemia by PARP inhibitors. Nat Med **21:**1481-1490.

54. **Mann M, Jensen ON.** 2003. Proteomic analysis of post-translational modifications. Nat Biotechnol **21:**255-261.

55. **Luo X, Kraus WL.** 2012. On PAR with PARP: cellular stress signaling through poly(ADP-ribose) and PARP-1. Genes Dev **26:**417-432.

56. **Gagne JP, Moreel X, Gagne P, Labelle Y, Droit A, Chevalier-Pare M, Bourassa S, McDonald D, Hendzel MJ, Prigent C, Poirier GG.** 2009. Proteomic investigation of phosphorylation sites in poly(ADP-ribose)

polymerase-1 and poly(ADP-ribose) glycohydrolase. J Proteome Res **8:**1014-1029.

57. **Kauppinen TM, Chan WY, Suh SW, Wiggins AK, Huang EJ, Swanson RA.** 2006. Direct phosphorylation and regulation of poly(ADP-ribose) polymerase-1 by extracellular signal-regulated kinases 1/2. Proc Natl Acad Sci U S A **103:**7136-7141.

58. **Zhang S, Lin Y, Kim YS, Hande MP, Liu ZG, Shen HM.** 2007. c-Jun N-terminal kinase mediates hydrogen peroxide-induced cell death via sustained poly(ADP-ribose) polymerase-1 activation. Cell Death Differ **14:**1001-1010.

59. **Bauer PI, Farkas G, Buday L, Mikala G, Meszaros G, Kun E, Farago A.** 1992. Inhibition of DNA binding by the phosphorylation of poly ADP-ribose polymerase protein catalysed by protein kinase C. Biochem Biophys Res Commun **187:**730-736.

60. **Beckert S, Farrahi F, Perveen Ghani Q, Aslam R, Scheuenstuhl H, Coerper S, Konigsrainer A, Hunt TK, Hussain MZ.** 2006. IGF-I-induced VEGF expression in HUVEC involves phosphorylation and inhibition of poly(ADP-ribose)polymerase. Biochem Biophys Res Commun **341:**67-72.

61. **Organ SL, Tsao MS.** 2011. An overview of the c-MET signaling pathway. Ther Adv Med Oncol **3:**S7-S19.

62. **Trusolino L, Comoglio PM.** 2002. Scatter-factor and semaphorin receptors: cell signalling for invasive growth. Nat Rev Cancer **2:**289-300.

63. **Weidner KM, Arakaki N, Hartmann G, Vandekerckhove J, Weingart S, Rieder H, Fonatsch C, Tsubouchi H, Hishida T, Daikuhara Y, et al.** 1991. Evidence for the identity of human scatter factor and human hepatocyte growth factor. Proc Natl Acad Sci U S A **88:**7001-7005.

64. **Basilico C, Arnesano A, Galluzzo M, Comoglio PM, Michieli P.** 2008. A high affinity hepatocyte growth factor-binding site in the immunoglobulin-like region of Met. J Biol Chem **283:**21267-21277.

65. **Fajardo-Puerta AB, Mato Prado M, Frampton AE, Jiao LR.** 2016. Gene of the month: HGF. J Clin Pathol doi:10.1136/jclinpath-2015-203575.

66. **Birchmeier C, Birchmeier W, Gherardi E, Vande Woude GF.** 2003. Met, metastasis, motility and more. Nat Rev Mol Cell Biol **4:**915-925.

67. **Ferracini R, Longati P, Naldini L, Vigna E, Comoglio PM.** 1991. Identification of the major autophosphorylation site of the Met/hepatocyte growth factor receptor tyrosine kinase. J Biol Chem **266:**19558-19564.

68. **Jeffers M, Taylor GA, Weidner KM, Omura S, Vande Woude GF.** 1997. Degradation of the Met tyrosine kinase receptor by the ubiquitin-proteasome pathway. Mol Cell Biol **17:**799-808.

69. **Corso S, Comoglio PM, Giordano S.** 2005. Cancer therapy: can the challenge be MET? Trends Mol Med **11:**284-292.

70. **Larue L, Bellacosa A.** 2005. Epithelial-mesenchymal transition in development and cancer: role of phosphatidylinositol 3' kinase/AKT pathways. Oncogene **24:**7443-7454.

71. **Garajova I, Giovannetti E, Biasco G, Peters GJ.** 2015. c-Met as a Target for Personalized Therapy. Transl Oncogenomics **7:**13-31.

72. **Reck M, Popat S, Reinmuth N, De Ruysscher D, Kerr KM, Peters S, Group EGW.** 2014. Metastatic non-small-cell lung cancer (NSCLC): ESMO Clinical Practice Guidelines for diagnosis, treatment and follow-up. Ann Oncol **25 Suppl 3:**iii27-39.

73. **Cappuzzo F, Moro-Sibilot D, Gautschi O, Boleti E, Felip E, Groen HJ, Germonpre P, Meldgaard P, Arriola E, Steele N, Fox J, Schnell P, Engelsberg A, Wolf J.** 2015. Management of crizotinib therapy for ALK-rearranged non-small cell lung carcinoma: an expert consensus. Lung Cancer **87:**89-95.

74. **Engelman JA, Zejnullahu K, Mitsudomi T, Song Y, Hyland C, Park JO, Lindeman N, Gale CM, Zhao X, Christensen J, Kosaka T, Holmes AJ, Rogers AM, Cappuzzo F, Mok T, Lee C, Johnson BE, Cantley LC, Janne PA.** 2007. MET amplification leads to gefitinib resistance in lung cancer by activating ERBB3 signaling. Science **316:**1039-1043.

75. **Shojaei F, Lee JH, Simmons BH, Wong A, Esparza CO, Plumlee PA, Feng J, Stewart AE, Hu-Lowe DD, Christensen JG.** 2010. HGF/c-Met acts as an alternative angiogenic pathway in sunitinib-resistant tumors. Cancer Res **70:**10090-10100.

76. **Minuti G, Cappuzzo F, Duchnowska R, Jassem J, Fabi A, O'Brien T, Mendoza AD, Landi L, Biernat W, Czartoryska-Arlukowicz B, Jankowski T, Zuziak D, Zok J, Szostakiewicz B, Foszczynska-Kloda M, Tempinska-**

Szalach A, Rossi E, Varella-Garcia M. 2012. Increased MET and HGF gene copy numbers are associated with trastuzumab failure in HER2-positive metastatic breast cancer. Br J Cancer **107:**793-799.

77. **Saito S, Morishima K, Ui T, Hoshino H, Matsubara D, Ishikawa S, Aburatani H, Fukayama M, Hosoya Y, Sata N, Lefor AK, Yasuda Y, Niki T.** 2015. The role of HGF/MET and FGF/FGFR in fibroblast-derived growth stimulation and lapatinib-resistance of esophageal squamous cell carcinoma. BMC Cancer **15:**82.

78. **Chapman PB, Hauschild A, Robert C, Haanen JB, Ascierto P, Larkin J, Dummer R, Garbe C, Testori A, Maio M, Hogg D, Lorigan P, Lebbe C, Jouary T, Schadendorf D, Ribas A, O'Day SJ, Sosman JA, Kirkwood JM, Eggermont AM, Dreno B, Nolop K, Li J, Nelson B, Hou J, Lee RJ, Flaherty KT, McArthur GA, Group B-S.** 2011. Improved survival with vemurafenib in melanoma with BRAF V600E mutation. N Engl J Med **364:**2507-2516.

79. **Ciamporcero E, Miles KM, Adelaiye R, Ramakrishnan S, Shen L, Ku S, Pizzimenti S, Sennino B, Barrera G, Pili R.** 2015. Combination strategy targeting VEGF and HGF/c-met in human renal cell carcinoma models. Mol Cancer Ther **14:**101-110.

80. **Burnett G, Kennedy EP.** 1954. The enzymatic phosphorylation of proteins. J Biol Chem **211:**969-980.

81. **Litchfield DW.** 2003. Protein kinase CK2: structure, regulation and role in cellular decisions of life and death. Biochem J **369:**1-15.

82. **Allende JEAaCC.** 1995. Protein kinase CK2: an enzyme with multiple substrated and a puzzling regulation. FASEB Journal **9:**11.

83. **Pagano MA, Sarno S, Poletto G, Cozza G, Pinna LA, Meggio F.** 2005. Autophosphorylation at the regulatory beta subunit reflects the supramolecular organization of protein kinase CK2. Mol Cell Biochem **274:**23-29.

84. **Dominguez I, Sonenshein GE, Seldin DC.** 2009. Protein kinase CK2 in health and disease: CK2 and its role in Wnt and NF-kappaB signaling: linking development and cancer. Cell Mol Life Sci **66:**1850-1857.

85. **Ahmad KA, Wang G, Unger G, Slaton J, Ahmed K.** 2008. Protein kinase CK2--a key suppressor of apoptosis. Adv Enzyme Regul **48:**179-187.

86. **Hanif IM, Shazib MA, Ahmad KA, Pervaiz S.** 2010. Casein Kinase II: an attractive target for anti-cancer drug design. Int J Biochem Cell Biol **42:**1602-1605.

87. **Seldin DC.** 1995. New models of lymphoma in transgenic mice. Curr Opin Immunol **7:**665-673.

88. **Landesman-Bollag E, Romieu-Mourez R, Song DH, Sonenshein GE, Cardiff RD, Seldin DC.** 2001. Protein kinase CK2 in mammary gland tumorigenesis. Oncogene **20:**3247-3257.

89. **de Thonel A, Hazoume A, Kochin V, Isoniemi K, Jego G, Fourmaux E, Hammann A, Mjahed H, Filhol O, Micheau O, Rocchi P, Mezger V, Eriksson JE, Rangnekar VM, Garrido C.** 2014. Regulation of the

proapoptotic functions of prostate apoptosis response-4 (Par-4) by casein kinase 2 in prostate cancer cells. Cell Death Dis **5:**e1016.

90. **Kim HR, Kim K, Lee KH, Kim SJ, Kim J.** 2008. Inhibition of casein kinase 2 enhances the death ligand- and natural kiler cell-induced hepatocellular carcinoma cell death. Clin Exp Immunol **152:**336-344.

91. **Deshiere A, Duchemin-Pelletier E, Spreux E, Ciais D, Combes F, Vandenbrouck Y, Coute Y, Mikaelian I, Giusiano S, Charpin C, Cochet C, Filhol O.** 2013. Unbalanced expression of CK2 kinase subunits is sufficient to drive epithelial-to-mesenchymal transition by Snail1 induction. Oncogene **32:**1373-1383.

92. **Hanahan D, Weinberg RA.** 2011. Hallmarks of cancer: the next generation. Cell **144:**646-674.

93. **Filhol O, Giacosa S, Wallez Y, Cochet C.** 2015. Protein kinase CK2 in breast cancer: the CK2beta regulatory subunit takes center stage in epithelial plasticity. Cell Mol Life Sci **72:**3305-3322.

94. **Landesman-Bollag E, Song DH, Romieu-Mourez R, Sussman DJ, Cardiff RD, Sonenshein GE, Seldin DC.** 2001. Protein kinase CK2: signaling and tumorigenesis in the mammary gland. Mol Cell Biochem **227:**153-165.

95. **Channavajhala P, Seldin DC.** 2002. Functional interaction of protein kinase CK2 and c-Myc in lymphomagenesis. Oncogene **21:**5280-5288.

96. **McKendrick L, Milne D, Meek D.** 1999. Protein kinase CK2-dependent regulation of p53 function: evidence that the phosphorylation status of the

serine 386 (CK2) site of p53 is constitutive and stable. Mol Cell Biochem **191:**187-199.

97. **Ortega CE, Seidner Y, Dominguez I.** 2014. Mining CK2 in cancer. PLoS One **9:**e115609.

98. **Thacker J, Zdzienicka MZ.** 2004. The XRCC genes: expanding roles in DNA double-strand break repair. DNA Repair (Amst) **3:**1081-1090.

99. **Heale JT, Ball AR, Jr., Schmiesing JA, Kim JS, Kong X, Zhou S, Hudson DF, Earnshaw WC, Yokomori K.** 2006. Condensin I interacts with the PARP-1-XRCC1 complex and functions in DNA single-strand break repair. Mol Cell **21:**837-848.

100. **Parsons JL, Dianova, II, Finch D, Tait PS, Strom CE, Helleday T, Dianov GL.** 2010. XRCC1 phosphorylation by CK2 is required for its stability and efficient DNA repair. DNA Repair (Amst) **9:**835-841.

101. **Mani RS, Yu Y, Fang S, Lu M, Fanta M, Zolner AE, Tahbaz N, Ramsden DA, Litchfield DW, Lees-Miller SP, Weinfeld M.** 2010. Dual modes of interaction between XRCC4 and polynucleotide kinase/phosphatase: implications for nonhomologous end joining. J Biol Chem **285:**37619-37629.

102. **Battistutta R, Cozza G, Pierre F, Papinutto E, Lolli G, Sarno S, O'Brien SE, Siddiqui-Jain A, Haddach M, Anderes K, Ryckman DM, Meggio F, Pinna LA.** 2011. Unprecedented selectivity and structural determinants of a new class of protein kinase CK2 inhibitors in clinical trials for the treatment of cancer. Biochemistry **50:**8478-8488.

103. **Juvekar A, Burga LN, Hu H, Lunsford EP, Ibrahim YH, Balmana J, Rajendran A, Papa A, Spencer K, Lyssiotis CA, Nardella C, Pandolfi PP, Baselga J, Scully R, Asara JM, Cantley LC, Wulf GM.** 2012. Combining a PI3K inhibitor with a PARP inhibitor provides an effective therapy for BRCA1-related breast cancer. Cancer Discov **2:**1048-1063.

104. **Siddiqui-Jain A, Drygin D, Streiner N, Chua P, Pierre F, O'Brien SE, Bliesath J, Omori M, Huser N, Ho C, Proffitt C, Schwaebe MK, Ryckman DM, Rice WG, Anderes K.** 2010. CX-4945, an orally bioavailable selective inhibitor of protein kinase CK2, inhibits prosurvival and angiogenic signaling and exhibits antitumor efficacy. Cancer Res **70:**10288-10298.

105. **Du Y, Yamaguchi H, Wei Y, Hsu JL, Wang HL, Hsu YH, Lin WC, Yu WH, Leonard PG, Lee GRt, Chen MK, Nakai K, Hsu MC, Chen CT, Sun Y, Wu Y, Chang WC, Huang WC, Liu CL, Chang YC, Chen CH, Park M, Jones P, Hortobagyi GN, Hung MC.** 2016. Blocking c-Met-mediated PARP1 phosphorylation enhances anti-tumor effects of PARP inhibitors. Nat Med **22:**194-201.

106. **Eisen MB, Spellman PT, Brown PO, Botstein D.** 1998. Cluster analysis and display of genome-wide expression patterns. Proc Natl Acad Sci U S A **95:**14863-14868.

107. **Olive PL, Banath JP.** 2006. The comet assay: a method to measure DNA damage in individual cells. Nat Protoc **1:**23-29.

108. **Chou TC.** 2010. Drug combination studies and their synergy quantification using the Chou-Talalay method. Cancer Res **70:**440-446.

109. **Toyokuni S, Okamoto K, Yodoi J, Hiai H.** 1995. Persistent oxidative stress in cancer. FEBS Lett **358:**1-3.

110. **Kim D, Koo JS, Lee S.** 2015. Overexpression of reactive oxygen species scavenger enzymes is associated with a good prognosis in triple-negative breast cancer. Oncology **88:**9-17.

111. **Aslan M, Ozben T.** 2003. Oxidants in receptor tyrosine kinase signal transduction pathways. Antioxid Redox Signal **5:**781-788.

112. **Gomes DA, Rodrigues MA, Leite MF, Gomez MV, Varnai P, Balla T, Bennett AM, Nathanson MH.** 2008. c-Met must translocate to the nucleus to initiate calcium signals. J Biol Chem **283:**4344-4351.

113. **Isabelle M, Moreel X, Gagne JP, Rouleau M, Ethier C, Gagne P, Hendzel MJ, Poirier GG.** 2010. Investigation of PARP-1, PARP-2, and PARG interactomes by affinity-purification mass spectrometry. Proteome Sci **8:**22.

114. **Bolin C, Boudra MT, Fernet M, Vaslin L, Pennaneach V, Zaremba T, Biard D, Cordelieres FP, Favaudon V, Megnin-Chanet F, Hall J.** 2012. The impact of cyclin-dependent kinase 5 depletion on poly(ADP-ribose) polymerase activity and responses to radiation. Cell Mol Life Sci **69:**951-962.

115. **Wright RH, Castellano G, Bonet J, Le Dily F, Font-Mateu J, Ballare C, Nacht AS, Soronellas D, Oliva B, Beato M.** 2012. CDK2-dependent activation of PARP-1 is required for hormonal gene regulation in breast cancer cells. Genes Dev **26:**1972-1983.

116. **Ju BG, Solum D, Song EJ, Lee KJ, Rose DW, Glass CK, Rosenfeld MG.** 2004. Activating the PARP-1 sensor component of the groucho/ TLE1 corepressor

complex mediates a CaMKinase IIdelta-dependent neurogenic gene activation pathway. Cell **119:**815-829.

117. **Tanaka Y, Koide SS, Yoshihara K, Kamiya T.** 1987. Poly (ADP-ribose) synthetase is phosphorylated by protein kinase C in vitro. Biochem Biophys Res Commun **148:**709-717.

118. **Lee DF, Kuo HP, Chen CT, Hsu JM, Chou CK, Wei Y, Sun HL, Li LY, Ping B, Huang WC, He X, Hung JY, Lai CC, Ding Q, Su JL, Yang JY, Sahin AA, Hortobagyi GN, Tsai FJ, Tsai CH, Hung MC.** 2007. IKK beta suppression of TSC1 links inflammation and tumor angiogenesis via the mTOR pathway. Cell **130:**440-455.

119. **Yang JY, Hung MC.** 2009. A new fork for clinical application: targeting forkhead transcription factors in cancer. Clin Cancer Res **15:**752-757.

120. **Yang JY, Zong CS, Xia W, Yamaguchi H, Ding Q, Xie X, Lang JY, Lai CC, Chang CJ, Huang WC, Huang H, Kuo HP, Lee DF, Li LY, Lien HC, Cheng X, Chang KJ, Hsiao CD, Tsai FJ, Tsai CH, Sahin AA, Muller WJ, Mills GB, Yu D, Hortobagyi GN, Hung MC.** 2008. ERK promotes tumorigenesis by inhibiting FOXO3a via MDM2-mediated degradation. Nat Cell Biol **10:**138-148.

121. **Meehan RS, Chen AP.** 2016. New treatment option for ovarian cancer: PARP inhibitors. Gynecologic Oncology Research and Practice **3**.

122. **Helen E. Bryant NS, Huw D. Thomas, Kayan M. Parker, Dan Flower, Elena Lopez, Suzanne Kyle, Mark Meuth,, Helleday NJCT.** 2005. Specific killing of BRCA2-deficient tumours with inhibitors of poly(ADP-ribose) polymerase. Nature **434:**4.

123. **Farmer H MN, Lord CJ, Tutt AN, Johnson DA, Richardson TB, Santarosa M, Dillon KJ, Hickson I, Knights C, Martin NM, Jackson SP, Smith GC, Ashworth A.** 2005. Targeting the DNA repair defect in BRCA mutant cells as a therapeutic strategy. Nature **434:**4.

124. **Ledermann J, Harter P, Gourley C, Friedlander M, Vergote I, Rustin G, Scott CL, Meier W, Shapira-Frommer R, Safra T, Matei D, Fielding A, Spencer S, Dougherty B, Orr M, Hodgson D, Barrett JC, Matulonis U.** 2014. Olaparib maintenance therapy in patients with platinum-sensitive relapsed serous ovarian cancer: a preplanned retrospective analysis of outcomes by BRCA status in a randomised phase 2 trial. Lancet Oncol **15:**852-861.

125. **Mateo J, Carreira S, Sandhu S, Miranda S, Mossop H, Perez-Lopez R, Nava Rodrigues D, Robinson D, Omlin A, Tunariu N, Boysen G, Porta N, Flohr P, Gillman A, Figueiredo I, Paulding C, Seed G, Jain S, Ralph C, Protheroe A, Hussain S, Jones R, Elliott T, McGovern U, Bianchini D, Goodall J, Zafeiriou Z, Williamson CT, Ferraldeschi R, Riisnaes R, Ebbs B, Fowler G, Roda D, Yuan W, Wu YM, Cao X, Brough R, Pemberton H, A'Hern R, Swain A, Kunju LP, Eeles R, Attard G, Lord CJ, Ashworth A, Rubin MA, Knudsen KE, Feng FY, Chinnaiyan AM, Hall E, et al.** 2015. DNA-Repair Defects and Olaparib in Metastatic Prostate Cancer. N Engl J Med **373:**1697-1708.

126. **Kathryn A. O'Brien SJL, Kimberley S. Cocke, R. Nagaraja Rao, and Richard P. Beckmann.** 1999. Casein Kinase 2 Binds to and Phosphorylates BRCA1. Biochemical and Biophysical Research Communications **260:**7.

127. **N. V. Malyuchenko EYK, O. I. Kulaeva, M. P. Kirpichnikov, V. M. Studitskiy.** 2014. PARP1 Inhibitors: Antitumor Drug Design. ACTA NATURE **7:**11.

128. **Shen Y, Aoyagi-Scharber M, Wang B.** 2015. Trapping Poly(ADP-Ribose) Polymerase. J Pharmacol Exp Ther **353:**446-457.

129. **Chapman JR, Jackson SP.** 2008. Phospho-dependent interactions between NBS1 and MDC1 mediate chromatin retention of the MRN complex at sites of DNA damage. EMBO Rep **9:**795-801.

130. **Zwicker F, Ebert M, Huber PE, Debus J, Weber KJ.** 2011. A specific inhibitor of protein kinase CK2 delays gamma-H2Ax foci removal and reduces clonogenic survival of irradiated mammalian cells. Radiat Oncol **6:**15.

131. **Wang Y, Ji P, Liu J, Broaddus RR, Xue F, Zhang W.** 2009. Centrosome-associated regulators of the G(2)/M checkpoint as targets for cancer therapy. Mol Cancer **8:**8.

132. **Jelinic P, Levine DA.** 2014. New insights into PARP inhibitors' effect on cell cycle and homology-directed DNA damage repair. Mol Cancer Ther **13:**1645-1654.

133. **Guerra B, Issinger OG, Wang JY.** 2003. Modulation of human checkpoint kinase Chk1 by the regulatory beta-subunit of protein kinase CK2. Oncogene **22:**4933-4942.

134. **Faust RA, Gapany M, Tristani P, Davis A, Adams GL, Ahmed K.** 1996. Elevated protein kinase CK2 activity in chromatin of head and neck tumors: association with malignant transformation. Cancer Lett **101:**31-35.

135. **Gapany M, Faust RA, Tawfic S, Davis A, Adams GL, Ahmed K.** 1995. Association of elevated protein kinase CK2 activity with aggressive behavior of squamous cell carcinoma of the head and neck. Mol Med **1:**659-666.

136. **Litchfield DW, Dobrowolska G, Krebs EG.** 1994. Regulation of casein kinase II by growth factors: a reevaluation. Cell Mol Biol Res **40:**373-381.

137. **Ji H, Wang J, Nika H, Hawke D, Keezer S, Ge Q, Fang B, Fang X, Fang D, Litchfield DW, Aldape K, Lu Z.** 2009. EGF-induced ERK activation promotes CK2-mediated disassociation of alpha-Catenin from beta-Catenin and transactivation of beta-Catenin. Mol Cell **36:**547-559.

138. **Davis AT, Wang H, Zhang P, Ahmed K.** 2002. Heat shock mediated modulation of protein kinase CK2 in the nuclear matrix. J Cell Biochem **85:**583-591.

139. **Wang YN, Lee HH, Lee HJ, Du Y, Yamaguchi H, Hung MC.** 2012. Membrane-bound trafficking regulates nuclear transport of integral epidermal growth factor receptor (EGFR) and ErbB-2. J Biol Chem **287:**16869-16879.

140. **Wang YN, Wang H, Yamaguchi H, Lee HJ, Lee HH, Hung MC.** 2010. COPI-mediated retrograde trafficking from the Golgi to the ER regulates EGFR nuclear transport. Biochem Biophys Res Commun **399:**498-504.

141. **Wang YN, Yamaguchi H, Hsu JM, Hung MC.** 2010. Nuclear trafficking of the epidermal growth factor receptor family membrane proteins. Oncogene **29:**3997-4006.

142. **Hung Y-NWaM-C.** 2012. Nuclear functions and subcellular trafficking mechanisms of the epidermal growth factor receptor family. Cell & Bioscience **2**.

143. **Lo HW, Ali-Seyed M, Wu Y, Bartholomeusz G, Hsu SC, Hung MC.** 2006. Nuclear-cytoplasmic transport of EGFR involves receptor endocytosis, importin beta1 and CRM1. J Cell Biochem **98:**1570-1583.

144. **Matteucci E, Bendinelli P, Desiderio MA.** 2009. Nuclear localization of active HGF receptor Met in aggressive MDA-MB231 breast carcinoma cells. Carcinogenesis **30:**937-945.

145. **Park HS, Jang MH, Kim EJ, Kim HJ, Lee HJ, Kim YJ, Kim JH, Kang E, Kim SW, Kim IA, Park SY.** 2014. High EGFR gene copy number predicts poor outcome in triple-negative breast cancer. Mod Pathol **27:**1212-1222.

146. **Nowsheen S, Cooper T, Stanley JA, Yang ES.** 2012. Synthetic lethal interactions between EGFR and PARP inhibition in human triple negative breast cancer cells. PLoS One **7:**e46614.

147. **Nowsheen S, Bonner JA, Lobuglio AF, Trummell H, Whitley AC, Dobelbower MC, Yang ES.** 2011. Cetuximab augments cytotoxicity with poly (adp-ribose) polymerase inhibition in head and neck cancer. PLoS One **6:**e24148.

VITA

Wen-Hsuan Yu was born in Taipei City, Taiwan on October 12th, 1983, the daughter of Chin-Lung Yu and Fang-Hui Lee. She received her degree of Bachelor of Science with major in life science and finance from National Taiwan University, Taiwan in 2007. From 2007 to 2009, she came to United States and worked as a research assistant in the field of biochemistry in University of North Carolina, Chapel Hill. In September 2009, she entered the Ph.D. program in the University of Texas Health Science Center at Houston Graduate School of Biomedical Sciences.